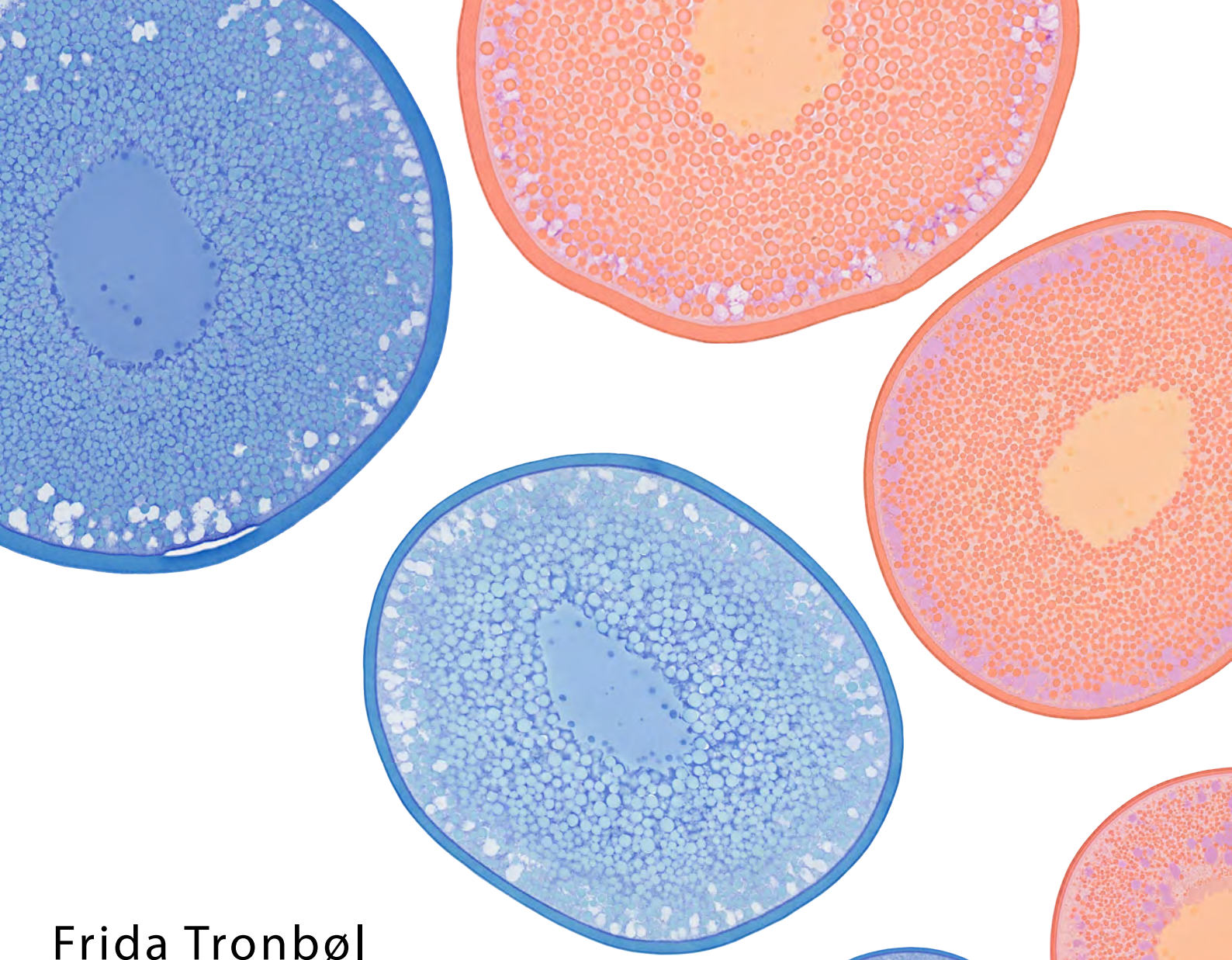

Frida Tronbøl

Tracking the time course of reproductive events in Northeast Arctic haddock (*Melanogrammus aeglefinus*)

Master of Science in Biology
- Fisheries Biology and Management

June 2021

UNIVERSITY OF BERGEN

Tracking the time course of reproductive events in the Northeast Arctic haddock (*Melanogrammus aeglefinus*)

Master of Science in **Fisheries Biology and Management**

University of Bergen

June 2021

Frida Tronbøl

Supervised by

Arild Folkvord

Edda Johannessen

Olav Sigurd Kjesbu

ACKNOWLEDGEMENTS

First of all, I would like to thank my three supervisors, Edda Johannesen, Olav Sigurd Kjesbu, and Arild Folkvord for all your time, commitment and scientific insight. Your constructive feedback and suggestions on numerous drafts, has pushed me to sharpen my thinking and critically assess my work from various points of view. I sincerely appreciate all the encouragement, patience, and guidance throughout this process. Olav, your seemingly endless knowledge of fish reproduction continues to amaze me, and I highly value your positive outlook and for introducing me to this fascinating field of research. Edda, your eye for detail and novel ideas has been instrumental to this process, and I truly appreciate the opportunity to continue studying the haddock in the course of this summer, as I am sure it will be an excellent learning experience - thank you for believing in me!

I am also deeply grateful to Grethe Thorsheim, for patiently teaching me your laboratory techniques, for processing my samples when time was running short, and for assisting collection of haddock ovaries onboard rolling vessels in the Barents Sea. And not to forget, for being moral support by phone when I, cold and barefoot, locked myself out on the fire escape stairs of 'høyblokka' on Easter Eve. Furthermore, I owe a special gratitude to Thassya Christina dos Santos Schmidt for always responding to my e-mails, tweaking my R-scripts and generally, for being so helpful. I also wish to express my deepest appreciation to Katerina Charitonidou, for taking your time answering the continuous stream of questions regarding odd histological structures found in my slides. Vemund Mangerud, thank you for continuously supplying me with formalin, tagging my samples and offering your assistance - it has truly been helpful. Additionally, I would like to thank Anders Thorsen for assisting with technical equipment and Image J - related headaches, and Ingrid Uglenes Fiksdal for staining my histological slides with PAS. Thank you, Thomas de Lange Wenneck for coordinating and letting me join the Winter Survey twice and handing over data progressively as they arrived. I am also grateful to Tom Williams for coordinating data collection with the Norwegian Reference Fleet and Maud Alix for assisting the retrieval of data and being great support in the lab. I highly appreciate the crew aboard various commercial and research vessels for their invaluable effort collecting samples forming the basis of this thesis.

Finally, I would like to thank my dear partner, Jostein Røstad, for patiently teaching me Adobe Illustrator, Word formatting, and most importantly, how to rewind. Thank you for encouraging me in everything I do. You are simply wonderful.

ABSTRACT

An important objective of fisheries management is to ensure harvest rates that allows the population to maintain its reproductive potential over time. Reproductive biology is thus of key importance when managing a fish stock as it largely determines the stock's productivity and resilience to exploitation, yet limited information is available regarding the reproductive cycle of the presently studied Northeast Arctic (NEA) haddock (*Melanogrammus aeglefinus*) stock. Additionally, as stock assessment routines include year-specific maturity-at-age data from surveys to provide estimates of the spawning stock biomass, it is important that these maturity stage estimates are validated with more accurate methods. The purpose of the present study was first to track the time course of reproductive events in field-caught NEA haddock, and second, to evaluate maturity data and explore a rapid technique to separate stages that appear macroscopically similar. Results showed that the NEA haddock commit to maturity well before August, as seen from the presence of cortical alveoli oocytes (CAO) which prevailed as the most advanced oocyte phase for 4-5 months. Despite the early appearance of the CAO phase, the first entrance into vitellogenesis occurred in late October, marking the time of separation between females that develop 'normally' and mature females that will skip the spawning season. The majority (73.8 %) of skipping females reached the CAO phase and thereafter started atretic reabsorption of these oocytes. Neither liver energy storage (somatic hepatosomatic index) nor body condition (Fulton's condition factor) could be directly linked to the occurrence of skipped spawning in the present study, although spatial and environmental factors potentially could have masked such effects. Notably, the occurrence of skipping was most common among second-time spawners (5-year-old females), apparently supporting a life-history driven mechanism for skipped spawning. The macroscopic maturity staging currently deployed during the annual Winter Survey at the Institute of Marine Research, was found to give correct estimates of the maturing portion of females but was not ideal for providing estimates of immature and skipping females. The subsequent attempt to use oocyte size frequency distributions to quickly separate immature and skipping females did not adequately provide a reliable tool for discrimination, due to the complexity of female maturity dynamics, confirmed by the ability to halt or revert the oocyte developmental process after the maturation and reproductive decision was made.

ABBREVIATIONS

Overview of frequently used technical abbreviations and their meaning

Abbreviation	Meaning	Page
CA-atresia	Cortical alveoli atresia	36
CAO	Cortical alveoli oocyte	8
CNR	Circumnuclear ring	17
ECAO	Early cortical alveoli oocyte	18
Ecosystem Survey	Joint Norwegian-Russian Ecosystem Survey in the Barents Sea	12
EVO	Early vitellogenic oocyte	18
Eα	Early alpha atresia	20
GSI_s	Somatic gonadosomatic index	22
HSI_s	Somatic hepatosomatic index	22
IMR	Norwegian Institute of Marine Research	12
K	Fulton's condition factor	22
LCAO	Late cortical alveoli oocyte	18
LC-H	Histological oocyte leading cohort	19
LC-W	Whole-mount oocyte leading cohort	15
LVO	Late vitellogenic oocyte	18
Lα	Late alpha atresia	20
NEA	Northeast Arctic	6
OSFD	Oocyte size frequency distribution	8
PG	Primary growth	8
POF	Post-ovulatory follicles	7
SG	Secondary growth	10
SSB	Spawning stock biomass	6
VO	Vitellogenic oocyte	8
Winter Survey	Joint Norwegian-Russian trawl-acoustic survey for demersal fish	6
β+γ	Beta and gamma atresia	20

TABLE OF CONTENTS

1 INTRODUCTION

Sustainable management of fish stocks is principally achieved by ensuring that the stock reproductive potential (Trippel 1999), often estimated as the spawning stock biomass (SSB), is kept above a level that secure an adequate recruitment of juvenile fish into the population (Kell et al. 2005). In this context, species-specific reproductive biology is of key importance as it largely defines a stocks' productivity, resilience to exploitation and capability of recovery (Morgan et al. 2009). For the Northeast Arctic (NEA) haddock (*Melanogrammus aeglefinus*) stock residing in the Barents Sea, central aspects of both its reproductive cycle and also maturity data used to estimate the SSB (ICES 2020a), remain understudied or even unexamined. Thus, the objective of the present study is first to enlighten unclear aspects of the NEA haddock reproductive cycle in terms of oogenesis and interruption of this process (i.e. skipped spawning), and second, to evaluate the accuracy of macroscopic maturity staging used in stock assessment and propose a possible method to reduce misclassification of these estimates.

Historically, the NEA haddock stock have exhibited tremendous variability in recruitment, often with weak coupling to the SSB (ICES 2020a), indicating that recruitment 'bottlenecks' may exists in various steps within its reproductive cycle from spawners to recruits (Bogstad et al. 2013; Landa et al. 2014; Filin and Russkikh 2019). Recruitment is affected by a multitude of physical and biological interactions, which for females start with factors controlling the level of egg production, which in turn can be traced back to mechanisms influencing oogenesis (Rothschild 2000). Uncovering the timing, mechanisms, and demographic attributes related to oocyte size and phase at which the haddock commit to maturity, could potentially aid further understanding of drivers in recruitment variability.

Annual estimates of the SSB in the NEA haddock stock include considerations of maturity-at-age data collected during the Joint Norwegian-Russian trawl-acoustic survey for demersal fish (hereafter referred to as the Winter Survey) (Fall et al. 2020). This on-board routine is based on visual inspection and classification of the gonads into five maturity stages: immature, maturing, spawning, spent and uncertain, with the latter being used if there is uncertainty whether the fish is immature or spent. These data are collected prior to the spawning season in order to generate a year-specific maturity ogive (i.e. the proportion of mature individuals at age), which supports a yearly estimation of the SSB. As the information collected during the Winter Survey constitutes the only source of maturity data entering the assessment of the haddock, it is essential that the proportion of individuals capable of spawning is estimated, as far as possible, accurately.

Recent research has revealed that misclassification occur frequently between immature and spent stages in NEA cod during the annual Winter Survey: Moksness (2019) found that out of the cod females macroscopically staged as immatures, 75.9 % turned out to be non-developing sexually mature females based on histology. Such findings highlight the inherent challenges of separating stages which appear macroscopically similar, but yet represent different demographic attributes of the population (Vitale and Cardinale 2006; Costa 2009). Currently, no such data are available for the NEA haddock, and the degree of misclassification of the macroscopic maturity estimates is largely unknown.

As an iteroparous species, the NEA haddock is assumed to follow an annual reproductive cycle that culminates in spawning once reached sexual maturity. Nonetheless, a growing body of evidence suggest that this pattern does not occur for at least a part (up to 64 %) of the sexually mature portion of the stock (Skjæraasen et al. 2015). This phenomenon, known as skipped spawning (i.e. the failure of iteroparous fishes to spawn annually following sexual maturation) has the potential to bias the SSB if not accounted for in assessment models (Rideout and Tomkiewicz 2011). However, putative skipping individuals of the NEA haddock stock are excluded from SSB estimates, and thus is unlikely to affect management advice (ICES 2020b). Nevertheless, classifying the proportion of skippers accurately in relation to immatures as well as SSB allows identifying any foreseen drivers underlying variability in skipping over time. Such time-series of skipped spawning could further provide insights into the degree of variation between years, and help to uncover under what conditions insufficient energy reserves (i.e. 'energy-constrained' skipped spawning) or trade-offs in energy allocation between growth, survival and reproduction (i.e. 'life history-driven' skipped spawning) (Skjæraasen et al. 2020) are controlling such interruption of the reproductive cycle .

Although skipped spawning has been recorded in both sexes, the focus of this study is towards female skippers, as it appears to play a greater role in the female reproductive cycle, as egg production requires higher energetic investment (Skjæraasen et al. 2009). The term skipped spawning is reserved to females that has partaken at least in one earlier spawning event and has therefore predominately been identified by the presence of post-ovulatory follicles (POF) and by the increased thickness of the ovarian wall in histological sections (Burton et al. 1997; Saborido-Rey and Junquera 1998; Witthames et al. 2010). Microscopic staging of ovaries provides higher accuracy than macroscopic field staging, and examines either the external appearance of the whole oocyte (whole mount) or the internal cellular structure (histology) (Brown-Peterson et al. 2011). Although histology can provide high-resolution micrographs of

minute detail, it is a time-consuming and costly method requiring specialised equipment, limiting the number of samples that can be processed in this manner (Tomkiewicz et al. 2003; Flores et al. 2019). Several studies have therefore instead used whole mount and associated oocyte size frequency distribution (OSFD) to rapidly quantify and study the progress of female maturity, especially for vitellogenic oocytes (VO) (Kjesbu et al. 1990, 2011; Thorsen and Kjesbu 2001; Kurita and Kjesbu 2009; Kennedy 2018; Anderson et al. 2020). Most studies have yet not focused on primary growth (PG) oocytes in OSFD due to the problem of clustering of PG oocytes and the low contrast between these oocytes and the background, obstructing the image analysis software to reliably detect these small, transparent cells (Thorsen and Kjesbu 2001; Kjesbu 2009; Kennedy 2018). Nevertheless, these challenges have recently largely been overcome by the staining of oocytes (Witthames et al. 2009), and the ultrasonication of ovarian tissue which enables separation of PG oocytes prior to measurements (Anderson et al. 2020). The use of ultrasound pen and staining in whole mount allows plentiful of PG oocytes to be captured by the image analysis system, and thereby could potentially provide a fast and cost-effective method for distinguishing between immature and skipping females during the annual Winter Survey, given that they possess dissimilar trends in OSFDs.

The occurrence of skipped spawning reflect the fact that the decision to spawn or not is made every year, depending on factors affecting females both prior to and during the spawning season (Rideout et al. 2005). During the reproductive cycle (Figure 1), regenerating female haddock are thought to be cued by declining day length after solstice in June (Davie et al. 2007) to commence development of cortical alveoli oocytes (CAO). It is generally accepted that the presence of CAO is the first marker that the female should spawn in the forthcoming spawning season, and has previously been shown to appear in NEA cod ovaries by September (Skjæraasen et al. 2010). The reproductive cycle of some females may, however, get arrested before this phase and never advance beyond the PG phases (i. Resting skippers) (Rideout et al. 2005). A second window of reproductive interruption has been observed before oogenesis progresses into VOs: the NEA cod and haddock have shown to halt further development by reabsorbing oocytes at the early CAO phase, a process which has been associated with insufficient energy reserves to continue the process of oogenesis (ii. Reabsorbing-CAO skippers) (Skjæraasen et al. 2009, 2015; Rideout and Tomkiewicz 2011).

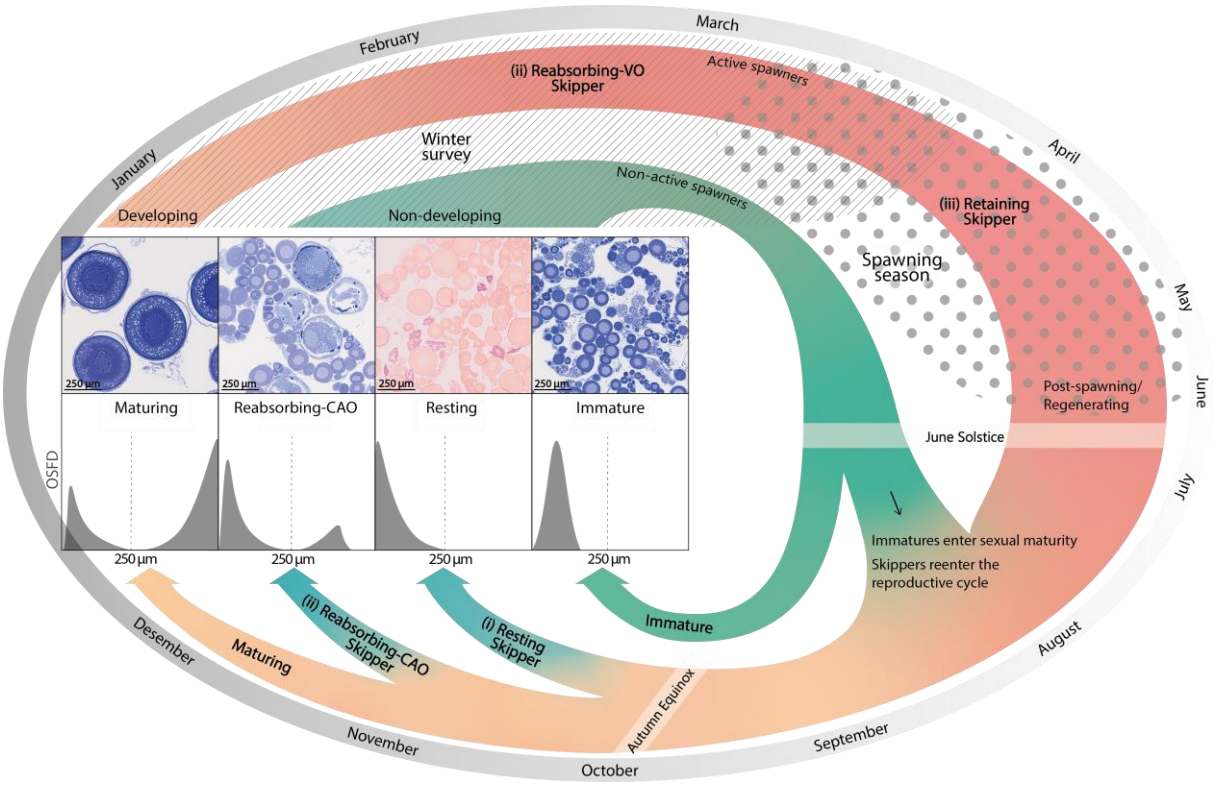

Figure 1. Conceptual figure of the proposed reproductive cycle of the NEA haddock, based on previous research of maturity in NEA cod and the northwest and northeast Atlantic stocks of haddock. Inserts to the left display the expected oocyte size frequency distribution (OSFD) and histological structures found in the ovaries prior to the spawning season (during the Winter Survey) in immatures, resting skippers, reabsorbing - cortical alveoli (CAO) skippers and maturing females. The dashed line in the OSFD indicates the size threshold between primary and secondary oocytes (250 µm). The interruption of oocyte development can occur at different times during the reproductive cycle as shown by the (i) resting (ii) reabsorbing-CAO and reabsorbing - vitellogenic oocytes (VO) and (iii) retaining modes of skipping.

Maturing female haddock are thought to continue oocyte development through vitellogenesis following the autumn equinox (i.e. when the night length exceeds the day length), as observed in the NEA cod (Kjesbu et al. 2011), and eventually migrate southwards to spawning grounds in January - February (Bergstad et al. 1987) (Figure 2). Meanwhile, some individuals may still interrupt their reproductive cycle by reabsorbing all VOs through follicular atresia (ii. Reabsorbing-VO skipper) or even retain their fully ripened eggs (iii. Retaining skipper) (Rideout and Tomkiewicz 2011). The research invested into skipped spawning of wild-caught NEA cod and haddock has mostly recorded the resting mode (Skjæraasen et al., 2009, 2012, 2015), which along with reabsorbing-CAO should be the only modes of skipped spawning possible to observe during the early parts of the Winter Survey. Macroscopically, these modes are ambiguous, and as previously mentioned, highly challenging to distinguish from immatures. To separate these categories, one could postulate that immature ovaries, which contain early phases of PG oocytes, should possess a normally distributed OSFD, while resting skippers with

more advanced stages for PG oocytes should be positively skewed (Figure 1). Meanwhile, reabsorbing-CAO, which have advanced beyond the 250 µm threshold into secondary growth (SG) oocytes, should exhibit bimodal OSFDs[1]. Identifying the characteristics of OSFD of immatures and skippers during the Winter Survey could provide a means of separating the two, at instances where there is uncertainty in maturity stage classification.

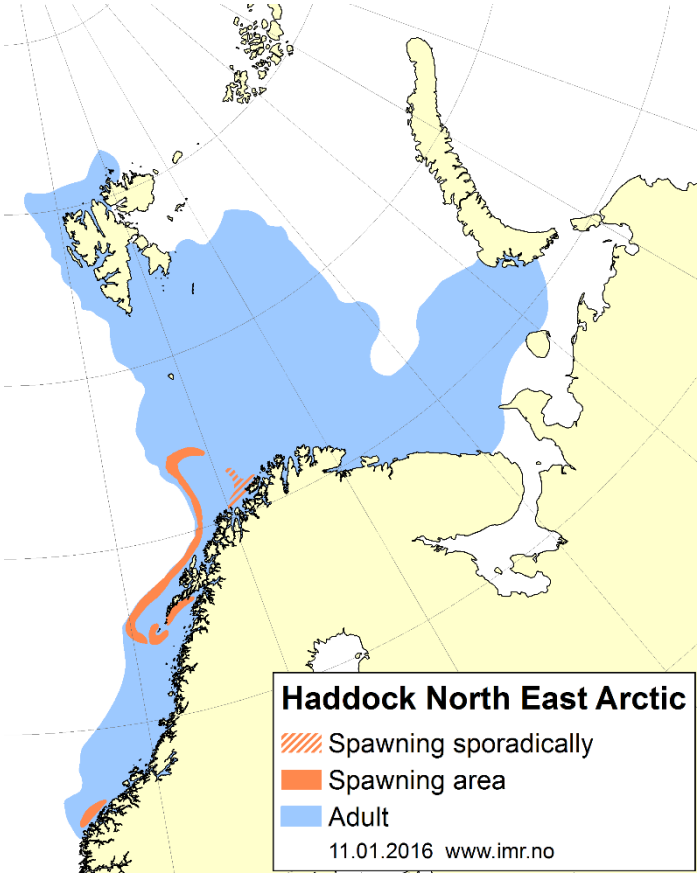

Figure 2. Official map of the NEA haddock distribution and spawning area, retrieved from the Institute of Marine Research. Recent research has revealed a genetic distinction between haddock north and south of the Lofoten Islands (~ 68°N), where spawning individuals found on the outer parts of the islands likely consists of migratory individuals from the Barents Sea (BS) (Berg et al. 2020). The NEA haddock is a determinate, group-synchronous, multiple batch spawner with peak spawning in late April to early May (Bergstad et al. 1987; Murua and Saborido-Rey 2003). In winter, adult haddock migrate along the continental slope of the western BS and north-western coast of Norway until it reaches its main spawning area at latitudes ~ 68 to 72°N (Sætersdal 1952; Bergstad et al. 1987). Pelagic eggs and larvae are transported with currents and eventually dispersed into the BS. Being an iteroparous species, the haddock spawns annually and adults are believed to return to feeding grounds in the BS in late summer, before repeating the reproductive cycle in early autumn.

[1] The reason for splitting modes of skipping into different categories, is that they likely will possess dissimilar trends in OSFD, and thus would have created large variability if the two modes were merged as one skipping category.

Although a few studies have been undertaken in regard to NEA haddock maturity dynamics (e.g. Skjæraasen et al. 2013, 2015), none have tracked the time course of oocyte development following the photoperiod cue in summer and autumn, when processes associated with the fish's energetic state may be important for the reproductive decision. By analysing ovary samples of NEA haddock by means of advanced image analysis techniques in combination with histology, the present study aims to enlighten central aspects of female oocyte- and maturity dynamics. More specifically, the objective of this thesis is to track the time course of reproductive events in field-caught NEA haddock through the initiation of the reproductive cycle in the autumn, until the onset of spawning to (i) examine oocyte development and timing of reproductive commitment, (ii) investigate the dominant mode and fundamental mechanisms determining skipping, (iii) evaluate current macroscopic maturity stage estimates deployed in assessment of the haddock, and finally (iv) explore a novel method of separating immature and skipping females based on OSFD.

2 MATERIAL AND METHODS

2.1 DATA SOURCES

Samples of the Northeast Arctic (NEA) haddock were collected at the time of initiation of maturity in the autumn until the inception of spawning, targeting the various phases of oocyte development and the occurrence of skipped spawning (Table 1). Ovary tissue and biometric information were collected monthly by the Norwegian Reference Fleet (Moan et al. 2020), which in the present study included four ocean-going commercial fishing vessels in the Barents Sea. Approximately eight samples were collected each week, resulting in 28 sampling stations across 5 consecutive months (Figure 3). Additionally, samples were collected from two annual surveys run jointly by the Norwegian Institute of Marine Research (IMR) and the Polar branch of the Russian Federal Research Institute of Fisheries and Aquaculture (PINRO): the Joint Norwegian-Russian Ecosystem Survey in the Barents Sea (Ecosystem survey) (van der Meeren and Prozorkevich 2020) and the Joint Norwegian-Russian Trawl-Acoustics Survey for demersal fish (Winter Survey) (Fall et al. 2020).

Table 1. Summary of data collection associated with each thesis objective. Sampling criteria included total length (TL), somatic gonadosomatic index (GSI_s) and maturity stages. n: number of sampled haddock from each survey.

Objectives	Time Period	Survey Type	Survey	Criteria	n
1. Track the the time course of oocyte development and the occurrence of skipped spawning	Aug - Sept (2020)	Fisheries Independent	Ecosystem Survey, The Institute of Marine Research (IMR)	TL > 40 cm Maturity stage: All stages*	71
	Aug - Dec (2020)	Fisheries Dependent	The Norwegian Reference Fleet		238
	Jan - Feb (2021)	Fisheries Independent	Winter Survey, IMR		163
2. Evaluate macroscopic maturity stage estimates and explore a method to separate immature and skipping females	Jan - Mar (2020)	Fisheries Independent	Winter Survey, IMR	TL > 40 cm $GSI_s \leq 2$ % Maturity stage: Immature and skipping	72

*Sampling criteria during the Ecosystem survey was altered due to technical issues and included additional females well below < 40 cm.

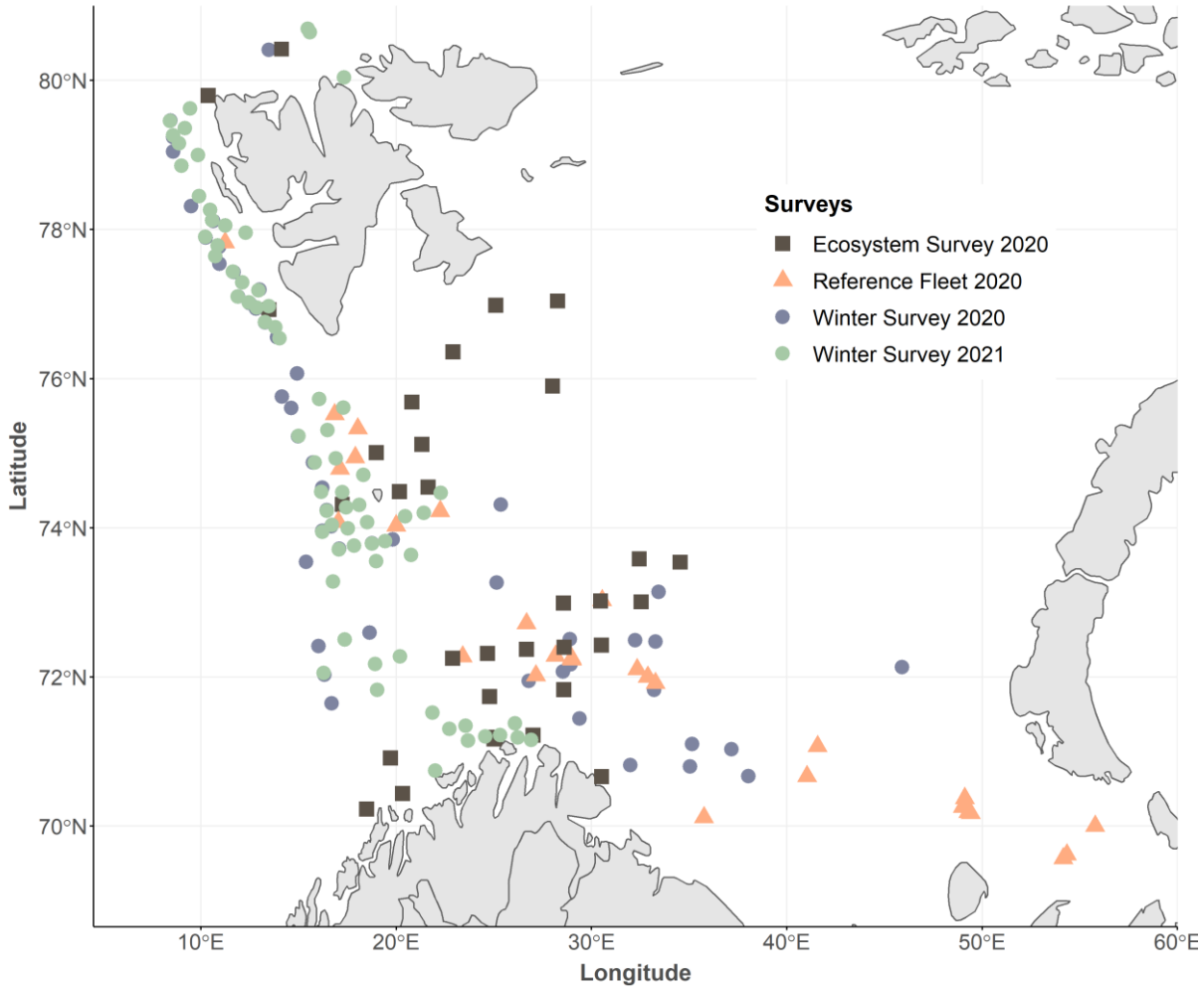

Figure 3. Map of sampling stations in the Barents Sea during the Ecosystem Survey 2020 (dark squares), fisheries-dependent Norwegian reference fleet sampling (orange triangles) and Winter Survey 2020 (blue dots) and 2021 (green dots), respectively.

2.2 BIOLOGICAL SAMPLING

Fish samples were handled immediately after the landing was onboard, and biometric information were collected according to instructions given by Mjanger et al. (2019). At the Winter and Ecosystem surveys, sampling is stratified into 5 cm length intervals, where one fish is sampled in each interval independent of sex. At the Norwegian Reference Fleet, otoliths and gonadal tissue are sampled from a maximum of 20 randomly selected fish per haul. In the present study, only females were selected and measurements of total length (nearest cm below), whole weight (nearest g below), gonad and liver weight (± 0.01 g) were recorded for all females, respectively. Otoliths were collected for age determination and later read by qualified technicians. Each female was assigned to one of five maturity stages upon visual inspection of

the ovary, based on a macroscopic classification used during field sampling at IMR (Table 2). Finally, a subsample of the ovary tissue (~2 g) was collected from the mid-section of the right lobe (assuming homogeneity; Kjesbu and Holm 1994) for each individual female. These subsamples were preserved on-board in 4 % formaldehyde solution (20 ml BiopSafe ® containers, Ax-lab, Denmark, https://www.axlab.dk/), immediately after completion of the biometric measurements.

Table 2. General description of macroscopic and microscopic (histology and whole mount) maturation stages and oocyte development phases in the reproductive cycle of female gadoids. The fifth stage, 'uncertain', is not included here, but is used when there exists uncertainty whether the fish is immature or spent. The size range of oocyte diameter at the various whole mount phases are based on research of the NEA cod, but have shown to be applicable also to the NEA haddock (Skjæraasen et al. 2015)

Maturity staging methods	Immature	Maturing	Spawning	Spent*
Macroscopic Mjanger et al. (2019)	Ovaries are small, firm and light pink in colour. Oocytes are not visible to the naked eye	Ovaries are larger and the colour have turned yellow to orange. Membrane contains numerous blood vessels. Visible opaque eggs that give the ovaries a granular appearance	Ovaries are very large. Contents consists of large translucent eggs. Eggs running freely with little to no pressure on the abdomen	Ovaries are small and firm. Membrane thin, but less transparent than an immature ovary. Pink/yellow to greyish colour
Microscopic				
Whole Mount Kjesbu et al. (2011)	< 250 µm Primary growth (PG) oocytes	250 - 850 µm Secondary growth (SG) oocytes	> 850 µm Hydrated and ovulated oocytes	< 250 µm PG oocytes or reabsorbing cortical alveoli oocytes (CAO) or vitellogenic oocytes (VO)
Histology Shirokova (1977); Kjesbu and Kryvi, (1989); Witthames et al. (2010)	Oogonia and PG phase 1, 2, 3 and 4 (a, b, c). Thin ovarian wall and little space between oocytes	Early and late CAO (ECAO, LCAO); early and late VO (EVO, LVO)	Hydrated and ovulated oocytes	PG oocytes, post-ovulatory follicles (POF), thick ovarian wall, and atretic oocytes: early alpha (Eα); late alpha (Lα); beta and gamma (β+γ)

* As the focus of this thesis is towards the reproductive cycle prior to the spawning season, no females would be classified as spent/regressing (post-spawners), thus 'spent' individuals are considered equivalent to skipping individuals.

2.3 LABORATORY ANALYSES

2.3.1 WHOLE MOUNT

Mean oocyte diameter of ovary samples were obtained using an automated image analysis system based on the auto-diametric method (Thorsen and Kjesbu 2001). All ovary samples included in the present study (n = 544) were subjected to digital image analysis, used to quantify both primary - and secondary growth oocytes, indicating the advancement of oocyte development in each individual female haddock. A subsample of ovary tissue was extracted from the BiopSafe containers and exposed to an ultrasound pen (Sonics & Materials Inc., Vibra-Cell™) for 5 to 10 seconds, depending on developmental phase (Anderson et al. 2020), to break the connective tissue between oocytes. For primary growth (PG) oocytes to be detectable, samples were stained with 2% toluidine blue and 1% sodium tetraborate (Appendix A) prior to being photographed under a dissecting microscope (magnification x12.5), where grey light level was standardised and set to 206 ± 2 at the start of each measurement series. Images were then imported and the diameter of at least 200 oocytes was measured (to the nearest µm) by the open-source ImageJ software (v. 1.52, https://imagej.nih.gov/ij/) with the plugin ObjectJ (https://sils.fnwi.uva.nl/bcb/objectj/) by taking a minimum of three micrographs of each ovary subsample (Thorsen and Kjesbu 2001). To ensure accurate and precise measurements of oocyte diameter, several tests were run on different values of threshold, roundness and ellipticity. These tests involved comparing the fit of measurement circles surrounding the oocytes (visually) and by noting the quantity of the PG oocytes detected between samples of different parameter values. The resulting images had a resolution of 0.1803 pixels/µ, and oocytes were measured based on a threshold value of 223 for sizes 50 – 1200 um, with roundness ≥ 0.8 and ellipticity ≥ 0.91. At instances where oocytes were not sufficiently dispersed or stained, the image analysis system detected and measured erroneous structures (i.e. debris or just small sections of oocytes), producing oocyte size frequency distributions (OSFD) either biased towards the smallest PG oocytes (without actually measuring them) or hardly any PG oocytes at all (Figure 4). In these cases, ovary subsamples were processed once more and new measurements were generated. The oocyte diameter measurements were then used to calculate the mean of the 20 largest oocytes in each ovary sample, hereafter referred to as the whole-mount oocyte leading cohort (LC-W), which is indicative of the female maturity development. Samples associated with Objective 1 was assigned to one of the following whole-mount maturity categories: non-developing, which included both immature and skipping: LC-W < 250; and maturing: 250 ≤ LC-W < 850 (Thorsen and Kjesbu 2001).

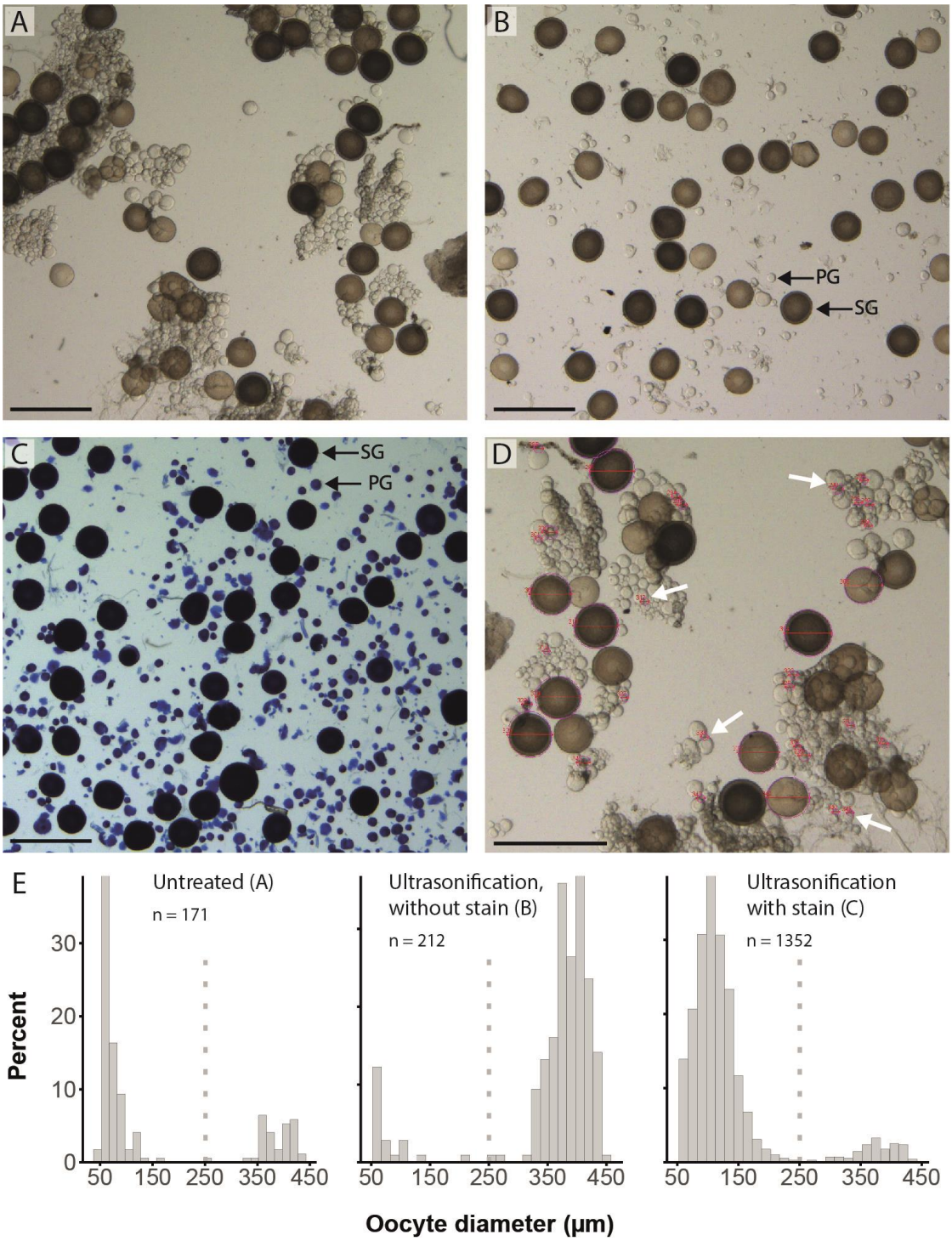

Figure 4. The effect of ultrasonification and staining in whole mount; A: untreated sample, both primary growth (PG) and secondary growth (SG) are clustered by connective tissue; B: oocytes have been dispersed by an ultrasound pen; C: oocytes have been dispersed by the ultrasound pen and stained with toluidine blue reagent; D: sample with insufficient contrast (not enough stain) between the PG oocytes and the background, generated inaccurate measurements by only detecting a small part of the oocyte (white arrows) or erroneously measuring debris. Scale bar: 1000 µm. E: the resulting oocyte size frequency distribution of the three treatments, including the number of oocytes measured (n) in each sample. Dashed line indicates the threshold separating PG and SG oocytes (250 µm), respectively.

2.3.2 HISTOLOGY

A selection of ovary samples was processed using histology to obtain highly detailed images of cellular substructures (i.e. oocyte development phases, post-ovulatory- and atretic follicles) that was further used to allocate females into categories based on maturity status (see section 2.3.2.1). All non-developing females and a random subsample of maturing females were selected for histological analysis. Ovary subsamples were processed using standard protocols for resin embedding (Kulzer, Technovit 7100®), involving dehydration, embedding and sectioning; producing two sets of 4 µm sections stained with 2% toluidine blue and 1% sodium tetraborate, or, alternatively, Periodic acid-Schiff (PAS) and Mallory trichrome, as the PAS reagent yields pronounced staining of the residual basement membrane in post-ovulatory follicles (POF) (Witthames et al. 2010). The sections were screened and converted to digital data by a high-resolution scanner (Hamamatsu, Nano Zoomer S60), allowing magnification of cell structures of minute detail. The digitalized micrographs were examined to determine the most advanced oocyte phase present in each individual female. PG oocytes was divided into four phases (PG1, PG2, PG3 and PG4), according to Shirokova (1977), with the latter being further divided into three subphases (4A, 4B, 4C) based on the shape and location of the circumnuclear ring (CNR) (Table 3; Figure 5).

Table 3. Histological description of the cytoplasm in different phases of primary (3, 4A, 4B, 4C) and secondary (cortical alveoli and vitellogenic) oocyte growth development in the NEA haddock. The oocyte size range and mean oocyte diameter (OD, ± standard deviation) associated with each oocyte phase are given in µm, and was measured manually from histological sections (n = 254).

Oocyte phases	Description of the cytoplasm	Size range	Mean OD
Primary growth oocyte		(µm)	(µm)
3	Homogeneous and uniform cytoplasm	72 - 138	106 ± 27
4A	Indistinct circumnuclear ring (CNR) covering the outer half of the cytoplasm	120 - 179	153 ± 17
4B	Distinct CNR located either centrally or towards the periphery	161 - 239	201 ± 16
4C	CNR dislocated towards the periphery and starts to disintegrate	194 - 256	232 ± 18
Cortical alveoli oocyte			
ECAO	Cortical alveoli (CA) appear at the periphery of the cytoplasm	198 - 309	261 ± 26
LCAO	CA increases in size and quantity, and the chorion becomes more pronounced	287 - 392	335 ± 26
Vitellogenic oocyte			
EVO	Small yolk granules (YG) appear on the periphery of the cytoplasm	409 - 456	433 ± 16
LVO	YG increases in number and size and occupy virtually all the cytoplasm	492 - 569	532 ± 24

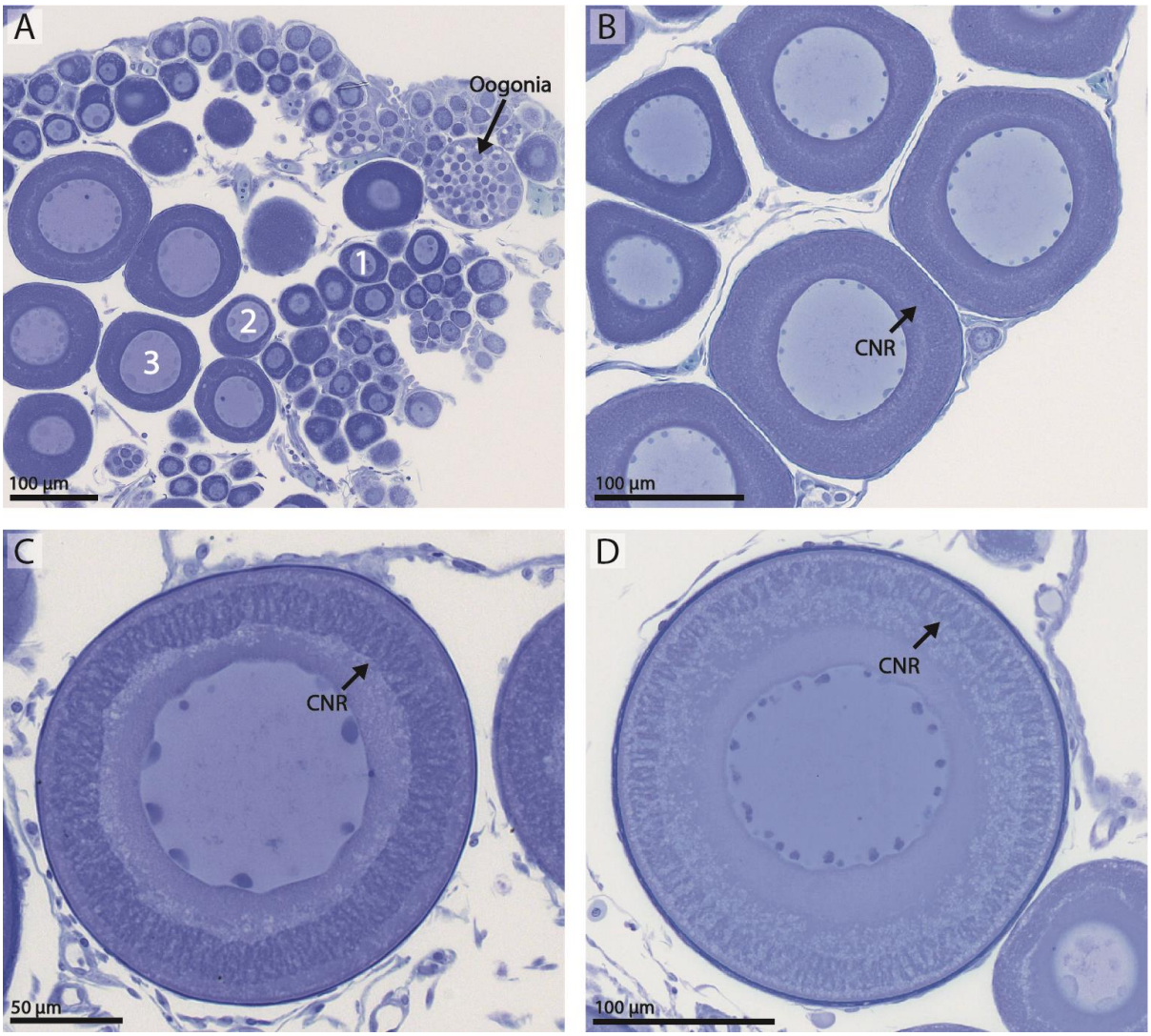

Figure 5. Histological sections of primary growth (PG) oocyte development phases of the NEA haddock stained with toluidine blue reagent. A: First developmental phases, oogonia and PG phases 1, 2 and 3, cytoplasm is uniform and homogenous; B: Phase 4A, a circumnuclear ring (CNR) appears in the cytoplasm as an indistinct feature located centrally; C: Phase 4B, the CNR has become distinct; D: Phase 4C, the CNR has migrated towards the periphery of the cytoplasm and is gradually disappearing. The chorion also becomes more pronounced through the various developmental phases.

The division of secondary growth (SG) phases was based on the oocyte size, appearance of the zona radiata (chorion) and the degree of accumulation of cortical alveoli and yolk granules, into early (ECAO) and late cortical alveoli (LCAO), and finally, early (EVO) and late vitellogenic (LVO) oocytes (Figure 6).

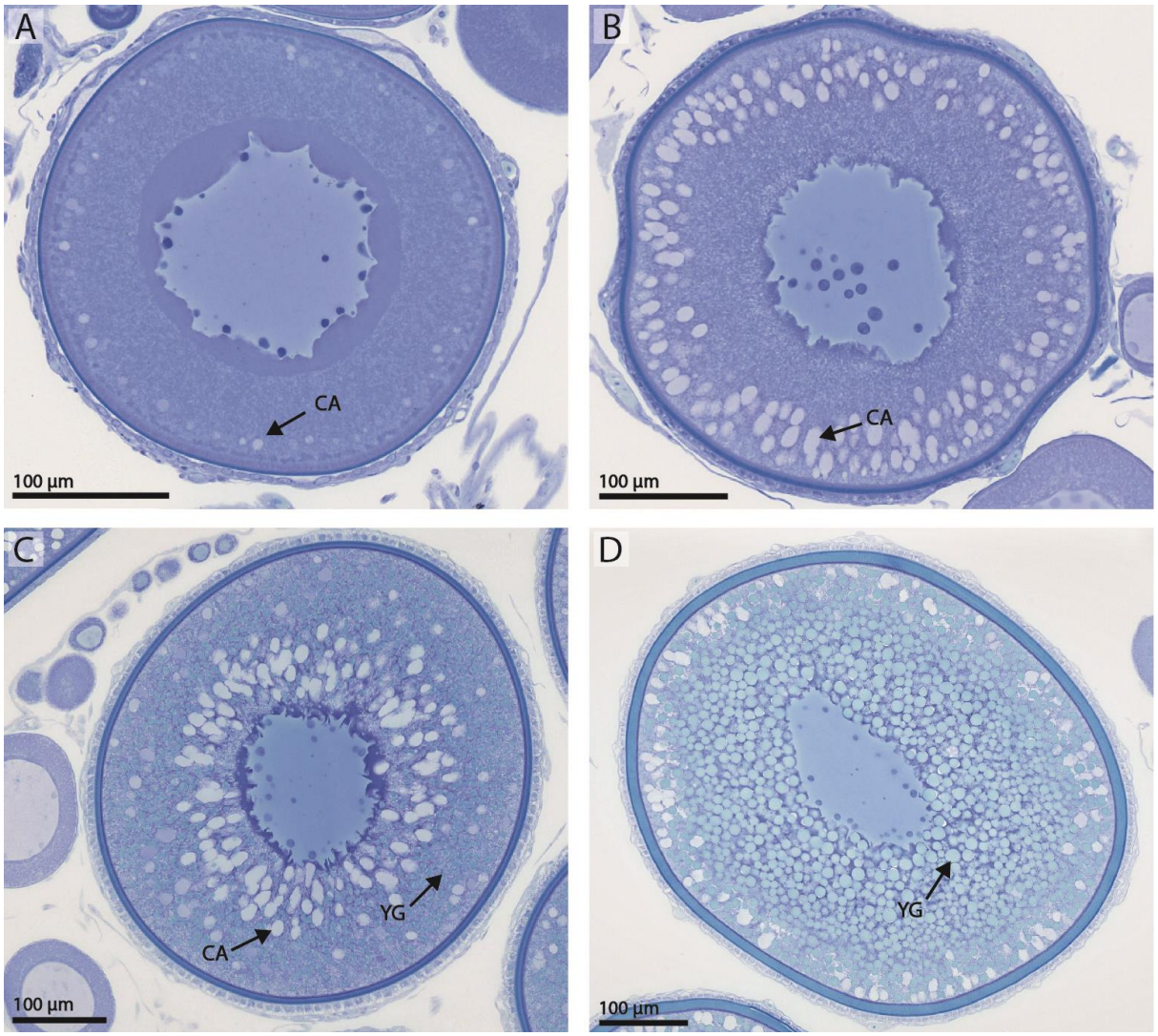

Figure 6. Histological sections of secondary growth oocyte development phases of the NEA haddock stained with toluidine blue. A: ECAO phase, commences when cortical alveoli (CA) appear at the periphery of the cytoplasm; B: LCAO phase, CA increases in size and quantity, and the chorion becomes more pronounced; C: EVO phase, small yolk granules (YG) appear on the periphery of the cytoplasm; D: LVO phase, increase in the number, size, and distribution of the yolk granules, which occupy virtually all the cytoplasm.

To quantify the most advanced oocyte phase for each female, the mean oocyte diameter of the 10 largest oocytes present were measured with the image viewing software Hamamatsu NanoZoomer Digital Pathology (NDP.view2), hereafter referred to as the histological oocyte leading cohort (LC-H). Oocyte diameter (OD) measurements were solely based on 'healthy', intact oocytes, and only oocytes sectioned through the nucleus were considered for measurements. Moreover, two axes were measured per oocyte to increase precision of measurements (Equation 1).

$$\mathrm{OD} = \frac{\mathrm{Axis}_{\mathrm{long}} + \mathrm{Axis}_{\mathrm{short}}}{2} \quad (1)$$

The prevalence of atresia was defined as the proportion of females possessing atretic cells in relation to the total number of females studied. The most advanced stage of atresia was noted, and the classification was based on the breakdown of the chorion into the three types: early alpha (Eα), indicated by small breaks in the chorion; late alpha (Lα), fragmentation of the chorion; and finally, a combined beta and gamma (β+γ) type, shown by disintegration of the chorion and significantly reduced follicle size (Witthames et al., 2010) (Figure 7).

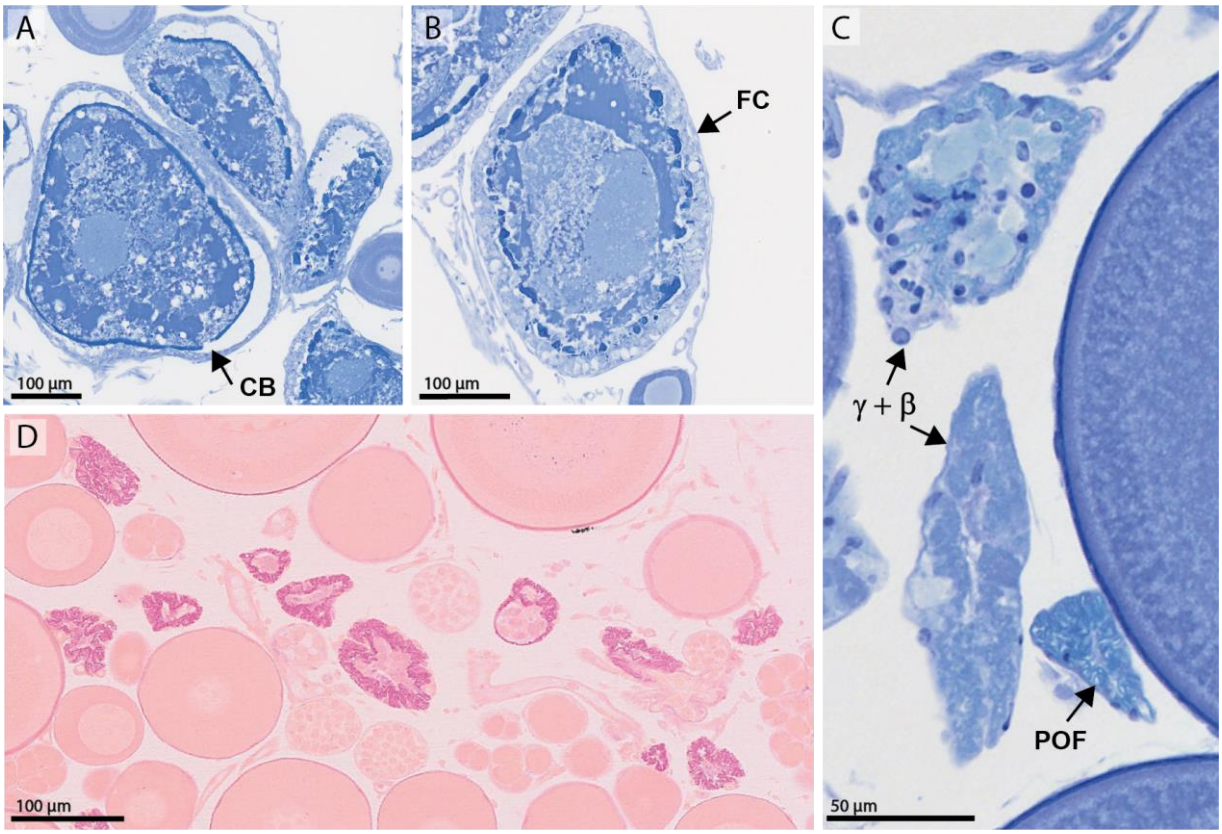

Figure 7. Histological sections of degenerating oocytes. A: early alpha atresia (Eα), breaks are visible in the chorion (CB); B: late alpha atresia (Lα), chorion appears fragmented (FC); C: combined beta and gamma atresia (β+γ), follicle is much smaller and the chorion has disintegrated. A post-ovulatory follicle (POF) is also visible; D: POFs (and possibly some β+γ) stained with Periodic acid-Schiff (PAS) and Mallory trichrome. The basement membrane in these structures becomes more pronounced, and thus more easily detectable when stained with PAS.

The intensity of atresia was noted as: very low (< 5 %); low (5 - 25 %); moderate (25 - 50 %) and massive (> 50 %) based on an overall judgment of the relative cell numbers present, at three different grids (magnification 5x) in each histological slide (Equation 2):

$$I_a = \frac{N_i}{N_i + N_j} \quad (2)$$

where, N_i is the number of atretic oocytes and N_j is the number of oocytes in the most advanced oocyte phase. The estimation of atresia in bins was considered sufficient for the present study. Any evidence for past spawning activity, i.e. POFs and the thickness of the tunica (immature females < 150 μm and spent females > 340 μm; for NEA cod) (Witthames et al., 2010) were also recorded when such structures were present in histological slides. Finally, diameter measurements of five atretic follicles for each stage of atresia, was recorded in all females showing reabsorption of cortical alveoli oocytes (i.e. reabsorbing-CAO skippers) to examine whether reabsorption occur simultaneously or over a prolonged period.

2.3.2.1 Examination of histological sections

Manual screening of all histological sections was carefully conducted to allocate females into maturity stage categories, reflecting past spawning history and current ability to spawn in the forthcoming spawning season. Allocation into immature, maturing, and skipping categories was based on the presence/absence of POFs, the most advanced oocyte phase and intensity of atretic oocytes. An uncertain category was adopted whenever criteria for the main three categories were not fully met. For instance, when ovary samples contained POF-like structures that could not be determined with certainty (e.g. odd shape or in very low quantity), females were allocated to the uncertain category. Moreover, classification of skipping females was based on both the intensity of atresia and the oocyte phase undergoing atresia: females possessing high intensity atresia of cortical alveoli phase oocytes or EVO were termed reabsorbing-CAO /or EVO skippers, while low intensity atresia of PG oocytes were termed resting skippers. Finally, examination of histological sections from the Winter Survey 2020 (in relation to Objective 2) revealed that all ovaries except two, contained POFs. Therefore, an additional eight females from the Winter Survey 2021 were included to supplement the dataset in order to provide necessary contrast in the OSFD between skippers and immatures to preform further analysis.

2.4 DATA ANALYSIS

2.4.1 RAW DATA

Biometric data associated with each individual female were retrieved from the IMR database (Sea2Data) and imported to Microsoft Office Excel 2019. Raw data were further checked for erroneous input data and modified if necessary. Proxies for individual body condition, ovary development and energy storage were calculated from the biometric data according to equations: (3) Fulton's condition factor, K; (4) somatic gonadosomatic index, GSI_s and (5) hepatosomatic index, HSI_s and included in the dataset.

$$K = \frac{\text{Whole Weight (g)}}{\text{Total Length}^3\text{(cm)}} \text{ x } 100 \quad (3)$$

$$GSI_s(\%) = \frac{\text{Ovary weight (g)}}{\text{Whole weight (g)} - \text{Ovary weight (g)}} \text{ x } 100\ (\%) \quad (4)$$

$$HSI_s(\%) = \frac{\text{Liver weight (g)}}{\text{Whole weight (g)} - \text{Liver weight (g)}} \text{ x } 100\ (\%) \quad (5)$$

The length-weight relationship was tested for allometry (H_0: $b\ (slope) = 3$, isometric growth) by applying a linear regression to a scatter plot of log-transformed data. The population exhibited isometric growth: $W = 0.0093L^{3.07}$ (one-sample t-test, df = 516, p = 0.16), with an exponent parameter (b) between 2.99 and 3.07 with 95 % confidence. Thus, using an exponent of 3 to calculate K was considered suitable for the data. Five non-developing females had GSI_s values > 1.7 (specifically: 3.22 ± 0.52 %), greatly exceeding the GSI_s threshold separating maturing and non-developing females in the NEA haddock (Skjæraasen et al. 2015). These gonad measurements were assumed to have been incorrectly punched during sampling and were marked as crosses in figures but excluded from statistical analysis. Samples collected during the Ecosystem Survey (August - September) included females well below the sampling criteria ≥ 40 cm (n = 25) but were still included in the analysis. Whole-mount oocyte diameter measurements generated in ImageJ were exported to Microsoft Office Excel and later transferred to R (v. 4.0.2, R Core Team 2020) for further statistical analysis and visualization (for specific R packages, see Appendix B). In addition to providing estimates of LC-W, the mean oocyte diameter measured from whole mount was also used to produce OSFD for skipping and immature females, in relation to Objective 2. Finally, the two measures for the oocyte leading cohort were used as follows: the LC-H was used in relation to histological oocyte

phases, while LC-W (regarded as the most accurate measure of oocyte size as shrinkage is negligible) was used to track oocyte development over time.

2.4.1 STATISTICAL ANALYSIS

Model assumptions were assessed by residual-fit plots and tested for normality and homogeneity of variance using Shapiro Wilk and studentized Breusch-Pagan tests. When deviations were detected, data were log transformed to meet assumptions of normality and correct for heteroskedasticity. Finally, Tukey's HSD (honestly significant difference) post hoc tests were used to examine the differences detected by the analysis of variance (ANOVA). All values are presented as mean ± standard deviation, and rejection of the null hypothesis was always set to $p < 0.05$.

Histological oocyte leading cohort in relation to oocyte phases

An unpaired two-sample t-test was used to test the difference in LC-H between PG (phases 3 - 4C) and SG oocytes (phases ECAO - LVO). The mean difference in LC-H between various phases of oocyte development was tested using a one-way ANOVA and Tukey's HSD test. Oocyte phases was treated as a categorical predictor with eight levels (i.e. 3, 4A, 4B, 4C, ECAO, LCAO, EVO and LVO), and LC-H as a continuous response variable.

Reproductive events

Maturity dynamics based on whole-mount analysis

The difference in age and length between whole-mount categories (i.e. maturing and non-developing females) were tested using an unpaired two-sample t-test. A two-way analysis of covariance (ANCOVA) was performed to examine if any demographic differences in LC-W could be detected over the sampling period. Prior to performing any test on the change in LC-W over time, the date variable was converted into number of days, where the earliest sampling day, August 14th, was coded as day 1, and subsequent sampling days were given a number equal to the number past this day (i.e. the final sampling day, February 10th, was coded 181). Sampling day was further treated as the continuous covariate of the response, LC-W, and length groups as a categorical predictor containing five levels (30-39, 40-49, 50-59, 60-69 and 70-79 cm). An interaction term was included to determine whether slopes differed between length groups. Furthermore, to examine monthly differences in GSI_s between whole-mount maturity categories, a two-way ANOVA was performed.

Maturity dynamics based on histological analysis

The change in LC-W over time was tested between histological maturity categories (i.e. immature, skipping and maturing females) by means of a two-way ANCOVA, including an interaction term to determine difference in slope between maturity categories. As no differences in LC-W over time could be detected between immature and skipping females, an unpaired two-sample t-test was performed to test for differences in LC-W between the two irrespective of sampling day. To examine the effect of female length on LC-W for females staged as maturing, a multiple linear regression was deployed, where LC-W was treated as a continuous response variable and female total length and sampling day as continuous predictors. Furthermore, a two-way ANOVA with Tukey HSD-test was performed to explore differences in total length and age between histological maturity categories to potentially uncover demographic variability in maturity status. Finally, a two-way ANOVA was used to examine if means of the continuous response variables GSI_s, HSI_s and K differed between the histological categories at different sampling months. The relationships were tested with an interaction term between the two categorical predictors (i.e. histological category and month).

Separation of immature and skipping females based on whole mount

To quantify and identify characteristic trends in OSFD displayed by immature and skipping females, skewness and kurtosis were calculated for each individual female and an unpaired two-sample t-test was used to examine differences between the two histological categories. To further assess whether the modes of skipped spawning individually differed in skewness and kurtosis from that of immatures, a one-way ANOVA was performed with Tukey's HSD test. Only resting and reabsorbing-CAO skippers were included in the analysis due to the insufficient sample size of reabsorbing-EVO skippers. Finally, a one-way ANOVA was used to examine differences in GSI_s and LC-W between immatures and the two modes of skipped spawning.

3 RESULTS

This section seeks to present the time course of oocyte development and ovary dynamics through the reproductive cycle of the Northeast Arctic (NEA) haddock (Objective 1) (Table 4). Furthermore, the issue of misclassification of samples collected during the annual Winter Survey is presented, along with a possible tool to improve confidence in maturity stage estimates between immature and skipping individuals (Objective 2).

Table 4. Overview of recorded biometrics associated with each thesis objective. Data collected towards Objective 1 were split into months to show temporal variability in the biometric data. The mean and standard deviation are given for (total) length, (whole) weight, age, Fulton's condition factor (K), somatic gonadosomatic index (GSI_s) and hepatosomatic index (HSI_s). Bold numbers represent samples collected and processed with whole mount, while numbers below represent a subsample of these processed with histological analysis. The sample size (n) is shown for each row of summary data.

Objectives		Data Source & time	Length (cm)	Weight (g)	Age (yr)	K	GSI_s (%)	HSI_s (%)	n
Objective 1	2020	Ecosystem Survey, Reference Fleet & Winter Survey	**51 ± 9.4** 50 ± 10.3	**1458 ± 837** 1390 ± 946	**5 ± 1.8** 5 ± 2.1	**0.99 ± 0.08** 0.99 ± 0.08	**1.39 ± 1.24** 1.33 ± 1.27	**4.18 ± 1.84** 3.99 ± 1.99	**450** 204
					BY MONTH				
		AUG	**44 ± 11.0** 42 ± 10.2	**987 ± 821** 880 ± 784	**4.4 ± 2.2** 4.2 ± 2.5	**0.98 ± 0.08** 1 ± 0.08	**0.64 ± 0.30** 0.6 ± 0.28	**3.43 ± 1.18** 3.2 ± 1.23	**55** 24
		SEPT	**53 ± 10.2** 54 ± 10.6	**1618 ± 855** 1749 ± 745	**5.6 ± 1.7** 5.8 ± 2.1	**1.02 ± 0.08** 1.02 ± 0.08	**0.99 ± 0.40** 1.09 ± 0.4	**4.00 ± 1.83** 4.06 ± 1.57	**67** 34
		OCT	**55 ± 7.7** 54 ± 8.7	**1733 ± 741** 1701 ± 856	**5.8 ± 1.9** 5.6 ± 2.1	**0.97 ± 0.08** 0.99 ± 0.08	**1.83 ± 1.42** 1.95 ± 1.61	**3.30 ± 1.75** 3.56 ± 2.03	**63** 27
		NOV	**49 ± 6.0** 46 ± 4.1	**1209 ± 486** 1012 ± 303	**4.5 ± 0.9** 4.2 ± 0.6	**0.99 ± 0.09** 1 ± 0.09	**1.64 ± 1.71** 1.72 ± 2.03	**3.60 ± 2.05** 3.23 ± 2.17	**82** 50
		DEC	**54 ± 8.8** 48 ± 7.8	**1636 ± 818** 1141 ± 595	**5.0 ± 1.2** 4.4 ± 0.9	**0.98 ± 0.09** 0.94 ± 0.09	**1.30 ± 0.68** 0.88 ± 0.54	**4.62 ± 1.43** 4.29 ± 1.51	**42** 18
	2021*	JAN	**52 ± 9.5** 54 ± 13	**1558 ± 972** 1853 ± 1304	**5.7 ± 1.9** 6.2 ± 2.7	**0.98 ± 0.08** 0.98 ± 0.08	**1.76 ± 1.58** 2.09 ± 1.77	**5.19 ± 1.76** 5.24 ± 2.14	**83** 18
		FEB	**52 ± 9.0** 53 ± 11	**1505 ± 902** 1677 ± 1222	**5.7 ± 1.5** 6.0 ± 2.0	**0.98 ± 0.07** 0.97 ± 0.08	**1.83 ± 1.60** 1.65 ± 1.38	**5.06 ± 1.48** 5.32 ± 1.50	**58** 17
Objective 2	2020	Winter Survey	**47 ± 9.9**	**1146 ± 719**	**4.8 ± 1.3**	**0.96 ± 0.1**	**0.68 ± 0.52**	**3.77 ± 1.35**	**72**

*Samples from the Winter Survey 2021 (January and February) were also included in Objective 2 in relation to section 3.2.

OOCYTE SHRINKAGE

The correspondence between the two methods (i.e. whole mount and histology) used to compute the oocyte leading cohort of each individual female, showed variability over the range of oocyte sizes. The dehydration procedure associated with histological analysis caused shrinkage of oocytes, resulting in deviations from the formaldehyde-fixed oocyte diameter measurements in whole-mounts. The oocyte leading cohort based on whole mount (LC-W) and histology (LC-H) exhibited stronger agreement in absolute terms at smaller than larger oocyte sizes (Figure 8), and LC-H measurements were generally lower compared to LC-W measurements.

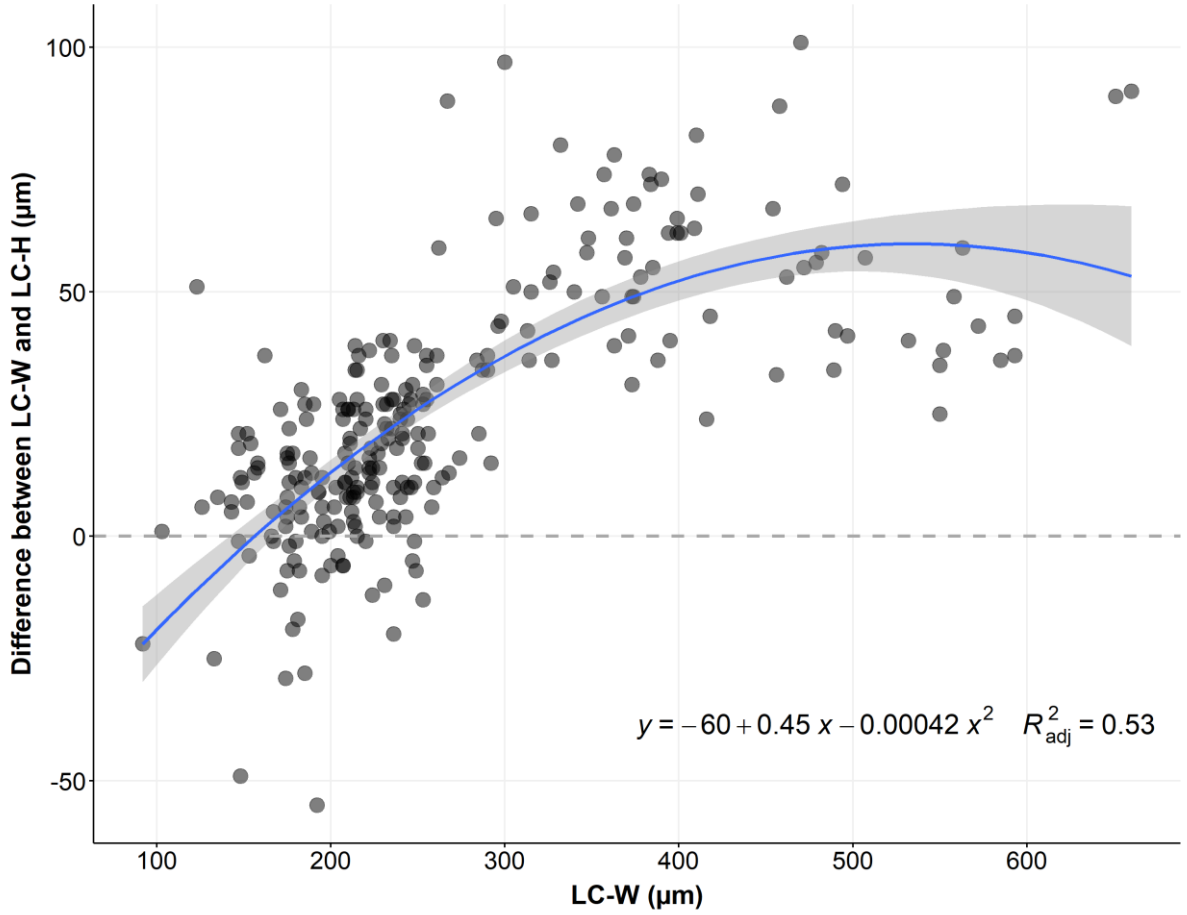

Figure 8. The absolute difference between whole-mount (LC-W) and histological (LC-H) oocyte leading cohort against LC-W, fitted with a second-degree polynomial regression line: $p < 0.001$. The horizontal dashed line denotes agreement (no difference) between the two methods.

HISTOLOGICAL OOCYTE LEADING COHORT IN RELATION TO MATURITY PHASES

Histological analysis showed that the transition between primary (PG) and secondary growth (SG) oocytes occurred at LC-H of around 250 µm, with the largest PG diameter at 256 µm and the smallest SG oocyte diameter at ~230 µm, although a few females (n = 5) exhibited cortical alveoli at oocyte diameters 198 - 230 µm (Figure 9). The LC-H of PG oocytes (208 ± 34 µm) was significantly smaller (unpaired two-sample t-test, df = 257, $p < 0.001$) compared to LC-H of the present selection of SG oocytes (402 ± 100 µm). A comparison of the LC-H between different oocyte phases showed that they were all significantly different from one another (Appendix C.1).

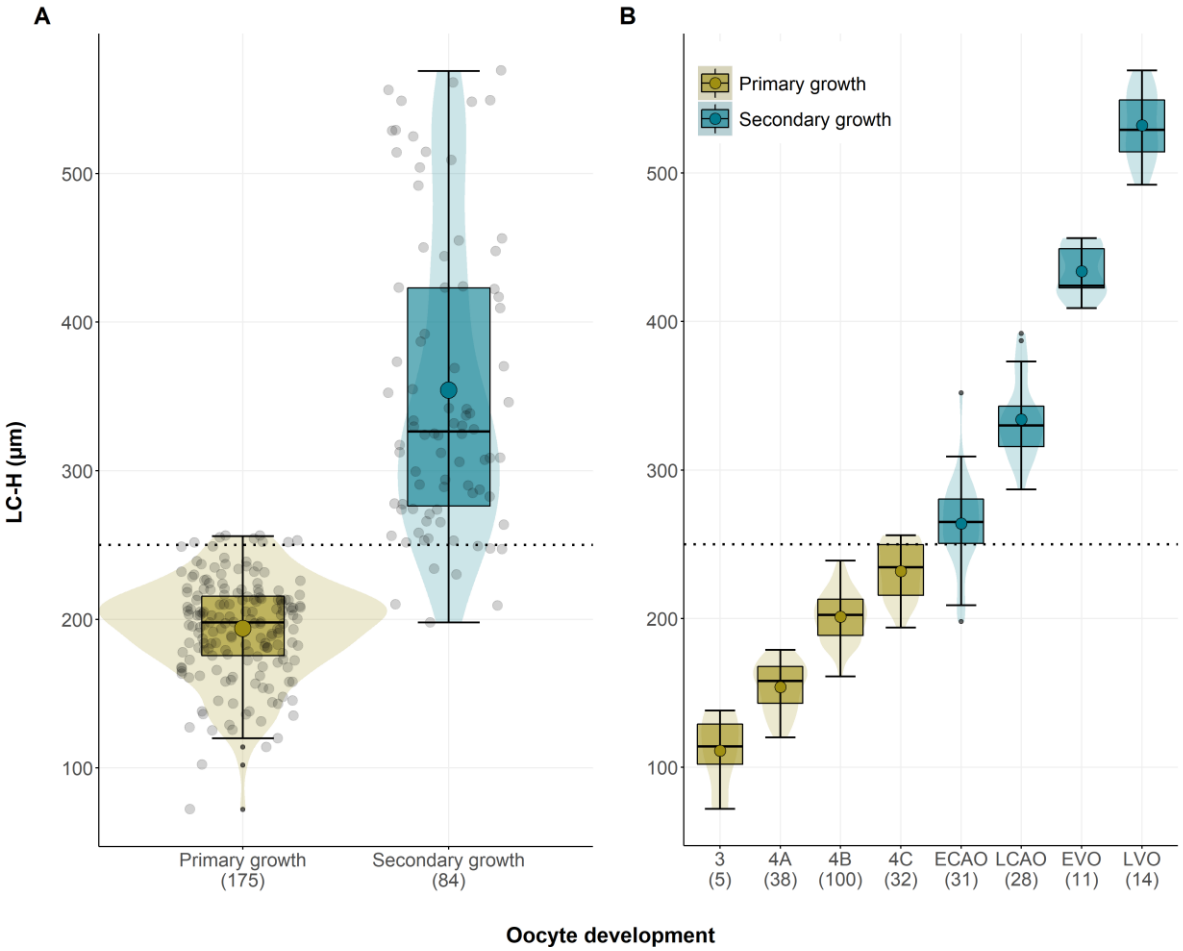

Figure 9. The histological oocyte leading cohort (LC-H) with corresponding phases of oocyte development. A: Oocyte phases 3, 4A, 4B and 4C were combined as primary growth (PG) oocytes, and early (ECAO) - and late (LCAO) cortical alveoli oocytes and early vitellogenic oocytes (EVO) as secondary growth (SG) oocytes; B: Difference in LC-H between the various oocyte phases. Crossbars, open circles, opaque dots, transparent circles and horizonal dotted lines represents range, median, mean, outliers, individual sample points and the threshold between PG and SG oocytes (250 µm), respectively. The numbers in brackets denote the number of observations. All samples processed with both whole mount and histology were considered (n = 259).

3.1 REPRODUCTIVE EVENTS

Maturity dynamics based on whole mount

A steady increase in oocyte size could be observed in ovaries during the autumn months before the upcoming spawning season. The mean LC-W in maturing (> 250 µm) females increased progressively from 290 ± 37 µm in August up to 529 ± 94 in February. From October onwards, a gap was observed between the PG and SG oocytes, becoming increasingly conspicuous by November, separating the non-developing females from those developing for the spawning season (Figure 10).

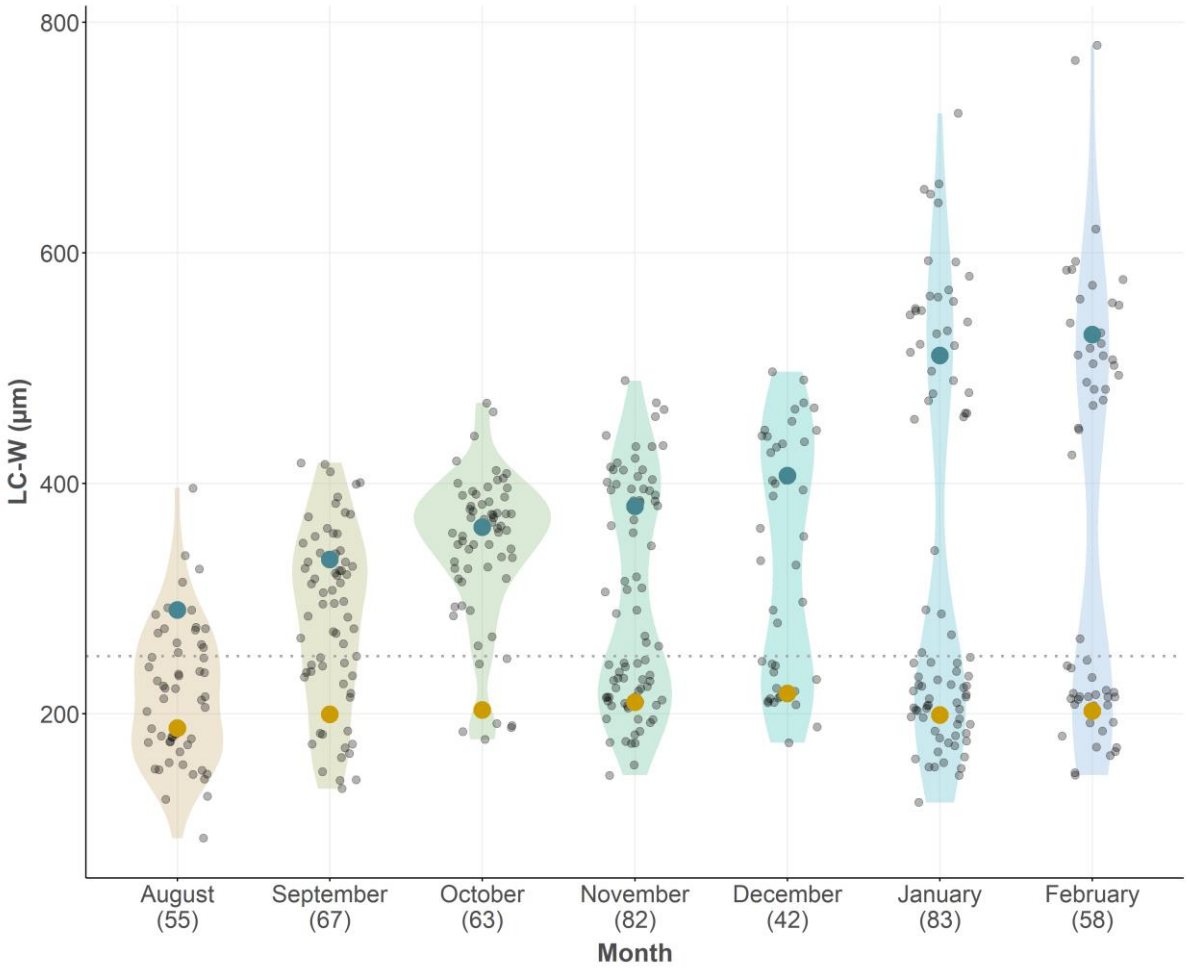

Figure 10. Distribution of the whole-mount oocyte leading cohort (LC-W) for each month prior to the onset of spawning in the NEA haddock (n = 450). The mean LC-W in maturing (blue circles) and non-developing (orange circles) are shown for each month. Transparent circles and the horizontal dotted line represent the individual sample points and the threshold between primary and secondary growth oocytes (250 µm), respectively. The numbers in brackets denote the number of observations per month.

The progression of oocyte development was evident already at the start of the sampling period in August, when 29 % of 55 females had progressed into SG oocytes (Figure 11). Further analysis showed that non-developing females (< 250 µm) were on average 11.5 cm smaller (total length) and 1.7 years younger compared to maturing females (unpaired two-sample t-test, df = 448, $p < 0.001$; Table 5). This biometric discrepancy was evident as females between 30 - 49 cm showed significantly lower increase in LC-W over time compared to females > 60 cm (two-way ANCOVA, df = 440, $p < 0.001$; Appendix C.2). Females between 40 - 49 cm (40 % of fish sampled) exhibited high variability in LC-W across the sampling period due to the large proportion of non-developing females within this length group from mid-October onwards. Furthermore, day length did not appear to have any noticable impact on oocyte growth, as no abrupt increase in LC-W could be observed following the autumn equinox.

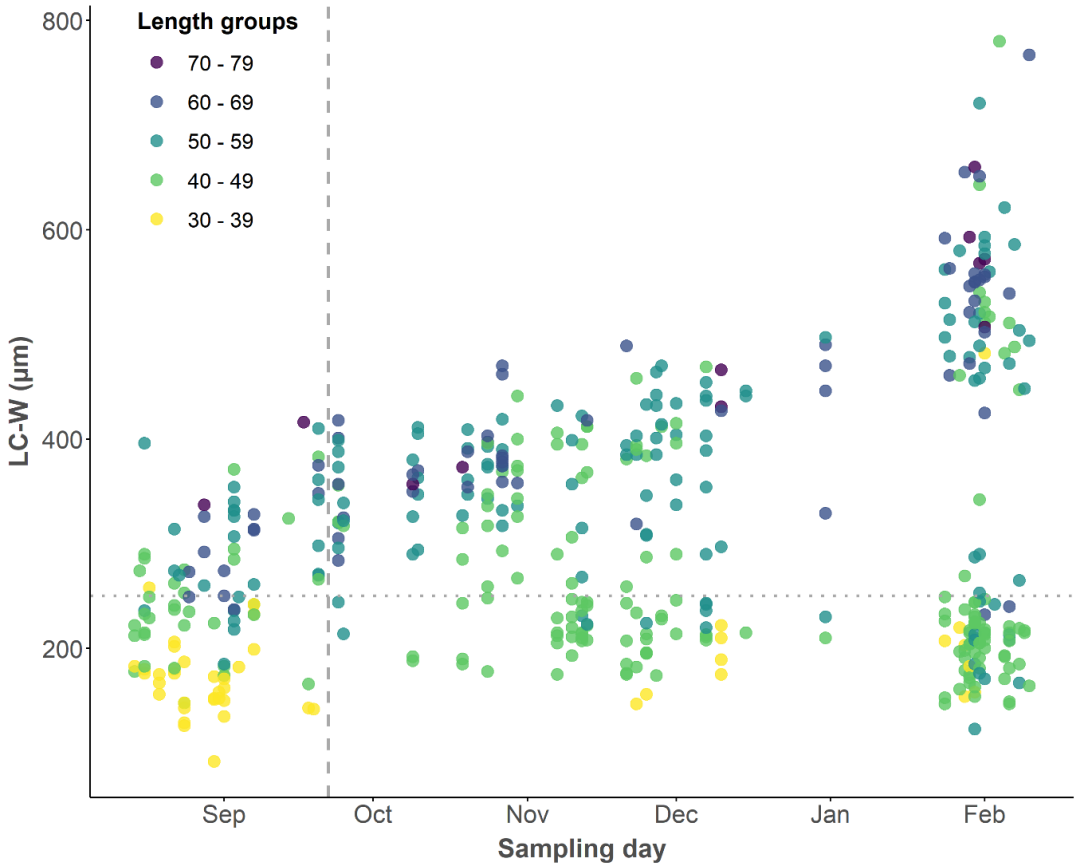

Figure 11. Development of the whole-mount oocyte leading cohort (LC-W) during the reproductive cycle (13 August 2020 - 10 February 2021) prior to the spawning season in NEA haddock (n = 450). Colours denote the five total length groups. The dotted horizontal line and the vertical dashed line represent the separation of non-developing and maturing females (250 µm), and the time of autumn equinox (set at September 22), respectively.

Table 5. The difference in total length and age between maturing and non-developing females, examined with an unpaired two-sample t-test.

PREDICTOR VARIABLE (Maturity category)	RESPONSE VARIABLE	df = 448		
		Mean ± SD	*t-value*	*p-value*
Non-developing	Age	4.3 ± 0.96	- 12.503	**< 0.001**
Maturing		6.0 ± 1.87		
Non-developing	Total length	44.8 ± 6.62	-16.615	**< 0.001**
Maturing		56.3 ± 8.10		

Ovary development

The somatic gonadosomatic index (GSI_s) of non-developing females showed a subtle increase from August (0.55 ± 0.22 %) to October (0.87 ± 0.31 %), but then sequentially decreased in the following months (Figure 12). Maturing females generally exhibited large variability in GSI_s, with some females possessing very low values in October and November. Nevertheless, maturing females had significantly higher GSI_s compared to non-developing females from September onwards (two-way ANOVA, df = 429, $p < 0.001$; Appendix C.3) with the differences being largest in January and February.

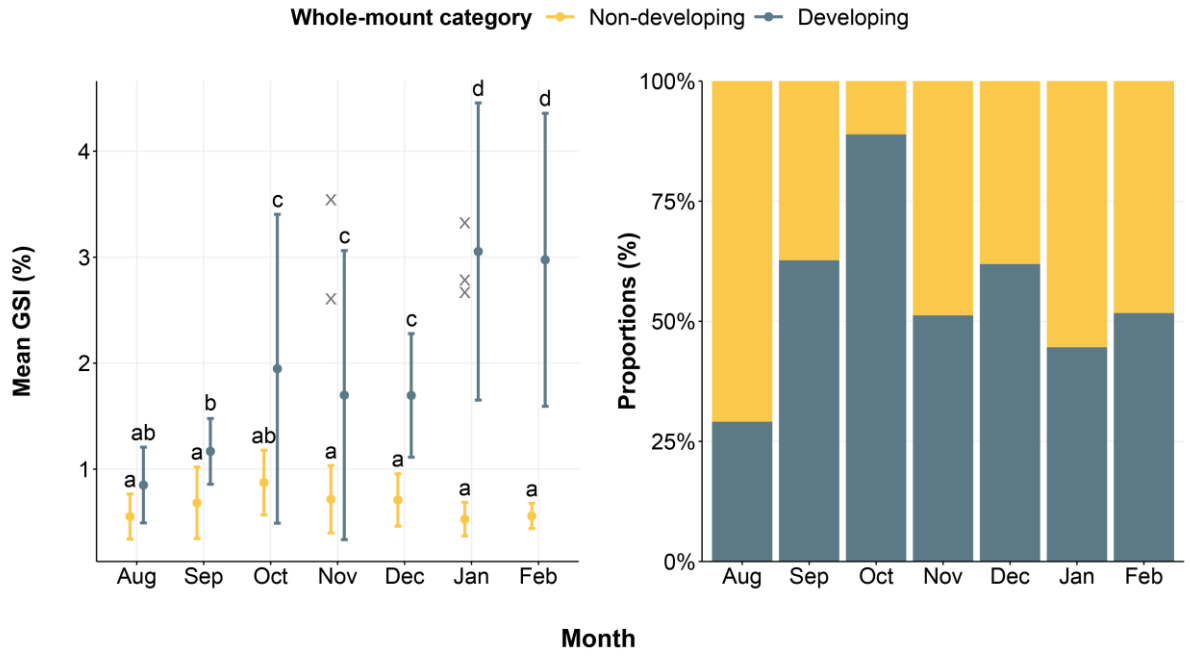

Figure 12. The mean somatic gonadosomatic index (GSI_s) and proportions of non-developing (yellow) and maturing (blue) females for each sampling month (August 2020 to February 2021) (n = 442). Closed circles and error bars represent the mean and standard deviation. Four samples were removed due to missing values of gonad weight. Crosses denote samples that were assumed to be measuring errors and removed from statistical analysis based on the 1.7 % GSI_s threshold separating maturing and non-developing females (see Material and Methods). Letters (letters a to d) above the error bars indicate the compact letter display of the statistically significant different groups in the two-way ANOVA after a post hoc test for multiple comparisons of groups.

Maturity dynamics based on histological analysis

Oocyte leading cohort

A a subsample of females collected during the reproductive cycle (from August 2020 to February 2021) was successfully separated into categories based on their histological maturity status as either immature (n = 45), skipping (n = 42) or maturing (n = 93) for the upcoming spawning season. A fourth category, uncertain (n = 29), was adopted whenever there was uncertainty in classification of three main categories and was excluded from further analysis. The change in LC-W over time was dependent on histological maturity category, where maturing females had a significantly steeper increase in LC-W over the sampling period compared to immature and skipping individuals (two-way ANCOVA, df = 174, $p < 0.001$; Figure 13, Appendix C.4).

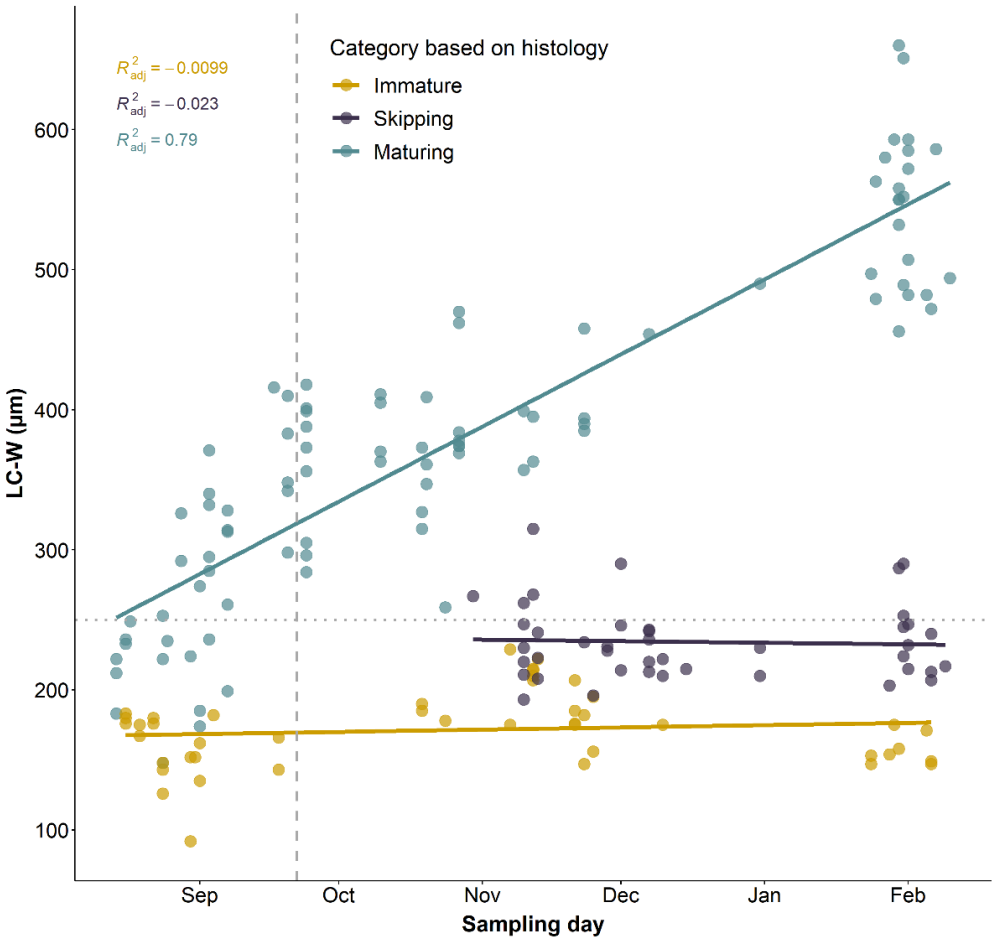

Figure 13. Development of whole-mount oocyte leading cohort (LC-W) over the sampling period for histological maturity categories: immature, skipping, maturing females (n = 180). The adjusted coefficient of determination (R^2_{adj}) denotes the goodness of fit of regression lines. The dotted horizontal line and the vertical dashed line represent the threshold between primary and secondary growth oocytes (250 µm), and the time of autumn equinox (set at September 22), respectively.

No significant increase in LC-W was detected for immature and skippers over the sampling period, although skipping females did possess significantly higher LC-W as such compared to immature females irrespective of sampling day (unpaired two-sample t-test, $p < 0.001$; Appendix C.5).

Further analysis showed that there was a tendency for larger, maturing females to exhibit higher LC-W sizes compared to smaller, maturing females (Figure 14) (multiple linear regression, df = 90, $p < 0.001$; Appendix C.6).

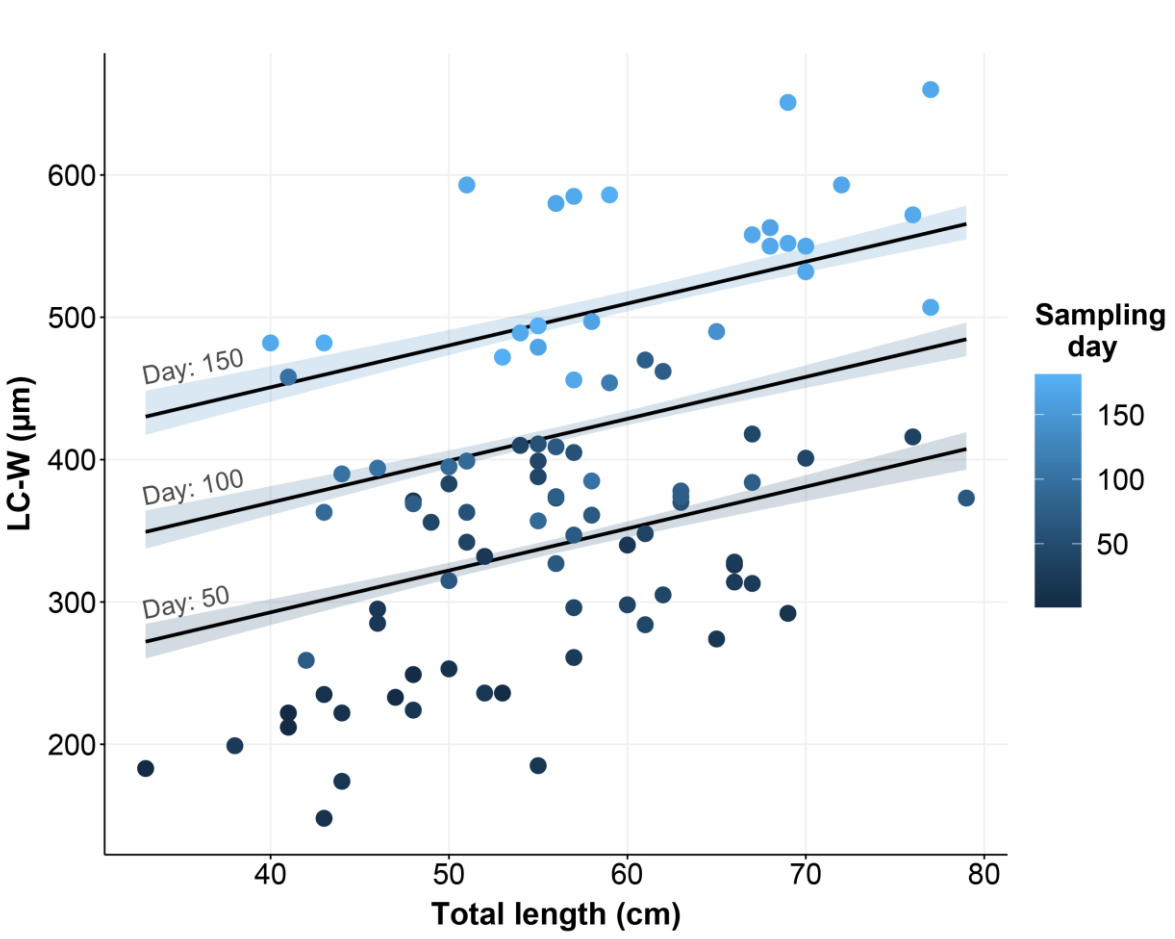

Figure 14. Relationship between female total length and whole-mount oocyte leading cohort (LC-W) when controlling for time (multiple regression), in females histologically staged as maturing (n = 93). Regression lines represent the correlation between LC-W and female length at sampling day 50 (early October), 100 (late November) and 150 (early January) (*slope* = 2.94, $p < 0.001$). Female total length and sampling day explained 84.6 % of the variability in LC-W.

Age and size of females were compared to detect potential differences among the maturity categories. As expected, immature females comprised the largest portion of the youngest and smallest individuals, while skippers were most prominent at intermediate sizes and ages. The proportion of maturing females increased with with increasing age and total length, finally comprising all females > 9 years and > 65 cm length (Figure 15). A significant difference in age and total length was further detected between the three maturity categories, where immature (3.6 ± 0.6 years; 39.4 ± 5.72 cm) < skipping (4.8 ± 1.1 years; 49.2 ± 5.79 cm) < maturing (6.3 ± 2.4 years; 56.4 ± 10.0 cm; Table 6).

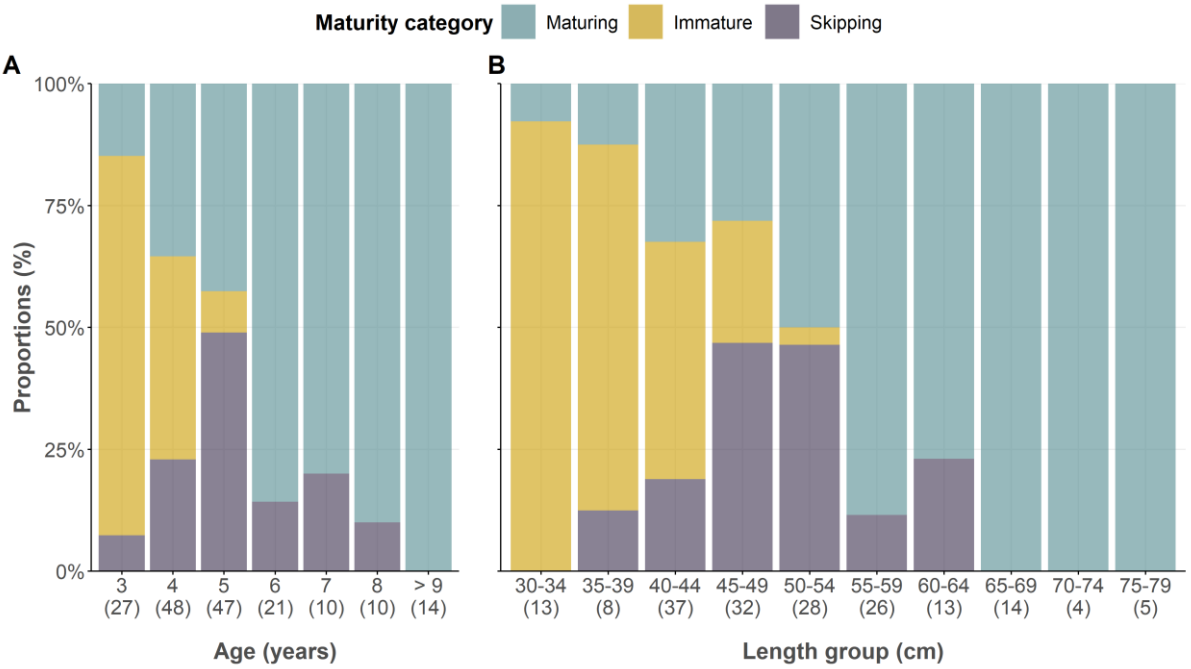

Figure 15. The proportion of maturing (blue), immature (yellow) and skipping (violet) females by age (A) and length group (B) during the sampling period. Numbers in brackets denotes the number of observations per age increment and length group.

Table 6. Difference in total length and age between the three histological maturity categories: immature, skipping and maturing females with a one-way ANOVA and Tukey HSD-test. Females with missing values on age (n = 3) were not included.

PREDICTOR VARIABLE	RESPONSE VARIABLES					
MATURITY CATEGORY	TOTAL LENGTH $F_{2,177}$ = 65.13			AGE $F_{2,174}$ = 33.87		
	Estimate ± SE	*t-value*	*p-value*	Estimate ± SE	*t-value*	*p-value*
Skipping - Immature	9.7 ± 1.77	5.49	**< 0.001**	1.20 ± 0.39	3.026	**0.008**
Maturing - Immature	16.9 ± 1.49	11.35	**< 0.001**	2.68 ± 0.33	8.020	**< 0.001**
Maturing - Skipping	7.3 ± 1.53	4.75	**< 0.001**	1.49 ± 0.34	4.361	**< 0.001**

Oocyte phase development

The monthly development of the most advanced oocyte phases showed that commitment to maturation could be observed already in August by the presence of early cortical alveoli oocytes (ECAO) (Figure 16). The ECAO phase exhibited a wide range of LC-H sizes, occasionally falling well below the 250 µm threshold between PG and SG oocytes in the subsequent months. Early vitellogenic oocyte (EVO) was first observed in October, marking a transition into vitellogenesis at LC-H of 400 µm. By January, both ECAO and late cortical alveoli oocyte (LCAO) phases had all transitioned into vitellogenic oocytes and was no longer present in ovary samples. The only exception was one skipping female in January undergoing cortical alveoli-atresia, but still possessing some intact (arrested) cortical alveoli oocytes. Finally, the late vitellogenic oocyte (LVO) phase appeared in January at LC-H of ~ 500 µm.

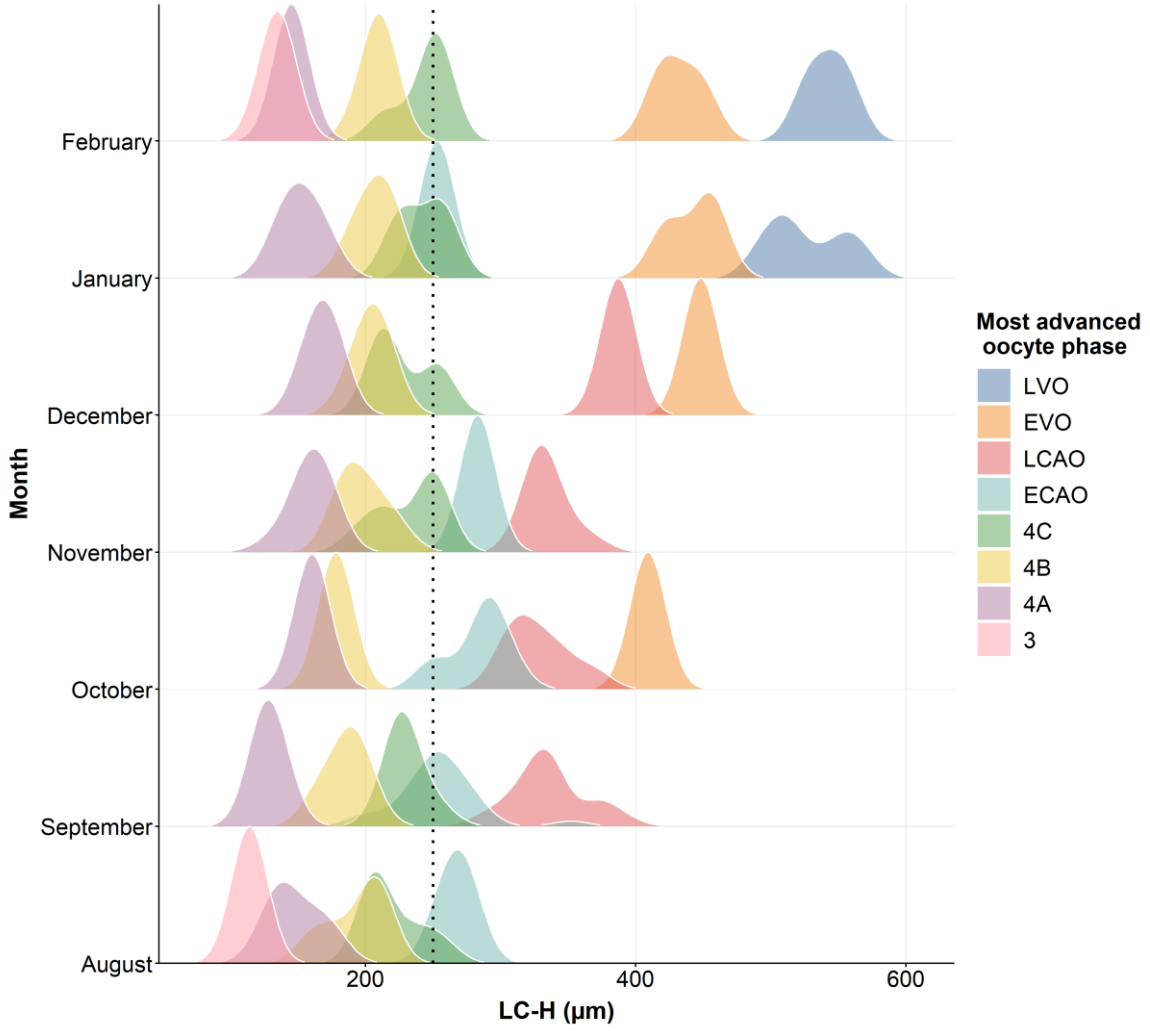

Figure 16. The monthly progression of the most advanced oocyte phases in relation to oocyte leading cohort (LC-H) as observed in histologically sectioned ovaries (n = 180). The vertical dashed line represents the threshold between primary and secondary growth oocytes (250 µm).

Histological analysis further showed a distinct difference in oocyte phases exhibited by the three maturity categories (Figure 17). Maturing females showed a steady transition starting with primarily PG phase oocytes early in the sampling period and ending with LVO in February. Of the 13 maturing females identified in August, 4 had reached the ECAO phase. By September, 70.5 % of 34 females had progressed to ECAO and LCAO phases. Approximately five weeks following the autumn equinox (set at September 22), yolk granules appeared in the cytoplasm of a 62-cm female (age 6), entering the EVO phase with LC-H at 392 µm. By January, all maturing females had transitioned into vitellogenesis.

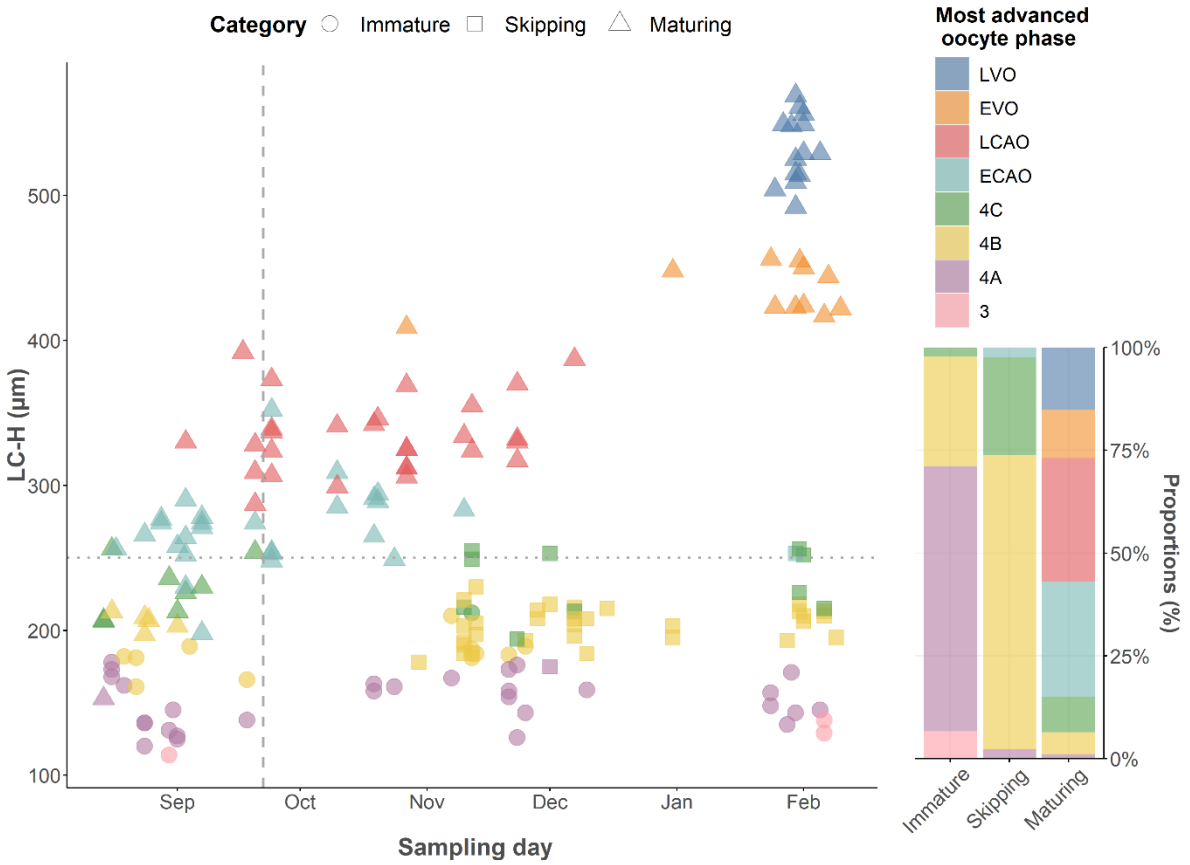

Figure 17. Development of the histological oocyte leading cohort (LC-H) during the reproductive cycle (13 August 2020 - 10 February 2021) in relation to the most advanced oocyte phase in NEA haddock (n = 180). Colours and shapes represent the phases of oocyte development and histological maturity categories, respectively. Phases 3, 4A, 4B and 4C are collectively primary growth oocytes, while early (ECAO) - and late (LCAO) cortical alveoli, early (EVO) and late (LVO) vitellogenic oocytes comprise the secondary growth oocytes. The dotted horizontal line and the vertical dashed line represent the threshold between primary and secondary growth oocytes (250 µm), and the time of autumn equinox (set at 22 September), respectively.

On the contrary, immature and skipping females exhibited little change in oocyte phases over time. The majority of immature females sampled (93.3 %) showed sign of early puberty, as indicated by the presence of the circumnuclear ring (see above), with a large proportion being

in the 4A phase. Skipping females was first identified late in October, with the vast majority possessing 4B phase oocytes as well as cortical alveoli atresia (CAO-atresia). The prevalence of atresia was 36.7 % (of 180 females) across the three maturity categories. Of these, 4.5 % were immature, 37.8 % maturing and 57.7 % was skipping (see below). Notably, the intensity of atresia was very low (< 5 %) for immature and maturing females.

Occurrence of skipped spawning

Skipping females was first identified in the end of October by the presence of mass atresia (>50 %) of cortical alveoli oocytes (CAO) at the late alpha (Lα) stage (Figure 18). From November onwards, the occurrence of skippers became more frequent and was observed in all subsequent months.

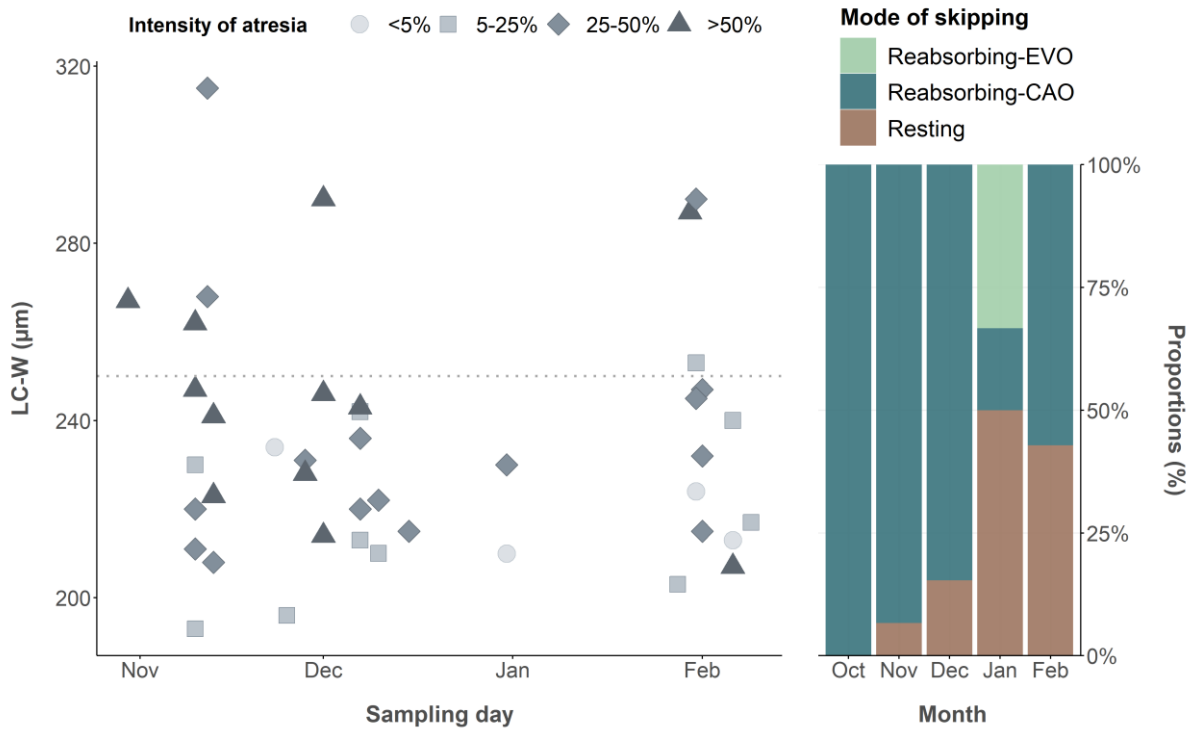

Figure 18. Whole-mount oocyte leading cohort size (LC-W) over time in relation to the intensity of atresia observed in reabsorbing cortical alveoli (reabsorbing-CAO), reabsorbing early vitellogenic oocyte (reabsorbing-EVO), and resting skippers (n = 42). The dotted horizontal line represents the threshold between primary and secondary growth oocytes (250 µm).

In total, 42 skipping females were identified during the present sampling period. Of these, the majority (73.8 %) was identified as reabsorbing-CAO skippers, exhibiting reabsorption of all CAOs, and 21.4 % were classified as resting skippers by the presence of advanced PG oocytes and occasionally, very low intensity (< 5 %) of atretic follicles. The remaining two females were identified as reabsorbing-EVO skippers, possessing atretic EVOs at the Lα stage. Females

collected in end of October to the start of December, showed the highest intensity of atresia, with 40 % of 25 females exhibiting reabsorption > 50 %.

Diameter measurements of atretic follicles were used to examine whether reabsorbing-CAO skippers undergo reabsorption simultaneously or over a prolonged period (i.e. if there is a specific time window at which they decide to skip spawning). Results showed that the vast majority of skipping females possessed both Lα and β+γ atresia throughout the sampling period, with no evident reduction in atretic follicle size over time, indicating that reabsorption may occur over a prolonged period (Figure 19).

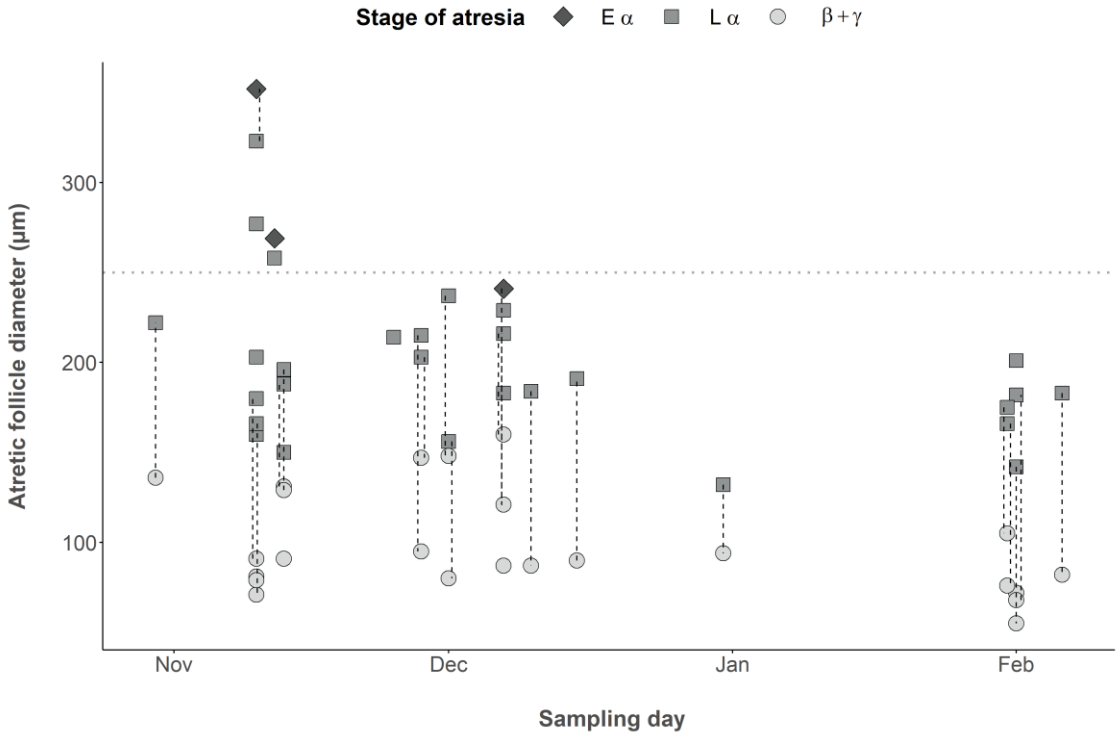

Figure 19. Progression of atretic follicles into early alpha (Eα), late alpha (Lα) and beta + gamma (β+γ) stages in reabsorbing-cortical alveoli oocyte (CAO) skippers over the sampling period (October 2020 - February 2021). The atretic follicle diameter was calculated as the average of 5 measurements for each atretic stage when present in the ovary subsample. Only cortical alveoli atretic follicles were measured in Eα and Lα stages, while the type of oocyte precursor of β+γ could not be determined with certainty but assumed to have been in the cortical alveoli phase when observed in conjunction with cortical alveoli α atresia. The dashed vertical lines between stages denotes measurements of different stages in the same female, and the dotted horizontal line represents the threshold between primary and secondary growth oocytes (250 µm). Finally, atretic follicles were measured in a total of 31 females.

Ovary development and energy proxies

Comparisons of ovary development between histological maturity categories showed that maturing females had significantly higher GSI_s from October onwards compared to immature females, and from December onwards compared to skipping females (two-way ANOVA, df = 155, $p < 0.001$; Figure 20; Appendix C.7). Moreover, the GSI_s in skipping females showed a steady decrease from 1.48 % in October to 0.63 % in February. The proxy for energy storage (somatic hepatosomatic index, HSI_s), was generally lower in skipping and immature females compared to those maturing, but a significant difference was only detected in January (two-way ANOVA, df = 157, $p < 0.001$), where immature (3.0 ± 0.87 %) and skipping (4.3 ± 1.20 %) < maturing (7.0 ± 1.41 %). No differences in HSI_s could be detected between skipping and immature females in any of the other months. Moreover, histological maturity category and sampling month could only explain 0.05 % of the variability in body condition (Fulton's condition factor, K), and no difference could be detected between categories (one-way ANOVA, df = 171, $p = 0.113$; Appendix C.8) nor between months ($p = 0.06$).

To further examine whether other factors than maturity category and months could explain the observed variability in HSI_s and K, a visual inspection of the spatial variability in these parameters were conducted, confirming that females distributed in the north-western Barents Sea showed somewhat higher values of HSI_s and K compared to the south-eastern region (Appendix C.9 and 10).

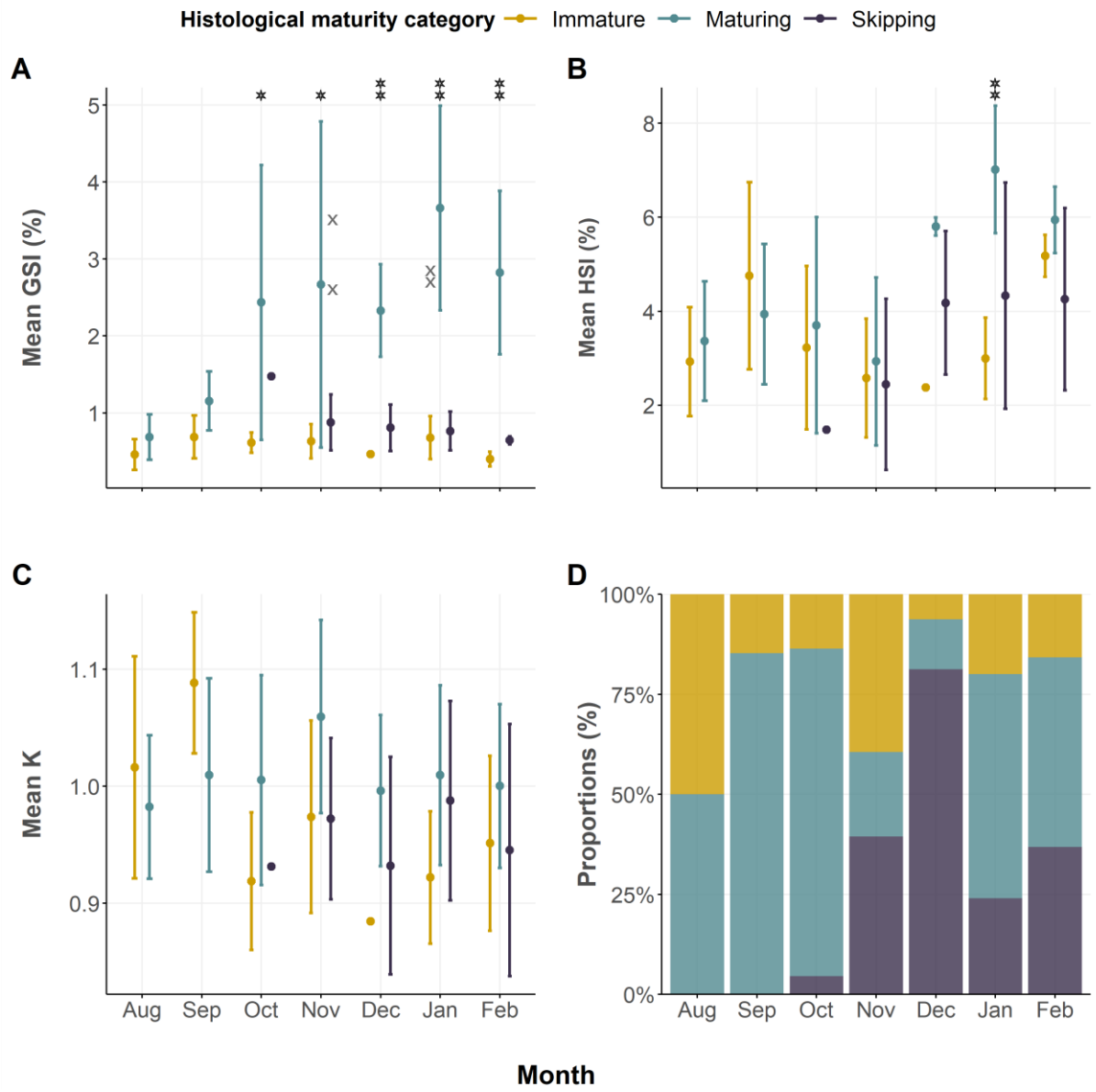

Figure 20. Biometric information for all females histologically analysed as immature (yellow), maturing (blue) and skipping (violet) over sampling months (August 2020 to February 2021). A: The mean somatic gonadosomatic index, GSI_s; B: somatic hepatosomatic index, HSI_s; C: Fulton's condition factor, K; D: monthly proportions of histological maturity categories. Closed circles and error bars represent the mean and standard deviation of measurements. Crosses denote samples that were assumed to be measuring errors and removed from statistical analysis, based on the 1.7 % GSI_s threshold separating maturing and non-developing females (see Material and Methods). Stars above boxes for the maturing category indicate significantly higher GSI_s or HSI_s values compared to immature (one star) and both immature and skipping females (two stars).

3.2 EVALUATION OF MACROSCOPIC MATURITY STAGES DURING THE WINTER SURVEY

To examine the degree of misclassification in maturity staging, macroscopic estimates was cross-examined with histological staging consulting the Winter Survey samples. Results showed that the correspondence between macroscopic and histological maturity stage estimations was high for maturing and spent[2] individuals, but less so for individuals staged as immature (Figure 21). Of the 41 females macroscopically staged as immature, only 24.4 % was classified correctly according to histological analysis. Histology confirmed that a large proportion of these females (56.1 %) was in fact skipping individuals, while the remaining 19.5 % could not be classified with certainty (see Materials and Methods). For individuals macroscopically staged as maturing, one female was found to be skipping by the presence of CAO-atresia, while the rest agreed with histological analysis. Of the 19 females macroscopically staged as spent, 18 were skipping according to histological analysis, while one female was identified as immature. Finally, the two females macroscopically staged as uncertain were both found to be skipping according to histology.

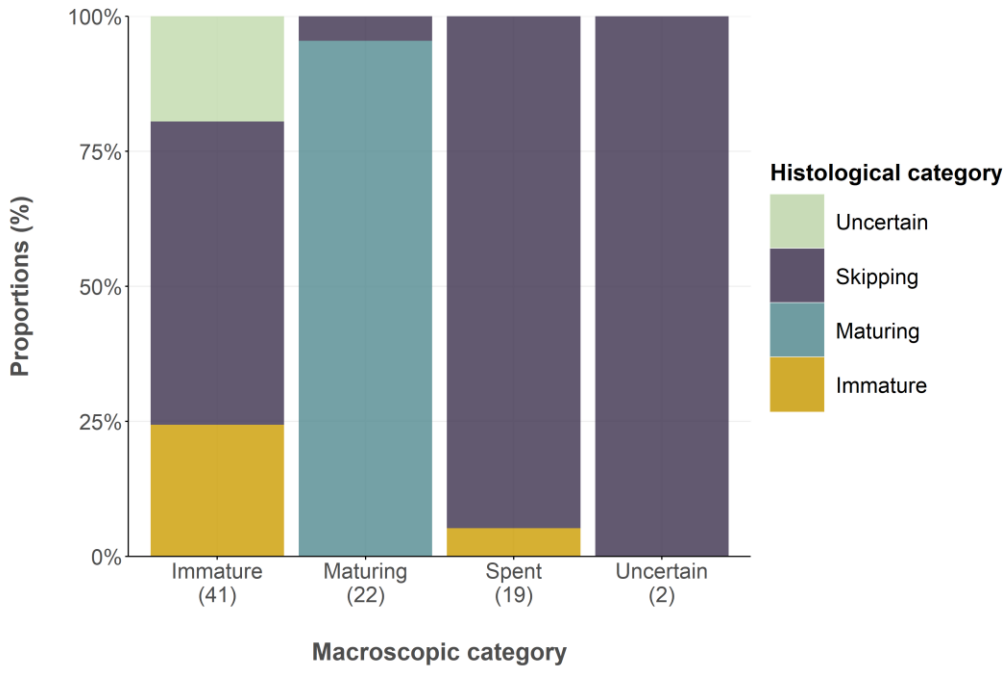

Figure 21. Correspondence between macroscopic and histological maturity stage estimates for NEA haddock samples collected during the Winter Survey 2020 and 2021. The numbers in brackets denote the number of observations per each maturity category.

[2] The macroscopic 'spent' stage (used in maturity stage estimation during annual surveys at IMR) refer to individuals with non-developing gonads that appear to have spawned before (i.e. skipping individuals; see Materials and Method section).

3.3 SEPARATION OF IMMATURE AND SKIPPING FEMALES BASED ON WHOLE MOUNT

The apparent difficulty in accurately identifying immature and skipping individuals during the Winter Survey highlights the need for alternative ways of quickly discriminate between the two categories. In an attempt to do so, immature (n = 12) and skipping (n = 46) females from the Winter Survey 2020 and 2021[3] were examined in more detail to assess potential differences in oocyte size frequency distributions (OSFD) exhibited by the two categories.

Results showed that both immature and skipping females exhibited unimodal OSFD, containing mainly PG oocytes < 250 µm. A comparison of shape of the OSFD between the two categories showed a significant difference in both skewness (unpaired t-test, df = 56, p = 0.002) and kurtosis (p = 0.027), where skippers on average had 0.52 higher value of skewness and 2.06 higher value of kurtosis compared to immature females (Table 7). Immature females exhibited a higher frequency of the smallest PG oocytes (50 - 80 µm range), with little advancement beyond 150 µm (Figure 22). Meanwhile, skipping females exhibited a wider and more positively skewed distribution (for individual OSFDs, see Appendix C.11 and 12).

Table 7. The difference in mean skewness and kurtosis between skipping (n = 46) and immature (n = 12) females from the Winter Survey 2020 and 2021 with an unpaired two-sample t-test.

PREDICTOR VARIABLE (Maturity category)	RESPONSE VARIABLE	df = 54		
		Mean ± SD	t-value	p-value
Skipping	Skewness	1.26 ± 0.53	-3.187	**0.002**
Immature		0.74 ± 0.46		
Skipping	Kurtosis	5.57 ± 3.08	-2.56	**0.027**
Immature		3.51 ± 1.11		

Although differences in OSFD between immature and skipping females were detected, the dissimilarity was relatively small, likely owing to the variability in OSFD within the skipping category (Appendix C.13). Three different modes of skipping were observed in samples collected from the Winter Survey 2020: resting (n = 24), reabsorbing-CAO (n = 20) and reabsorbing-EVO (n = 2) skippers. Notably, resting skippers could not be distinguished from immature females based on skewness (one-way ANOVA, df = 54, p = 0.208; Figure 23

[3] Eight immature females from the the Winter Survey 2021 were included, due to the insufficient sample size of immature females from Winter Survey 2020.

Appendix C.14) and kurtosis (p = 0.549), making it virtually impossible to confidently separate these two categories when looking at individual samples.

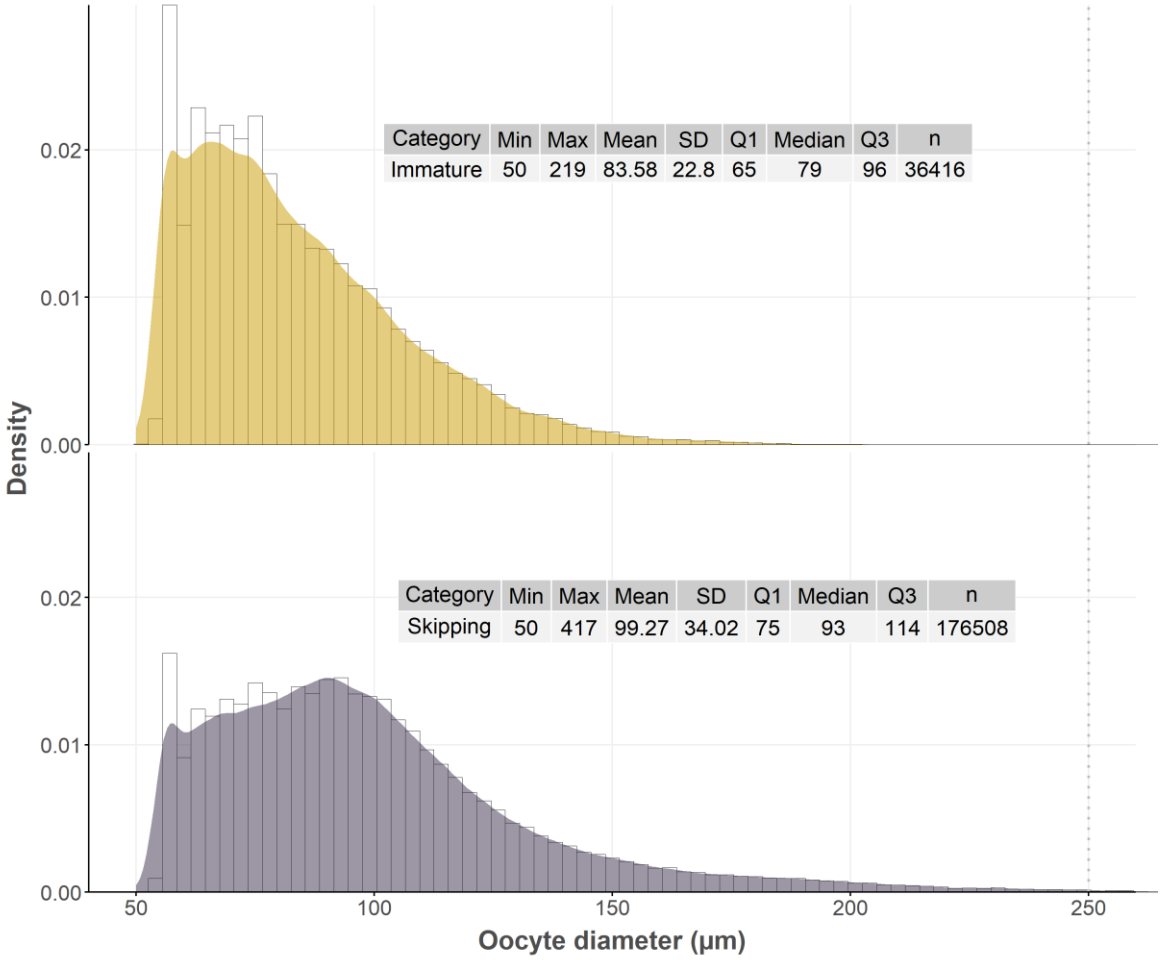

Figure 22. Oocyte size frequency distributions of immature (yellow) and skipping (violet) females during the Winter Survey 2020 and 2021. Histograms are overlayed with a smoothed density function for visualization of the distributions. Descriptive statistics for the OSFD are shown in each panel as the minimum and maximum (Min, Max) oocyte diameter measured, the mean and standard deviation (Mean, SD) and the interquartile range (Q1: 25th quartile, Median, Q3: 75th quartile) of the distribution and finally, the number of oocytes measured per category (n). The vertical dotted line represents the threshold between primary and secondary growth oocytes (250 µm), respectively.

On another note, significant differences were detected between immature females and the two skipping modes (reabsorbing-EVO skippers were removed from the analysis due to insufficient sample size) in terms of GSI_s and LC-W (Figure 23; Appendix C.15), being potentially important measures of comparison when skewness and kurtosis do not suffice.

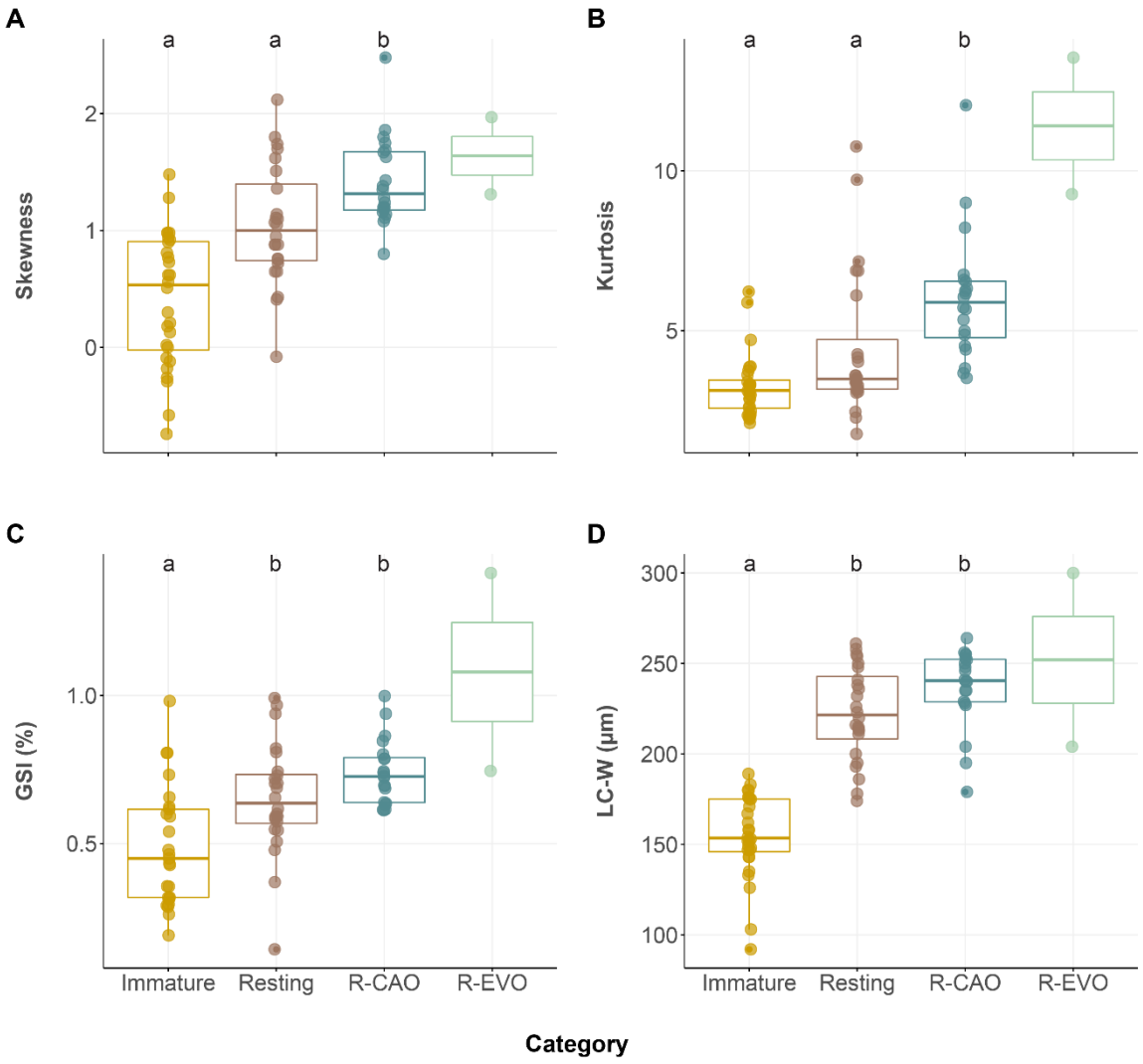

Figure 23. Difference in A: skewness; B: kurtosis; C: somatic gonadosomatic index (GSI_s) and; D: whole-mount leading oocyte cohort (LC-W) between immature (yellow) and the three modes of skipped spawning: resting (brown), reabsorbing-CAO (R-CAO; blue) and reabsorbing-EVO (R-EVO; green) skippers. Letters (letters a and b) above the boxes indicate the compact letter display of the statistically significant different groups in the one-way ANOVA after a post hoc test for multiple comparisons of groups. Reabsorbing-EVO skippers were excluded from the statistical analysis due to insufficient sample size.

It is worth mentioning that, of the 72 non-developing ovary samples histologically analysed during the Winter Survey 2020, 22 samples could not be allocated to any histological maturity category with certainty (i.e. immature or skipping). Notably, this relatively large portion of 'uncertain' females would likely have obscured the the present OSFDs and biometric comparisons of immature and skipping females if included in the data analysis. Many of the uncertain females possessed normally distributed OSFDs (and thereby lower skewness and kurtosis), and slightly higher LC-W sizes compared to immatures. They were also in-between immature and skipping females in terms of age and total length (Appendix C.16, 17 and 18).

Seasonal variability in oocyte size frequency distribution

The OSFD of immature and skipping females displayed some variability during the reproductive cycle (Figure 24). Development of oocytes could be seen in immature females (recruit spawners) in August by a reduction of the smallest oocyte size ranges as the females started to develop, resulting in a more normally distributed OSFD. After October, a sequential reduction in the mean OSFD could be observed, and a similar trend was also evident in skipping females. From November onwards, both categories displayed a higher frequency of the smallest PG oocytes, resulting in the right skewed distribution observed during the Winter Survey.

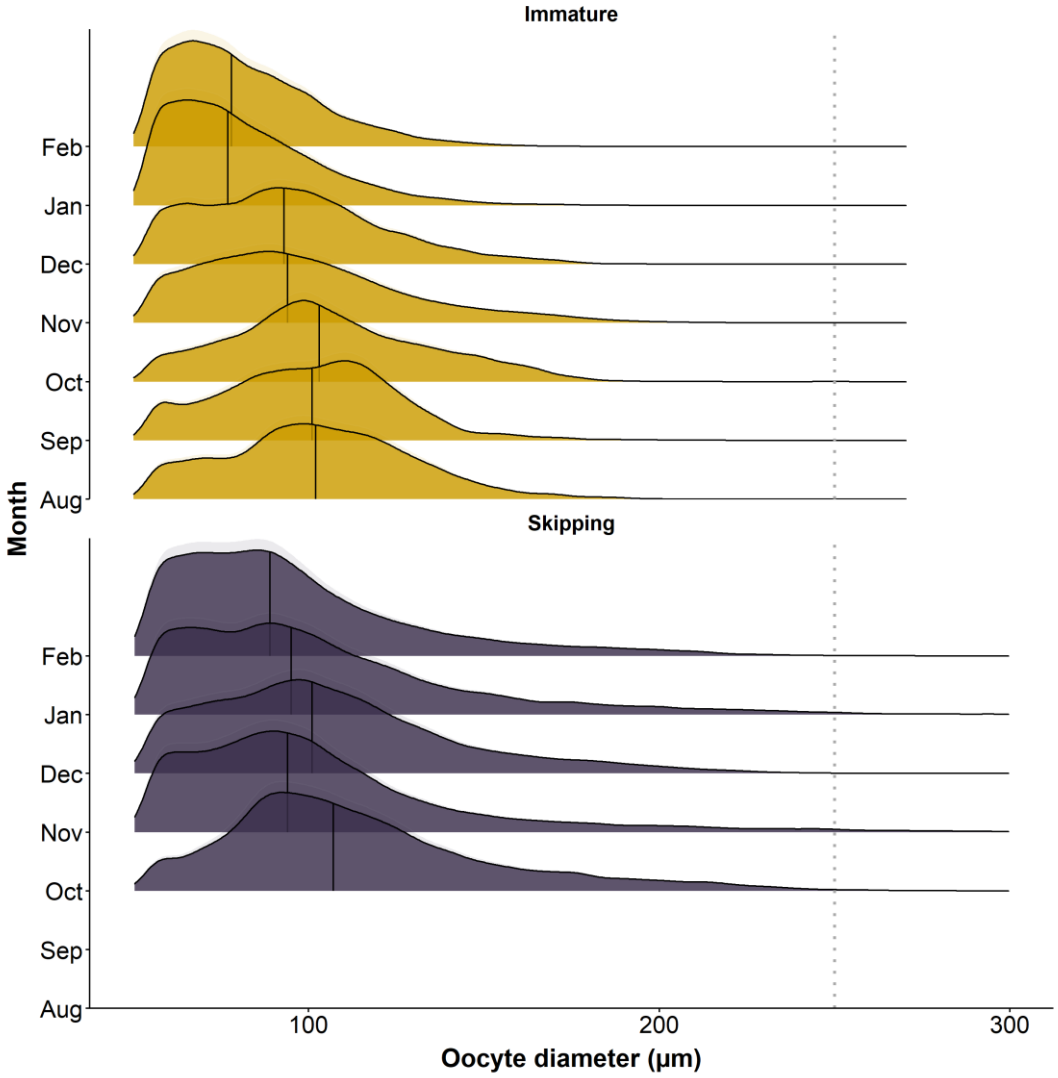

Figure 24. Monthly change in oocyte size frequency distribution in immature and skipping females collected during the reproductive cycle (13 August 2020 - 10 February 2021) prior to the spawning season. The vertical line within each oocyte size frequency distribution represents the mean oocyte diameter, and the dotted vertical line denote the threshold between primary and secondary growth oocytes (250 µm).

4 DISCUSSION

The reproductive success of individuals is what allows a population to replenish and persist over time, and at the population level it depends on both the total reproductive output of all individuals (i.e. egg production) and the processes affecting the survival of that output. (Lowerre-Barbieri et al. 2011). An in-depth understanding of the initial biological processes leading up to female fecundity and thus egg production, is key information for defining the stock reproductive potential (Trippel 1999). Although a few studies have been undertaken in regard to the Northeast Arctic (NEA) haddock oocyte and maturity dynamics (Skjæraasen et al. 2013, 2015), central aspects of its reproductive cycle are presently poorly understood and require closer attention. Thus, the aim of the present thesis was to track the time course of oocyte development and skipped spawning through the reproductive cycle, by means of image and histological analysis, and to evaluate the accuracy of maturity data used in assessment of the haddock. Results showed that the haddock starts production of cortical alveoli early in the autumn (August), and enter vitellogenesis approximately 5 weeks following the autumn equinox (late October). The majority of skipping females were undergoing mass atresia of cortical alveoli oocytes (CAO), and were significantly younger and smaller compared to maturing females. Evaluation of macroscopic stage estimates conducted annually during the Winter Survey revealed a high level of accuracy in correctly staging maturing females but was not optimal for estimating immature vs skipping females. Accordingly, the whole-mount derived oocyte size frequency distributions (OSFD) used for rapid separation of these two categories, did not offer an adequately reliable way to discriminate immature and skipping females in the present study.

4.1 Timing of reproductive commitment

Image analysis (whole mount) confirmed that nearly a third of females sampled in August had developed secondary growth oocytes (>250 µm), indicating that the first decision window to commence preparation of oocyte development ought to be prior to August. These findings are in line with the coupling of photoperiod with maturity decision that has been demonstrated in the North Sea haddock (Martin-Robichaud and Berlinsky 2004; Davie et al. 2007), with June summer solstice proposed as trigger for a first-decision window to start preparation of oocyte development. The somatic gonadosomatic index (GSI_s) showed an abrupt increase by October, consistent with the observed oocyte size development during this time. The whole-mount oocyte leading cohort (LC-W) also showed a steady increase thereafter, with a few females

reaching a maximum LC-W of 780 µm at the end of the sampling period in February, indicating proximity to the spawning season (Skjæraasen et al. 2013). Females that did not possess secondary growth oocytes (non-developing females), evidently belonged to a different demographic category, shown by being significantly smaller and younger compared to maturing females developing for the spawning season.

Histological analysis confirmed that the early cortical alveoli oocyte (CAO) phase was present in haddock ovaries already in August, as opposed to in September, which has been demonstrated in the NEA cod (*Gadus morhua*) (Skjæraasen et al. 2009, 2010). Even so, the onset of vitellogenesis appeared to be later in the autumn compared to cod, which commence deposition of yolk granules approximately two weeks following the autumn equinox (Skjæraasen et al. 2009; Kjesbu et al. 2010). The first appearance of early vitellogenic oocyte (EVO) in the present study (October 27th) closely resembles that of a recent study of the North Sea saithe (Skjæraasen et al. 2017), demonstrating entrance into vitellogenesis by late October - early November, nearly a month later than the cod. Skjæraasen et al. (2017) speculated whether the laboratory settings associated with their study could have shifted the timing of vitellogenesis, however, along with the results from the present study, this discrepancy could indicate potential real species differences in the onset of vitellogenesis between these gadoids. In terms of timing and duration of the spawning season, differences in the onset of vitellogenesis seems reasonable, as the haddock spawns somewhat later than the cod (Bergstad et al. 1987), although there exists a great deal of uncertainty around the timing of spawning in the haddock. Nevertheless, the reason why the haddock would progress into CAO earlier than the cod, despite entering vitellogenesis later and subsequently spawning later in the spring, is perhaps not so intuitive.

The CAO phase persisted from August through December, indicating that (i) this phase has a long duration in the haddock, (ii) these oocytes could be remnants of CAOs arrested in skipping females from the previous reproductive cycle, or (iii) that there exists substantial individual variability in the initial timing and development of oogenesis. If the latter is true, the individual timing of oocyte development and spawning may vary by haddock age and/or size (Wright and Trippel 2009). Firstly, immature females developing for their first spawning season (recruit spawners) may start the formation of CAO later in the autumn compared to already sexually mature females (repeat spawners). For instance, Tobin et al. (2010) observed that CAO appeared first in October in recruit spawning North Sea haddock, followed by deposition of yolk granules as late as November and December. Similar results have been demonstrated for

recruit spawners of cultured Atlantic cod, showing first commitment to maturity by the production of CAO following the autumn equinox (Kjesbu et al. 2011). Secondly, larger mature females may exhibit more advanced oocytes (higher LC-W) at a given time than smaller mature females. In the present study, LC-W in females histologically staged as maturing was positively correlated with female length when controlling for time (i.e. sampling day). Size-specific differences in LC-W have been demonstrated in the Atlantic cod (Skjæraasen et al. 2010; Kjesbu et al. 2010), but have not previously been documented in the NEA haddock (Skjæraasen et al. 2013), and may thus be a contributing factor to the long CAO phase observed in the present study. Furthermore, as the LC-W is closely related to the time of spawning (Kjesbu 1994), it could indicate that there is a tendency for larger females to start spawning earlier in the NEA haddock.

The underlying reasons for such demographic differences are unclear (Wright and Trippel 2009), although it has been suggested that a smaller and larger body size may exhibit different physiological responses to elevated water temperatures (Kjesbu et al. 2010). The size-specific difference in LC-W is presently small, but with future increases in sea water temperature this disparity could potentially become more pronounced. From a population aspect, the timing and duration of spawning is important as it affects the early environmental conditions experienced by the progeny, by either matching or mismatching the temporal overlap between the larvae and the zooplankton peak abundance in spring (Cushing 1990). Accordingly, the timing of oocyte development and subsequently, the timing of spawning, may have substantial bearing on survival of offspring and female reproductive success (Wright and Trippel 2009), comprising one of many factors potentially affecting year-class strength and recruitment variability in the haddock.

4.2 Occurrence of skipped spawning

The first evidence of reproductive interruption in the NEA haddock was observed in the end of October. Contrary to what has previously been reported for skipped spawning in the NEA haddock (Skjæraasen et al. 2015), the majority of skipping females separated from those maturing at the early or late CAO phases by undergoing massive atresia. Skjæraasen et al. (2015) reported resting (i.e. skipping females that do not advance beyond primary growth oocytes) as being the dominant mode (95.6 up to 98.8 % in 2009 - 2012) during the months from November to March, with the remaining proportions of skipping females classified as either reabsorbing-CAO or EVO. One possible explanation for the differences in allocation of skipping mode, could be that their study was conducted in January to March which is closer to

the spawning season, when cortical alveoli atresia (CA-atresia) could potentially have degenerated to the extent that they no longer could be observed. Although this is plausible, results from the present study showed that CA-atresia were prominent also in samples collected from January to early March (2020 and 2021 seasons pooled) although to a lower extent, indicating that differences in interpretation of atretic structures may be the cause of the disparity in allocation of skipping mode. Nevertheless, both field-caught and experimentally monitored cod have demonstrated similar results to the present study, where nearly all females underwent mass reabsorption after reaching the CAO phase (Rideout et al. 2000; Skjæraasen et al. 2009).

Only females that possessed unambiguous CA-atresia were classified as reabsorbing-CAO skippers in the present study. The degeneration of these atretic follicles to the β+γ stage may be the reason why resting skippers were more frequently found from December onwards. When the β+γ stages degenerate (shrink) further over time, they become increasingly challenging to distinguish from post-ovulatory follicles (POF). It is thus possible that a larger proportion of the resting females were in fact late reabsorbing-CAO skippers. Unexpectedly, CA-atresia in both Lα and β+γ stages could be observed in ovaries in all consecutive months following October. This finding is surprising in that atretic follicles often have a short lifetime (Kjesbu et al. 1991). Witthames et al (2010) demonstrated that the α atretic stage in the NEA cod lasted approximately 9.7 days at an ambient temperature of 4.5°C. However, their research was based on degeneration of vitellogenic oocytes containing yolk granules. It could thus be possible that degeneration is much longer for follicles that do not contain yolk, as the extraction of nutrients would be less important. Another possible explanation for the apparent long duration of CA-atresia could be that CAO get arrested for an extended period of time before degeneration commences (Rideout and Tomkiewicz 2011). Although caution should be taken when interpreting atretic follicle sizes (due to uncertainties associated with orientation of these structures when sectioning histological samples), the presence of these structures provide evidence that the females had advanced into CAO and then undergone reabsorption.

4.3 Mechanisms for skipped spawning

One of the main energetic costs associated with reproduction in teleost's is the sequestration of vitellogenin into developing oocytes (Tyler and Sumpter 1996) and additionally, for the NEA haddock, the lengthy migrations to spawning grounds (Bergstad et al. 1987). Two altering hypothesis has been proposed as mechanisms for skipped spawning: the 'energy-constrained' skipped spawning, where poor body condition is thought to inhibit sufficient accumulation of energy reserves to support oogenesis and ovary development, and 'life history-driven' skipped

spawning, which is based on trade-offs associated with energy allocation between growth, survival and reproduction (see below; Skjæraasen et al. 2020). A number of studies have found a link between low energy storage and skipped spawning in the NEA cod and haddock (Skjæraasen et al. 2009, 2012, 2015), where skipping individuals generally have exhibited lower energy reserves compared to females maturing for the spawning season. In the two latter studies however, data on energy storage were only available in the months after the decision to spawn or not was made (January – March). As the body condition and energy storage tend to vary among seasons according to variation in physiological processes, observing the level of female 'well-being' at the time of reproductive commitment, could potentially reveal underlying mechanisms causing some females to skip spawning. Results from the present study did not reveal any clear evidence that energy storage (somatic hepatosomatic index, HSI_s) nor body condition (Fulton's condition factor, K) were significantly lower at the time of reproductive commitment in skipping females (late October - early November). Generally, skipping females exhibited lower values of HSI_s and K compared to maturing females, but so did immature females. Notably, all three maturity categories generally exhibited high variability in K and HSI_s indicating that other factors than maturity status or temporal variability may have affected these parameters. For instance, females sampled in the south eastern Barents Sea appeared to exhibit lower values of HSI_s and K compared to females collected west of Spitsbergen, which could be related to lower food availability or less favourable oceanographic conditions in this region, as found in Eriksen et al. (2017). Thus, geographic variability could potentially mask any underlying drivers for skipped spawning related to energy reserves in the present study. Alternatively, Rideout et al (2005) suggested that the most appropriate time to collect data on condition and liver size would be immediately after the spawning season when post-spawning individuals are feeding to elevate lipid storage for the upcoming spawning season. Any failure to increase condition and energy storage during this time, could potentially cause the fish to skip their next spawning opportunity.

Although insufficient energy reserves provide one possible explanation for skipped spawning other studies have suggested skipping as an evolutionary adaptive trait to allocate more energy into body growth and thereby increase reproductive output in subsequent years (Jørgensen et al. 2006; Skjæraasen et al. 2009; Folkvord et al. 2014). Skipping females in the present study were on average 5 years old and 49 cm long, indicating that a considerable proportion of females that had completed their first spawning season as 4 year olds (Olsen et al. 2010), would have skipped their next spawning opportunity. A possible explanation for this observation could be

that recruit spawners may have difficulties in acquiring enough energy following their first spawning season to repeat the development process for next year's spawning opportunity. Demographic effects of skipped spawning have also been demonstrated previously in the NEA haddock (Skjæraasen et al. 2015) and other gadoids (Skjæraasen et al. 2012; Macchi et al. 2016), suggesting links to both energy constraints and life history theory.

The interruption of maturity prior to the onset of vitellogenesis and the start of the lengthy spawning migration, seem to be highly beneficial to conserve and divert energy into other physiological processes. However, the underlying reasons why females would advance to the CAO phase, rather than remain at the CNR phases (i.e. 4A, 4B, 4C), and then decide not to spawn, remains unclear. Though there seem to be a low energetic cost associated with deposition of cortical alveoli (i.e. endogenous vitellogenesis) (Wallace and Selman 1981). Notably, no skipping females were detected among females above 9 years and 65 cm, indicating that older, larger females generally spawn annually, investing energy into reproduction rather than body growth. The apparent demographic effect on skipped spawning suggests that the proportions of skippers presently should be high as the strong year-class of 2016 (now at age 5) comprise a large proportion of the population (ICES 2020a).

4.4 Evaluation of macroscopic maturity stages during the Winter Survey

To effectively assess and manage the NEA haddock stock, information regarding the spawning stock biomass (SSB) is required, which in turn depend on accurate macroscopic evaluation of gonads during the annual Winter Survey (ICES 2020b). These maturity estimates have not previously been validated microscopically in the NEA haddock. Results from the present study showed that misclassification was low for females macroscopically staged as maturing, confirming that the current estimates used to produce maturity ogives for the NEA haddock stock assessment, are accurate and effective. Results also showed that females refraining to spawn after reaching the EVO phase (reabsorbing-EVO skippers) was the most likely source of misclassification of maturing females. Only two skipping females (of 42) was assigned to this mode in the present study, of which one of them was staged as maturing at visual inspection. Thus, as these skippers can appear similar to maturing females macroscopically, they may be staged as maturing, and thereby potentially influence estimates of the SSB.

On the other hand, misclassification of immature females was relatively high, with only 24.4 % of females classified correctly as immature according to histology. Notably, even with the use of histology, some females could not be allocated to either immature or skipping categories

with certainty (see below). However, even if the 19.5 % of females histologically staged as uncertain were in fact immature, there is still a high percentage (56.1 %) of females macroscopically staged as immature, that were in fact skipping females. These findings confirm that there exists a clear challenge in separating immature and skipping individuals macroscopically, which has also been recently demonstrated in the NEA cod (Moksness 2019).

Histology is currently the most reliable and accurate method to identify skipping individuals (Rideout et al. 2005). Even so, certain cellular substructures are inherently challenging to distinguish and interpret consistently, creating some difficulties in allocation of categories. In the present study, this became evident in that 22 of 72 females analysed histologically from the Winter Survey 2020, could not be placed into any maturity category with certainty. Some of these females, termed 'uncertain', appeared to be immature in terms of oocyte size and phase, but evidently also contained a few (typically < 5) structures resembling POFs. Several authors have reported difficulty in separation of old POFs and β+γ atresia (Ganias et al. 2007; Brown-Peterson et al. 2011) due to largely similar size and appearance, which is problematic as these structures are essential in distinguishing between maturity categories. Additional challenges emerge when atresia of primary growth oocytes are present, which currently is poorly documented in the literature, although it seems to be a common occurrence in several species (Rideout et al. 2005; Skjæraasen et al. 2009) as well as in the present study. Identification of skippers based on POFs alone can therefore be inconclusive. As a result, ovarian wall thickness is often adopted as a tool for determining maturity status. However, the use of ovarian wall thickness could only be used as identification on a small fraction of samples in the present study, which is unfortunate as it could have assisted further separation when POFs did not fully suffice.

4.5 Separation of immature and skipping females based on whole mount

Finding a reliable technique to discriminate between maturity stages that appear macroscopically similar has been sought after for some time on-board scientific surveys collecting data for stock assessment. Accordingly, a secondary objective of this thesis was to explore a rapid technique to separate immature and skipping females based on image analysis (whole mount). Results showed that immature and skipping females could not be separated with certainty using OSFD in the present study. Significant differences in skewness and kurtosis were detected between immature and reabsorbing skippers, but for skipping females in the resting mode, the OSFD was indistinguishable from that of immatures. The results did, however, show a difference in GSI_s and LC-W between immatures and all three skipping

modes, where skipping females possessed higher GSI_s values and larger, more advanced oocytes compared to immature females. It should be noted that the sample size of immature females was very low and had to be pooled from two seasons. In retrospect, sampling criterion during the Winter Survey should have been set at a lower size (e.g. 30 or 35 cm total length) to ensure an adequate sample size of immature females. Nevertheless, it is worth mentioning that the inclusion of the uncertain category into the above-mentioned analysis would undoubtably have made the distinction between immature and skipping females even less pronounced.

The OSFD is a dynamic feature that changes seasonally according to female maturity status: for instance, Tobin et al (2010) reported that during the spawning season in the North Sea haddock, several immature females was observed to be arrested at the CNR-phases, resulting in normally distributed OSFDs. Similar results have been demonstrated in sole (*Solea solea*) (Ramsay and Witthames 1996) and cod (Burton et al. 1997; Kjesbu et al. 2011), where some immature females have shown to pause oogenesis in more advanced primary growth phases than that of other immatures. It is likely that a large proportion of the females assigned to the uncertain category, were in this adolescent phase, as many of them possessed normally distributed OSFDs and were in-between immatures and skippers in terms of age and size. In summary, these findings highlight the complexity of factors affecting the reproductive decision in female haddock, by showing that reversion of maturity (and maturation: adolescent phase) is a common occurrence for both immature and sexually mature females. Although oocyte size may not be a reliable metric to separate immature and skipping females, internal appearance characterisation in whole-mounts could potentially offer quick means of separation by analysing the presence of blood vessels and organisation of ovarian tissue in individual females (Kjesbu 1991). Such unprocessed, unstained samples were photographed under a stereo microscope during the Winter Survey 2020 and could potentially be examined further in future projects.

5 CONCLUSION

The present study has enlightened a number of important processes related to the reproductive cycle of the NEA haddock, many of which have not previously been investigated. These results have implications for future reproductive studies of the haddock, by providing detailed descriptions of oocyte development and characteristics of females deciding to skip the spawning season. The present study further confirms that there exists a high degree of misclassification of macroscopic stage estimates, which should be accounted for, as classifying skippers correctly in relation to immatures may help defining any foreseen drivers underlying variability in skipping over time.

It would be beneficial if ovary samples of the NEA haddock in future studies were collected earlier in the reproductive cycle (e.g. immediately after the spawning season), to assess nutritional status of females in relation to skipped spawning, at the time when the physiological decision to spawn may be determined. Such sampling could also verify whether the early appearance of CAO in the present study was in fact due to early timing of oogenesis, and not due to females being arrested at the CAO phase in the previous reproductive cycle. Moreover, although the methodology presented here was not adequate for separating immature and skipping females during the Winter Survey, a greater sample size of immature females could potentially have offered a better insight into the nature of their OSFDs and early oocyte recruitment patterns. Alternatively, the use of internal appearance characterisation may also provide an informative approach for separation of immature and skipping females in future studies.

To conclude, the NEA haddock showed reproductive commitment well before August, by the presence of CAO which prevailed as the most advanced oocyte phase for 4-5 months. The long duration of the CAO phase was further linked to individual variability in female length, where recruit spawners may start oocyte development later than repeat spawners, and smaller repeat spawners may possess less advanced oocytes than larger repeat spawners. The entrance into vitellogenesis was first observed in late October, simultaneously as the first skipping female appeared, marking the time of separation between females that develop ‘normally’ and those that will skip the spawning season. The majority of skipping females identified in October to March had reached the CAO phase and started atretic reabsorption of these oocytes. Neither energy storage nor body condition could be directly linked to the occurrence of skipped spawning in the present study, although spatial and environmental factors potentially could

have masked such effects. The occurrence of skipping was most common among second-time spawners (5 years old females), seemingly supporting a life-history driven mechanism for skipping, where the benefit of growing larger in body size to increase fecundity and probability of survival in the future outweighs present reproductive success.

The macroscopic maturity stage estimation currently deployed during the annual Winter Survey at the IMR was found to give correct estimates of the maturing portion of females but was not ideal for providing estimates of immature vs skipping females. The attempt to use whole-mount derived OSFD to quickly separate immature and skipping females did not adequately provide a reliable tool for discrimination between the two categories in the present study. The complexity of female maturity dynamics, confirmed by the ability to revert the oocyte developmental process after the maturation and reproductive decision was made, hindered currently any clear separation of immature and skipping females.

Finally, progressing beyond oogenesis and egg production, future studies should also be directed towards spatio-temporal aspects of the NEA haddock spawning season, as egg and larval survival largely hinge on the timing and duration of adult spawning due to various oceanographic and biotic interactions (Filin and Russkikh 2019). Defining the spawning period could further assist a more comprehensive understanding of the formation of year-class strength and subsequently, recruitment variability in terms of match-mismatch hypothesis and other intricate aspects linked to the reproductive cycle of the NEA haddock.

REFERENCES

Anderson, K.C., Alix, M., Charitonidou, K., Thorsen, A., Thorsheim, G., Ganias, K., Schmidt, T.C. dos S., and Kjesbu, O.S. 2020. Development of a new 'ultrametric' method for assessing spawning progression in female teleost serial spawners. Scientific Reports **10**(1): 9677. doi:10.1038/s41598-020-66601-w.

Berg, P.R., Jorde, P.E., Glover, K.A., Dahle, G., Taggart, J.B., Korsbrekke, K., Dingsør, G.E., Skjæraasen, J.E., Wright, P.J., Cadrin, S.X., Knutsen, H., and Westgaard, J.-I. 2020. Genetic structuring in Atlantic haddock contrasts with current management regimes. ICES Journal of Marine Science **78**(1): 1-13. doi:10.1093/icesjms/fsaa204.

Bergstad, O.A., Jørgensen, T., and Dragesund, O. 1987. Life history and ecology of the gadoid resources of the Barents Sea. Fisheries Research **5**(2): 119–161. doi:10.1016/0165-7836(87)90037-3.

Bogstad, B., Dingsør, G.E., Ingvaldsen, R.B., and Gjøsæter, H. 2013. Changes in the relationship between sea temperature and recruitment of cod, haddock and herring in the Barents Sea. Marine Biology Research **9**(9): 895–907. doi:10.1080/17451000.2013.775451.

Brown-Peterson, N.J., Wyanski, D.M., Saborido-Rey, F., Macewicz, B.J., and Lowerre-Barbieri, S.K. 2011. A standardized terminology for describing reproductive development in fishes. Marine and Coastal Fisheries **3**(1): 52–70. doi:10.1080/19425120.2011.555724.

Burton, M.P.M., Penneyl, R.M., and Biddiscombe, S. 1997. Time course of gametogenesis in Northwest Atlantic cod (*Gadus morhua*). Canadian Journal of Fisheries and Aquatic Sciences **54**(Suppl.1): 122–131. doi:10.1139/cjfas-54-S1-122.

Costa, A.M. 2009. Macroscopic vs. microscopic identification of the maturity stages of female horse mackerel. ICES Journal of Marine Science **66**(3): 509–516. doi:10.1093/icesjms/fsn216.

Cushing, D.H. 1990. Plankton production and year-class strength in fish populations: an update of the match/mismatch hypothesis. *In* Advances in Marine Biology. *Edited by* J.H.S. Blaxter and A.J. Southward. Academic Press. pp. 249–293. doi:10.1016/S0065-2881(08)60202-3.

Davie, A., Mazorra de Quero, C., Bromage, N., Treasurer, J., and Migaud, H. 2007. Inhibition of sexual maturation in tank reared haddock (*Melanogrammus aeglefinus*) through the use of constant light photoperiods. Aquaculture **270**(1): 379–389. doi:10.1016/j.aquaculture.2007.04.052.

Eriksen, E., Skjoldal, H.R., Gjøsæter, H., and Primicerio, R. 2017. Spatial and temporal changes in the Barents Sea pelagic compartment during the recent warming. Progress in Oceanography **151**: 206–226. doi:10.1016/j.pocean.2016.12.009.

Fall, J.J.E., Wenneck, T. de L., Bogstad, B., Fuglebakk, E., Gjøsæter, H., Seim, S.E., Skage, M.L., Staby, A., Tranang, C.A., Windsland, K., Russkikh, A.A., and Fomin, K. 2020. Fish investigations in the Barents Sea winter 2020. The Institute of Marine Research, Bergen, Norway. Available from https://imr.brage.unit.no/imr-xmlui/handle/11250/2755566 [accessed 24 May 2021].

Filin, A.A., and Russkikh, A.A. 2019. Specific features of the formation of the year-class abundance of Northeastern Arctic haddock *Melanogrammus aeglefinus* during the warming of the Barents Sea. Journal of Ichthyology **59**(2): 225–233. doi:10.1134/S0032945219020061.

Flores, A., Wiff, R., Ganias, K., and Marshall, C.T. 2019. Accuracy of gonadosomatic index in maturity classification and estimation of maturity ogive. Fisheries Research **210**: 50–62. doi:10.1016/j.fishres.2018.10.009.

Folkvord, A., Jørgensen, C., Korsbrekke, K., Nash, R.D.M., Nilsen, T., and Skjæraasen, J.E. 2014. Trade-offs between growth and reproduction in wild Atlantic cod. Canadian Journal of Fisheries and Aquatic Sciences **71**(7): 1106–1112. doi:10.1139/cjfas-2013-0600.

Ganias, K., Nunes, C., and Stratoudakis, Y. 2007. Degeneration of postovulatory follicles in the Iberian sardine (*Sardina pilchardus*): Structural changes and factors affecting resorption. Fishery Bulletin- National Oceanic and Atmospheric Administration **105**: 131–139.

ICES. 2020a. Arctic Fisheries Working Group (AFWG). ICES Scientific Reports **2:52**: 577 pp. ICES. doi:http://doi.org/10.17895/ices.pub.6050.

ICES. 2020b. Stock Annex: Haddock (*Melanogrammus aeglefinus*) in Subareas 1 and 2 (Northeast Arctic). Available from https://www.ices.dk/sites/pub/Publication%20Reports/Stock%20 Annexes/2020/had.27.1-2_SA.pdf.

Jørgensen, C., Ernande, B., Fiksen, Ø., and Dieckmann, U. 2006. The logic of skipped spawning in fish. Canadian Journal of Fisheries and Aquatic Sciences **63**: 200–211. doi:10.1139/f05-210.

Kell, L.T., Pilling, G.M., Kirkwood, G.P., Pastoors, M., Mesnil, B., Korsbrekke, K., Abaunza, P., Aps, R., Biseau, A., Kunzlik, P., Needle, C., Roel, B.A., and Ulrich-Rescan, C. 2005. An evaluation of the implicit management procedure used for some ICES roundfish stocks. ICES Journal of Marine Science **62**(4): 750–759. doi:10.1016/j.icesjms.2005.01.001.

Kennedy, J. 2018. Oocyte size distribution reveals ovary development strategy, number and relative size of egg batches in lumpfish (*Cyclopterus lumpus*). Polar Biology **41**(6): 1091–1103. doi:10.1007/s00300-018-2266-9.

Kjesbu, O., Righton, D., Krüger-Johnsen, M., Thorsen, A., Michalsen, K., Fonn, M., and Witthames, P. 2010. Thermal dynamics of ovarian maturation in Atlantic cod (*Gadus morhua*). Canadian Journal of Fisheries and Aquatic Sciences **67**: 605–625. doi:10.1139/F10-011.

Kjesbu, O.S. 1991. A simple method for determining the maturity stages of Northeast Arctic cod (*Gadus morhua* L.) by in vitro examination of oocytes. Sarsia **75**(4): 335–338. doi:10.1080/00364827.1991.10413458.

Kjesbu, O.S. 1994. Time of start of spawning in Atlantic cod (*Gadus morhua*) females in relation to vitellogenic oocyte diameter, temperature, fish length and condition. Journal of Fish Biology **45**(5): 719–735. doi:10.1111/j.1095-8649.1994.tb00939.x.

Kjesbu, O.S. 2009. Applied Fish Reproductive Biology: Contribution of Individual Reproductive Potential to Recruitment and Fisheries Management. *In* Fish Reproductive Biology: Implications for Assessment and Management. John Wiley & Sons, Ltd. pp. 459–463. doi:10.1002/9781444312133.ch8.

Kjesbu, O.S., and Holm, J.C. 1994. Oocyte recruitment in first-time spawning Atlantic cod (*Gadus morhua*) in relation to feeding regime. Canadian Journal of Fisheries and Aquatic Sciences **51**: 1893–1898. doi:10.1139/f94-189.

Kjesbu, O.S., Klungsøyr, J., Kryvi, H., Witthames, P.R., and Walker, M.G. 1991. Fecundity, atresia, and egg size of captive Atlantic cod (*Gadus morhua*) in relation to proximate body composition. Canadian Journal of Fisheries and Aquatic Sciences **48**(12): 2333–2343. doi:10.1139/f91-274.

Kjesbu, O.S., Thorsen, A., and Fonn, M. 2011. Quantification of primary and secondary oocyte production in Atlantic cod by simple oocyte packing density theory. Marine and Coastal Fisheries **3**(1): 92–105. doi:10.1080/19425120.2011.555714.

Kjesbu, O.S., Witthames, P.R., Solemdal, P., and WalKer, M.G. 1990. Ovulatory rhythm and a method to determine the stage of spawning in Atlantic cod (*Gadus morhua*). Canadian Journal of Fisheries and Aquatic Sciences **47**(6): 1185–1193. doi:10.1139/f90-138.

Kurita, Y., and Kjesbu, O.S. 2009. Fecundity estimation by oocyte packing density formulae in determinate and indeterminate spawners: Theoretical considerations and applications. Journal of Sea Research **61**(3): 188–196. doi:10.1016/j.seares.2008.10.010.

Landa, C.S., Ottersen, G., Sundby, S., Dingsør, G.E., and Stiansen, J.E. 2014. Recruitment, distribution boundary and habitat temperature of an arcto-boreal gadoid in a climatically changing environment: a case study on Northeast Arctic haddock (*Melanogrammus aeglefinus*). Fisheries Oceanography **23**(6): 506–520. doi:10.1111/fog.12085.

Lowerre-Barbieri, S.K., Brown-Peterson, N.J., Murua, H., Tomkiewicz, J., Wyanski, D.M., and Saborido-Rey, F. 2011. Emerging issues and methodological advances in fisheries reproductive biology. Marine and Coastal Fisheries **3**(1): 32–51.

Macchi, G.J., Diaz, M.V., Leonarduzzi, E., Militelli, M.I., and Rodrigues, K. 2016. Skipped spawning in the Patagonian stock of Argentine hake (*Merluccius hubbsi*). Fishery Bulletin **114**(4): 397–408. doi:10.7755/FB.114.4.3.

Martin-Robichaud, D.J., and Berlinsky, D.L. 2004. The effects of photothermal manipulation on reproductive development in female haddock (*Melanogrammus aeglefinus* L.). Aquaculture Research **35**(5): 465–472. doi:10.1111/j.1365-2109.2004.01040.x.

van der Meeren, G.I., and Prozorkevich, D. 2020. Survey report from the joint Norwegian/Russian ecosystem survey in the Barents Sea and adjacent waters, August-November 2020. The Institute of Marine Research. Available from https://imr.brage.unit.no/imr-xmlui/handle/11250/2755574 [accessed 24 May 2021].

Mjanger, H., Svendsen, B.V., Senneset, H., Fuglebakk, E., Skage, M.L., Diaz, J., Johansen, G.O., and Vollen, T. 2019. Handbook for sampling fish, crustaceans and other invertebrates. Version 1.0. Ref.id.: FOU.SPD.HB-02, Institute of Marine Research: 157 pp.

Moan, A., Skern-Mauritzen, M., Vølstad, J.H., and Bjørge, A. 2020. Assessing the impact of fisheries-related mortality of harbour porpoise (*Phocoena phocoena*) caused by incidental bycatch in the dynamic Norwegian gillnet fisheries. ICES Journal of Marine Science **77**(7–8): 3039–3049. doi:10.1093/icesjms/fsaa186.

Moksness, I.E. 2019. Comparing maturation dynamics of Atlantic cod (*Gadus morhua*) in the Barents Sea by macroscopic and microscopic tools. M.Sc. in Fisheries Biology and Management, Department of Biological Sciences, University of Bergen.

Morgan, M.J.M.J., Murua, H.M., Kraus, G.K., Lambert, Y.L., Marteinsdóttir, G.M., Marshall, C.T.M.T., O'Brien, L.O., and Tomkiewicz, J.T. 2009. The evaluation of reference points and stock productivity in the context of alternative indices of stock reproductive potential. Canadian Journal of Fisheries and Aquatic Sciences **66**: 404–414. doi:10.1139/F09-009.

Murua, H., and Saborido-Rey, F. 2003. Female reproductive strategies of marine fish species of the North Atlantic. Journal of Northwest Atlantic Fishery Science **33**: 23–31. doi:10.2960/J.v33.a2.

Olsen, E., Aanes, S., Mehl, S., Holst, J.C., Aglen, A., and Gjøsæter, H. 2010. Cod, haddock, saithe, herring, and capelin in the Barents Sea and adjacent waters: a review of the biological value of the area. ICES Journal of Marine Science **67**(1): 87–101. doi:10.1093/icesjms/fsp229.

R Core Team. 2020. R: A language and environment for statistical computing. R Foundation for Statistical Computing, Vienna, Austria. Available from https://www.R-project.org/.

Ramsay, K., and Witthames, P.R. 1996. Using oocyte size to assess seasonal ovarian development in *Solea solea* (L.). Journal of Sea Research **36**(3–4): 275–283. doi:10.1016/S1385-1101(96)90796-0.

Rideout, R.M., Burton, M.P.M., and Rose, G.A. 2000. Observations on mass atresia and skipped spawning in northern Atlantic cod, from Smith Sound, Newfoundland. Journal of Fish Biology **57**(6): 1429–1440. doi:10.1111/j.1095-8649.2000.tb02222.x.

Rideout, R.M., Rose, G.A., and Burton, M.P.M. 2005. Skipped spawning in female iteroparous fishes. Fish and Fisheries **6**(1): 50–72. doi:10.1111/j.1467-2679.2005.00174.x.

Rideout, R.M., and Tomkiewicz, J. 2011. Skipped spawning in fishes: more common than you might think. Marine and Coastal Fisheries **3**(1): 176–189. doi:10.1080/19425120.2011.556943.

Rothschild, B.J. 2000. "Fish stocks and recruitment": the past thirty years. ICES Journal of Marine Science **57**(2): 191–201. doi:10.1006/jmsc.2000.0645.

Saborido-Rey, F., and Junquera, S. 1998. Histological assessment of variations in sexual maturity of cod (*Gadus morhua* L.) at the Flemish Cap (north-west Atlantic). ICES Journal of Marine Science **55**(3): 515–521. doi:10.1006/jmsc.1997.0344.

Sætersdal, G.S. 1952. The haddock in Norwegian waters - I. Vertebrae counts and brood strength variations of young fish. Report on Norwegian Fishery and Marine Investigations **10**: 1–14.

Shirokova, M.Y. 1977. Peculiarities of the sexual maturation of females of the Baltic cod, *Gadus morhua callarias*. Journal of Ichthyology **17(4)**: 574–581.

Skjæraasen, J., Korsbrekke, K., Nilsen, T., Fonn, M., Kjesbu, O., Dingsør, G., and Nash, R. 2015. Skipped spawning in Northeast Arctic haddock *Melanogrammus aeglefinus*. Marine Ecology Progress Series **526**: 143–155. doi:10.3354/meps11222.

Skjæraasen, J.E., Devine, J.A., Godiksen, J.A., Fonn, M., OtterÅ, H., Kjesbu, O.S., Norberg, B., Langangen, Ø., and Karlsen, Ø. 2017. Timecourse of oocyte development in saithe *Pollachius virens*. Journal of Fish Biology **90**(1): 109–128. doi:https://doi.org/10.1111/jfb.13161.

Skjæraasen, J.E., Kennedy, J., Thorsen, A., Fonn, M., Strand, B.N., Mayer, I., and Kjesbu, O.S. 2009. Mechanisms regulating oocyte recruitment and skipped spawning in Northeast Arctic cod (*Gadus morhua*). Canadian Journal of Fisheries and Aquatic Sciences **66**(9): 1582–1596. doi:10.1139/F09-102.

Skjæraasen, J.E., Korsbrekke, K., Dingsør, G.E., Langangen, Ø., Opdal, A.F., and Jørgensen, C. 2020. Large annual variation in the amount of skipped spawning for female Northeast Arctic haddock *Melanogrammus aeglefinus*. Fisheries Research **230**: 105670. doi:10.1016/j.fishres.2020.105670.

Skjæraasen, J.E., Korsbrekke, K., Kjesbu, O.S., Fonn, M., Nilsen, T., and Nash, R.D.M. 2013. Size-, energy- and stage-dependent fecundity and the occurrence of atresia in the Northeast Arctic haddock *Melanogrammus aeglefinus*. Fisheries Research **138**: 120–127. doi:10.1016/j.fishres.2012.04.003.

Skjæraasen, J.E., Nash, R.D.M., Kennedy, J., Thorsen, A., Nilsen, T., and Kjesbu, O.S. 2010. Liver energy, atresia and oocyte stage influence fecundity regulation in Northeast Arctic cod. Marine Ecology Progress Series **404**: 173–183. doi:10.1016/j.fishres.2012.04.003.

Skjæraasen, J.E., Nash, R.D.M., Korsbrekke, K., Fonn, M., Nilsen, T., Kennedy, J., Nedreaas, K.H., Thorsen, A., Witthames, P.R., Geffen, A.J., Hoie, H., and Kjesbu, O.S. 2012. Frequent skipped spawning in the world's largest cod population. Proceedings of the National Academy of Sciences **109**(23): 8995–8999. doi:10.1073/pnas.1200223109.

Thorsen, A., and Kjesbu, O.S. 2001. A rapid method for estimation of oocyte size and potential fecundity in Atlantic cod using a computer-aided particle analysis system. Journal of Sea Research **46**(3): 295–308. doi:10.1016/S1385-1101(01)00090-9.

Tobin, D., Wright, P.J., and O'Sullivan, M. 2010. Timing of the maturation transition in haddock *Melanogrammus aeglefinus*. Journal of Fish Biology **77**(6): 1252–1267. doi:10.1111/j.1095-8649.2010.02739.x.

Tomkiewicz, J., Tybjerg, L., and Jespersen, Å. 2003. Micro- and macroscopic characteristics to stage gonadal maturation of female Baltic cod. Journal of Fish Biology **62**(2): 253–275. doi:10.1046/j.1095-8649.2003.00001.x.

Trippel, E.A. 1999. Estimation of stock reproductive potential: history and challenges for Canadian Atlantic gadoid stock assessments. Journal of Northwest Atlantic Fishery Science **25**: 61–81. doi:10.2960/J.v25.a6.

Tyler, C.R., and Sumpter, J.P. 1996. Oocyte growth and development in teleosts. Reviews in Fish Biology and Fisheries **6**(3): 287–318. doi:10.1007/BF00122584.

Vitale, F. and Cardinale. 2006. Histological analysis invalidates maturity ogives of cod (*Gadus morhua*) based on visual inspections. Optimization of maturity surveys and use of alternative criteria in estimating maturity. ICES Journal of Marine Science. doi:10.1016/j.icesjms.2005.09.001.

Wallace, R.A., and Selman, K. 1981. Cellular and dynamic aspects of oocyte growth in teleosts. Integrative and Comparative Biology **21**(2): 325–343. doi:10.1093/icb/21.2.325.

Witthames, P.R., Thorsen, A., and Kjesbu, O.S. 2010. The fate of vitellogenic follicles in experimentally monitored Atlantic cod *Gadus morhua* (L.): Application to stock assessment. Fisheries Research **104**(1): 27–37. doi:10.1016/j.fishres.2009.11.008.

Witthames, P.R., Thorsen, A., Murua, H., Saborido-Rey, F., Greenwood, L.N., Dominguez, R., Korta, M., and Kjesbu, O.S. 2009. Advances in methods for determining fecundity: application of the new methods to some marine fishes. Fishery Bulletin **107**(2): 148–164.

Wright, P.J., and Trippel, E.A. 2009. Fishery-induced demographic changes in the timing of spawning: consequences for reproductive success*. Fish and Fisheries **10**(3): 283–304. doi:10.1111/j.1467-2979.2008.00322.x.

APPENDIX A

IMAGE ANALYSIS

THE WHOLE MOUNT STAINING METHOD

One-third of the ovarian tissue was extracted from each BiopSafe container and placed in an Eppendorf tube filled with 1 ml of 4 % phosphate-buffered formaldehyde (PBF). The tissue was exposed to an ultrasound pen (Sonics & Materials Inc., Vibra-Cell™) for 5 - 10 seconds and stained with 60 µl of 2% toluidine blue and 1% sodium tetraborate colouring. The Eppendorf tube was then shaken, and the homogeneously stained tissue was carefully poured into 74 µm-mesh netwells, settled on a petri dish filled with PBF. The petri dish was placed on a stirring machine while the PBF was replaced 2 - 4 times to dilute and remove excess stain. After profound rinsing, the tissue was ejected onto a petri dish with PBF and placed under a light microscope with a digital camera mounted onto it. Prior to photographing the sample, a small drop of dishwashing detergent was added on to the petri dish to avoid oocytes from being attached to the water surface (Thorsen and Kjesbu 2001).

APPENDIX B

R PACKAGES

R PACKAGE	REFERENCE
emmeans	Russell V. Lenth (2021). emmeans: Estimated Marginal Means, aka Least-Squares Means. R package version 1.5.5-1. https://CRAN.R-project.org/package=emmeans
ggpubr	Alboukadel Kassambara (2018). ggpubr: 'ggplot2' Based Publication Ready Plots. R ggpubr package version 0.2. https://CRAN.R-project.org/package=ggpubr
ggridges	Claus O. Wilke (2021). ggridges: Ridgeline Plots in 'ggplot2'. R package version 0.5.3. https://CRAN.R-project.org/package=ggridges
ggspatial	Dewey Dunnington (2020). ggspatial: Spatial Data Framework for ggplot2. R package version 1.1.4. https://CRAN.R-project.org/package=ggspatial
gridExtra	Baptiste Auguie (2015). gridExtra: Miscellaneous Functions for "Grid" Graphics. R package version 2.0.0. http://CRAN.R-project.org/package=gridExtra
MASS	Venables, W. N. & Ripley, B.D. (2002). Modern Applied Statistics with S. Fourth MASS Edition. Springer, New York. ISBN 0-387-95457-0
moments	Lukasz Komsta and Frederick Novomestky (2015). moments: Moments, cumulants, skewness, kurtosis and related tests. R package version 0.14. https://CRAN.R-project.org/package=moments
multcomp	Torsten Hothorn, Frank Bretz and Peter Westfall (2008). Simultaneous Inference in multcomp General Models Biometrical Journal 50(3), 346-363.
multcompView	Spencer Graves, Hans-Peter Piepho and Luciano Selzer with help from Sundar Dorai-Raj (2019). multcompView: Visualizations of Paired Comparisons. R package version 0.1-8. https://CRAN.R-project.org/package=multcompView
RColorBrewer	Erich Neuwirth (2014). RColorBrewer: ColorBrewer Palettes. R package version 1.1-2. https://CRAN.R-project.org/package=RColorBrewer
rgeos	Roger Bivand and Colin Rundel (2020). rgeos: Interface to Geometry Engine - Open Source ('GEOS'). R package version 0.5-5. https://CRAN.R-project.org/package=rgeos
rnaturalearth	Andy South (2017). rnaturalearth: World Map Data from Natural Earth. R package version 0.1.0. https://CRAN.R-project.org/package=rnaturalearth
sf	Pebesma, E., 2018. Simple Features for R: Standardized Support for Spatial Vector Data. The R Journal 10 (1), 439-446, https://doi.org/10.32614/RJ-2018-009
scales	Hadley Wickham and Dana Seidel (2020). scales: Scale Functions for Visualization. R package version 1.1.1. https://CRAN.R-project.org/package=scales
tidyverse	Hadley Wickham (2017). tidyverse: Easily Install and Load the 'Tidyverse'. R package version 1.2.1. https://CRAN.R-project.org/package=tidyverse
viridis	Simon Garnier (2018). viridis: Default Color Maps from 'matplotlib'. R package version 0.5.1. https://CRAN.R-project.org/package=viridis

APPENDIX C

STATISTICAL RESULTS AND ADDITIONAL FIGURES

Appendix C.1. The difference in histological oocyte leading cohort (LC-H, µm) between various histological oocyte phases, examined with a one-way analysis of variance (ANOVA) with Tukey HSD (honestly significant difference) post hoc test. Data have been pooled across surveys to consider the consistency of oocyte size measurements and assignment of oocyte phases.

MOST ADVANCED PHASE OF OOCYTE DEVELOPMENT	$F_{7,251}$ = 805, R^2 = 0.956			
	Estimate	SE	*t-values*	*p-values*
3 - 4A	42..89	9.78	4.385	< 0.001
3 - 4B	78.60	10.48	7.497	< 0.001
3 - 4C	111.31	11.38	9.779	< 0.001
3 - ECAO	163.85	11.42	14.345	< 0.001
3 - LCAO	258.56	11.55	22.369	< 0.001
3 - EVO	355.74	13.55	26.237	< 0.001
3 - LVO	436.48	12.88	33.867	< 0.001
4A - 4B	51.69	5.01	10.321	< 0.001
4A - 4C	84.39	6.68	12.625	< 0.001
4A - ECAO	136.93	6.75	20.277	< 0.001
4A - LCAO	231.64	6.98	33.177	< 0.001
4A - EVO	328.83	9.95	33.053	< 0.001
4A - LVO	409	9.01	45.439	< 0.001
4B - 4C	32.70	6.11	5.356	< 0.001
4B - ECAO	85.24	6.18	13.794	< 0.001
4B - LCAO	179.95	6.43	27.990	< 0.001
4B - EVO	277.13	9.56	28.963	< 0.001
4B - LVO	357.88	8.59	41.650	< 0.001
4C - ECAO	52.54	7.60	6.911	< 0.001
4C - LCAO	147.250	7.80	18.863	< 0.001
4C - EVO	244.43	10.54	23.184	< 0.001
4C - LVO	325.18	9.66	33.641	< 0.001
ECAO - LCAO	94.71	7.86	12.042	< 0.001
ECAO - EVO	191.89	10.58	18.126	< 0.001
ECAO - LVO	272.63	9.71	28.068	< 0.001
EVO - LCAO	97.18	10.73	9.053	< 0.001
LCAO - LVO	80.75	12.15	6.644	< 0.001
EVO - LVO	177.93	9.87	18.020	< 0.001

Appendix C.2. Simple effects and interaction contrasts of the change in whole-mount oocyte leading cohort (LC-W, µm) over time between different length groups of the NEA haddock, performed by a two-way analysis of covariance (ANCOVA) with Tukey's HSD test.

PREDICTOR VARIABLES		RESPONSE VARIABLE: LC-W $F_{9,440}$ = 39.9, R^2_{adj} = 0.428			
Sampling day	Length groups	Estimate	SE	*t-values*	*p-values*
Sampling day	30 - 39 - 40 - 49	-0.26	0.26	-0.999	0.318
Sampling day	30 - 39 - 50 - 59	0.32	0.28	1.140	0.254
Sampling day	30 - 39 - 60 - 69	1.10	0.31	3.562	**< 0.001**
Sampling day	30 - 39 - 70 - 79	1.24	0.54	2.280	**0.023**
Sampling day	40 - 49 - 50 - 59	0.58	0.19	3.049	**0.002**
Sampling day	40 - 49 - 60 - 69	1.37	0.24	5.795	**< 0.001**
Sampling day	40 - 49 - 70 - 79	1.50	0.51	2.973	**0.003**
Sampling day	50 - 59 - 60 - 69	0.79	0.25	3.146	**0.002**
Sampling day	50 - 59 - 70 - 79	0.93	0.51	1.805	0.072
Sampling day	60 - 69 - 70 - 79	0.14	0.53	0.256	0.797

Appendix C.3. Simple effects and interaction contrasts between the two whole-mount maturity categories: maturing (M) and non-developing females (ND) of the mean difference in somatic gonadosomatic index (GSI_s, %) over the sampling months performed by a two- way ANOVA with Tukey's HSD test. Females with missing values for GSI_s (n = 8) were not included in the analysis. Results are given on log transformed scale.

PREDICTOR VARIABLES		RESPONSE VARIABLE GSI_s $F_{13,428}$ = 46.99, R^2_{adj} = 0.576			
MONTH	Maturity category	Estimate	SE	*t-value*	*p-value*
Aug	ND - M	-0.38	0.15	-2.557	0.372
Sep	ND - M	-0.65	0.12	- 5.152	**< 0.001**
Oct	ND - M	-0.64	0.19	-4.238	**0.035**
Nov	ND - M	-0.71	0.11	-6.376	**< 0.001**
Dec	ND - M	-0.86	0.16	-5.311	**< 0.001**
Jan	ND - M	-1.66	0.11	-14.855	**< 0.001**
Feb	ND - M	-1.59	0.13	-12.224	**< 0.001**

Appendix C.4. Simple effects and interaction contrasts of histological maturity categories (i.e. immature, maturing and skipping females) in relation to whole-mount oocyte leading cohort (LC-W, µm) over the sampling period, performed by of a two-way ANCOVA with Tukey's HSD test.

PREDICTOR VARIABLE		RESPONSE VARIABLE: LC-W $F_{5,174}$ = 276.8, R^2_{adj} = 0.885			
Sampling day	Maturity category	**Estimate**	**SE**	***t-values***	***p-values***
Sampling day	Immature - Maturing	-1.67	0.13	-12.511	**< 0.001**
Sampling day	Immature - Skipping	0.09	0.23	0.392	0.919
Sampling day	Maturing - Skipping	1.76	0.21	8.422	**< 0.001**

Appendix C.5. The difference in mean whole-mount oocyte leading cohort (LC-W, µm) between immature and skipping females examined with an unpaired two-sample t-test.

PREDICTOR VARIABLE (Maturity category)	RESPONSE VARIABLE	df = 85		
		Mean ± SD	***t-value***	***p-value***
Immature	LC-W	171.4 ± 26.8	-10.852	**< 0.001**
Skipping		234.2 ± 27.8		

Appendix C.6. The relationship between whole-mount oocyte leading cohort (LC-W, µm), total length and sampling day in maturing females, examined with a multiple linear regression analysis.

PREDICTOR VARIABLES	RESPONSE VARIABLE: LC-W $F_{2,90}$ = 253, R^2_{adj} = 0.846			
	Estimate	**SE**	***t-value***	***p-value***
Intercept	96.32	27.76	3.470	**< 0.001**
Female total length	2.94	0.51	5.765	**< 0.001**
Sampling day	1.56	0.01	18.598	**< 0.001**

Appendix C.7. Simple effects and interaction contrasts of the change in GSI_s (%) and HSI_s (%) over the sampling period for histological maturity categories (i.e. immature, skipping and maturing females) performed by a two- way ANOVA with Tukey's HSD test. Females with missing values for GSI_s (n = 6) and HSI_s (n = 4) have been removed. Results of GSI_s are given on log transformed scale.

PREDICTOR VARIABLES		RESPONSE VARIABLES					
MONTH	MATURITY CATEGORY	GSI_s $F_{18,155}$ = 14.85, R^2_{adj} = 0.590			HSI_s $F_{18,157}$ = 6.16, R^2_{adj} = 0.347		
		Estimate ± SE	*t-value*	*p-value*	Estimate ± SE	*t-value*	*p-value*
Aug	Immature - Skipping	-	-	-	-	-	-
	Immature - Maturing	-0.37 ± 0.20	-1.846	0.957	-0.44 ± +.65	-0.668	1
	Maturing - Skipping	-	-	-	-	-	-
Sep	Immature - Skipping	-	-	-	-	-	-
	Immature - Maturing	-051 ± 0.24	-2.094	0.871	0.82 ± 0.78	1.048	1
	Maturing - Skipping	-	-	-	-	-	-
Oct	Immature - Skipping	-0.89 ± 0.58	-1.532	0.994	1.74 ± 1.85	0.944	1
	Immature - Maturing	-1.15 ± 0.31	-3.663	**0.039**	-0.48 ± 0.99	-0.480	1
	Maturing - Skipping	0.26 ± 0.51	0.501	1	2.23 ± 1.65	1.352	0.999
Nov	Immature - Skipping	-0.31 ± 0.19	-1.588	0.991	0.13 ± 0.59	0.225	1
	Immature - Maturing	-1.12 ± 0.22	-5.086	**< 0.001**	-0.35 ± 0.71	-0.501	1
	Maturing - Skipping	0.81 ± 0.22	3.530	0.068	0.49 ± 0.71	0.684	1
Dec	Immature - Skipping	-0.48 ± 0.52	-0.927	1	-1.79 ± 1.66	-1.081	1
	Immature - Maturing	1.59 ± 0.61	-3.830	**0.026**	-3.42 ± 1.96	-1.745	0.976
	Maturing - Skipping	1.10 ± 0.38	3.908	**0.021**	1.63 ± 1.22	1.336	0.999
Jan	Immature - Skipping	-0.13 ± 0.35	-0.036	1	-1.34 ± 0.97	-1.376	0.999
	Immature - Maturing	-1.67 ± 0.32	-4.819	**< 0.001**	-4.02 ± 0.84	-4.815	**< 0.001**
	Maturing - Skipping	1.54 ± 0.24	6.231	**< 0.001**	2.68 ± 0.78	4.599	**0.002**
Feb	Immature - Skipping	-0.49 ± 0.34	-1.416	0.998	0.92 ± 1.11	0.831	1
	Immature - Maturing	-1.91 ± 0.33	-5.674	**< 0.001**	-0.77 ± 1.07	-0.719	1
	Maturing - Skipping	1.42 ± 0.25	5.567	**< 0.001**	1.69 ± 0.81	2.090	0.873

Appendix C.8. The difference in Fulton's condition factor (K) between histological maturity categories (i.e. immature, skipping and maturing females) and months. The model was initially tested with an interaction term between histological maturity categories and months, but was removed as it was non-significant.

PREDICTOR VARIABLES	RESPONSE VARIABLES K $F_{8,171}$ = 2.033, R^2_{adj} = 0.047				
	df	Sum of squares	Mean square	*F-value*	*p-value*
Month	6	0.09	0.01	2.062	0.060
Maturity category	2	0.03	0.02	2.207	0.113

Appendix C.9. Map of the spatial variability in hepatosomatic index (HSI_s) of all samples histologically analysed as a part of thesis Objective 1 (n = 180). Lighter colours denote higher HSI_s values, while darker colours denote lower values of HSI_s.

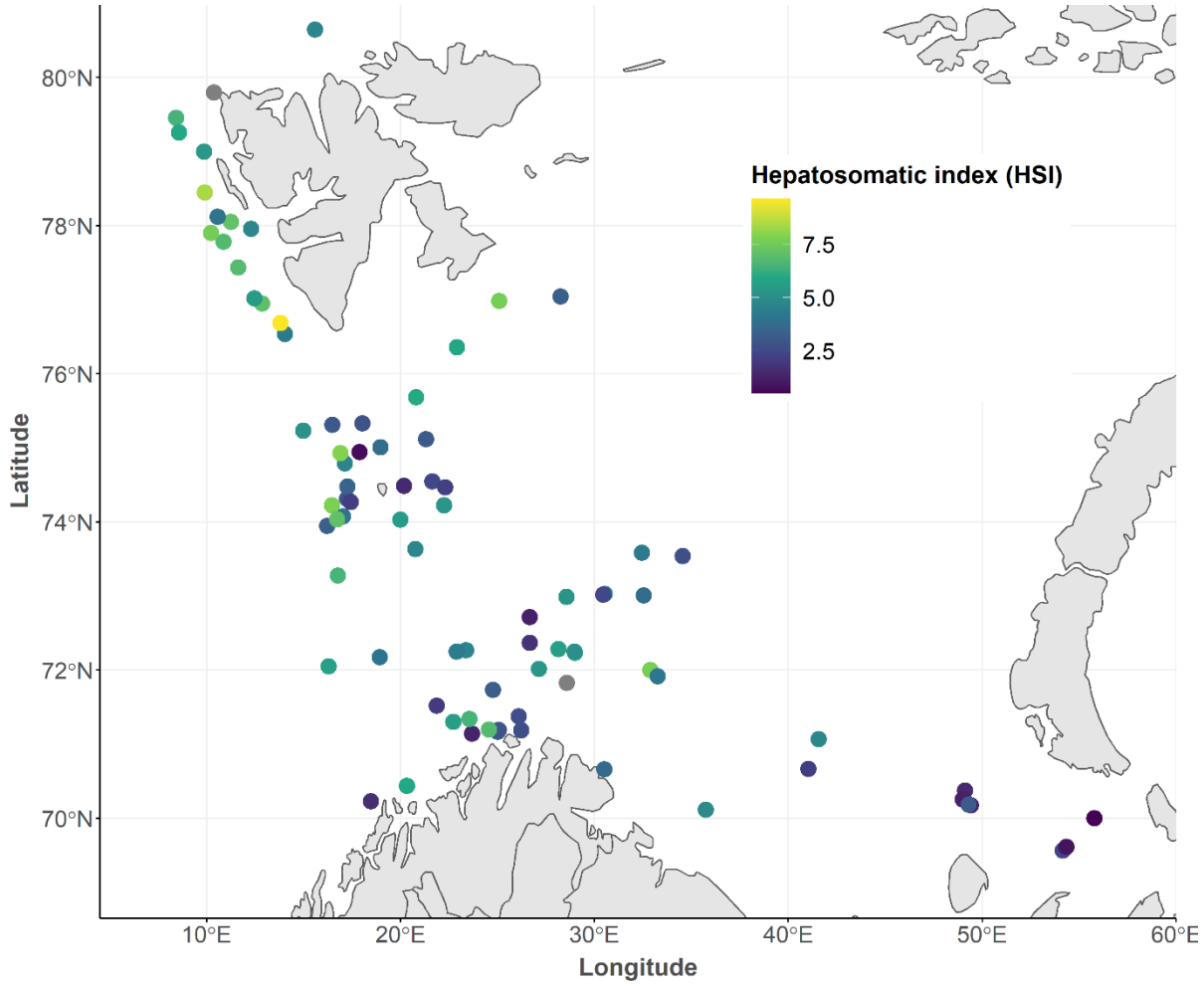

Appendix C.10. Map of the spatial variability in Fulton's condition factor (K) of all samples histologically analysed as a part of thesis Objective 1 (n = 180). Lighter colours denote higher K values, while darker colours denote lower values of K.

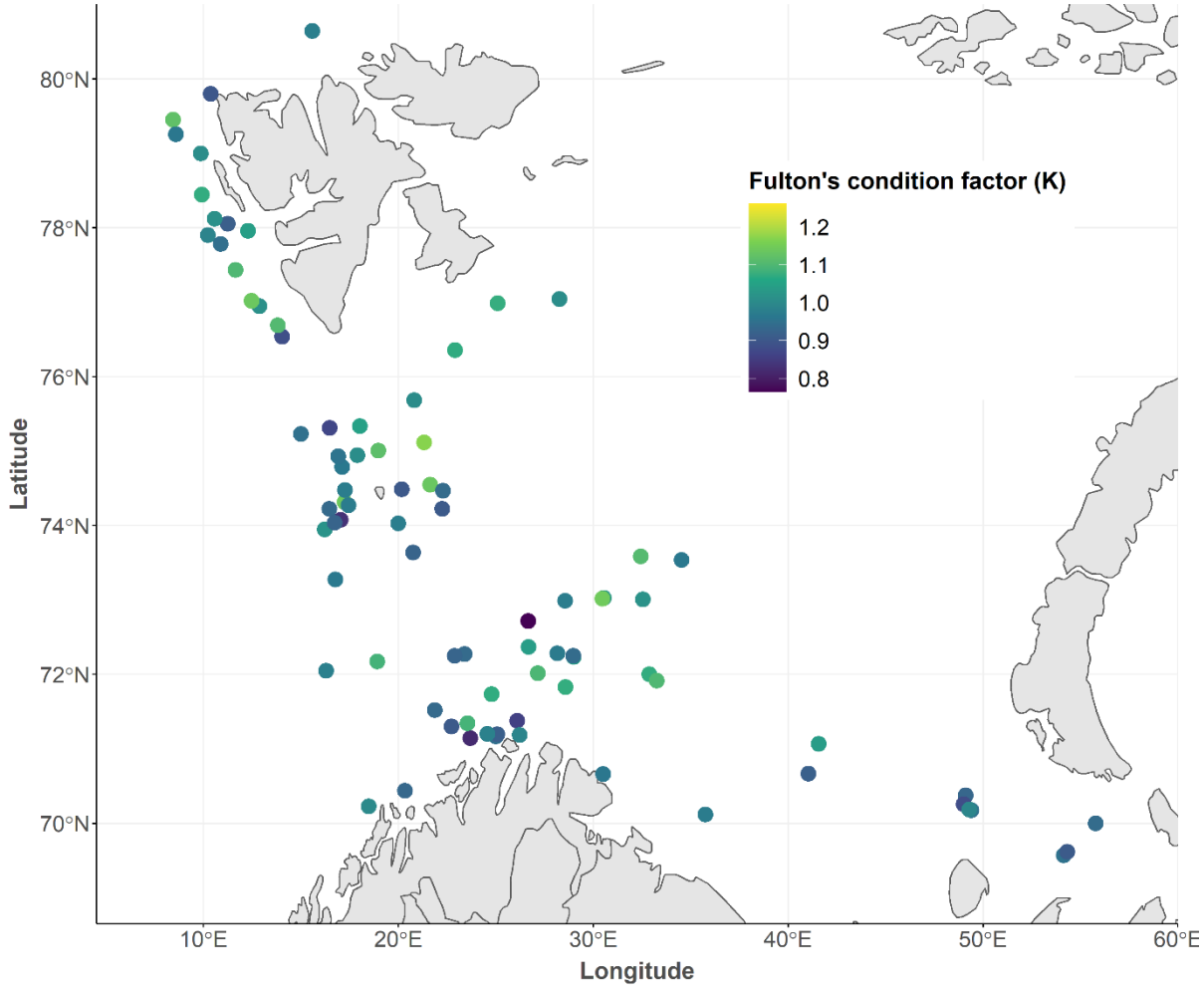

Appendix C.11. Oocyte size frequency distributions of individual immature females (n = 12) collected during the Winter Survey 2020 (green) and 2021 (blue). Collectively, these individuals have been combined as one category and used for analysis of skewness and kurtosis in relation to thesis Objective 2.

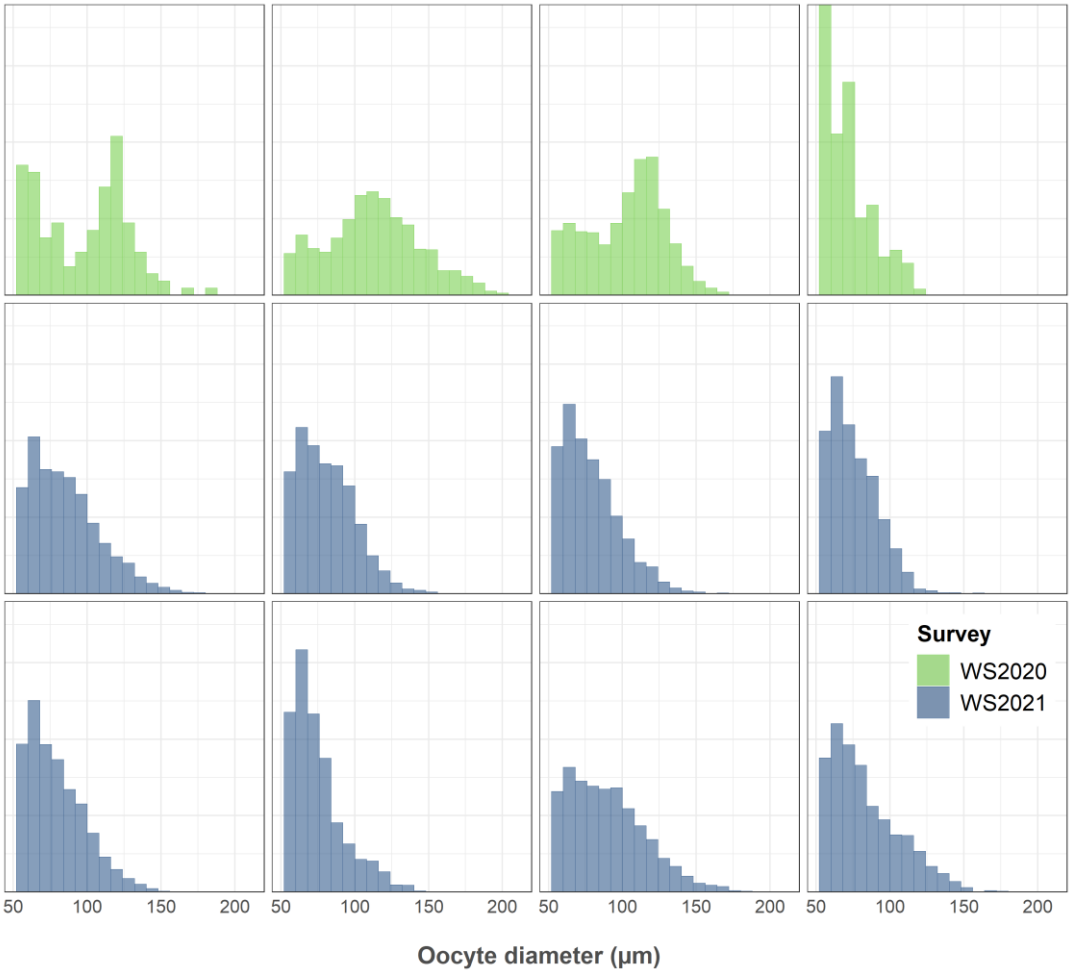

Appendix C.12. Oocyte size frequency distributions of individual skipping females (n = 46) collected during the Winter Survey 2020. Collectively, these individuals have been combined as one category and used for analysis of skewness and kurtosis in relation to thesis Objective 2.

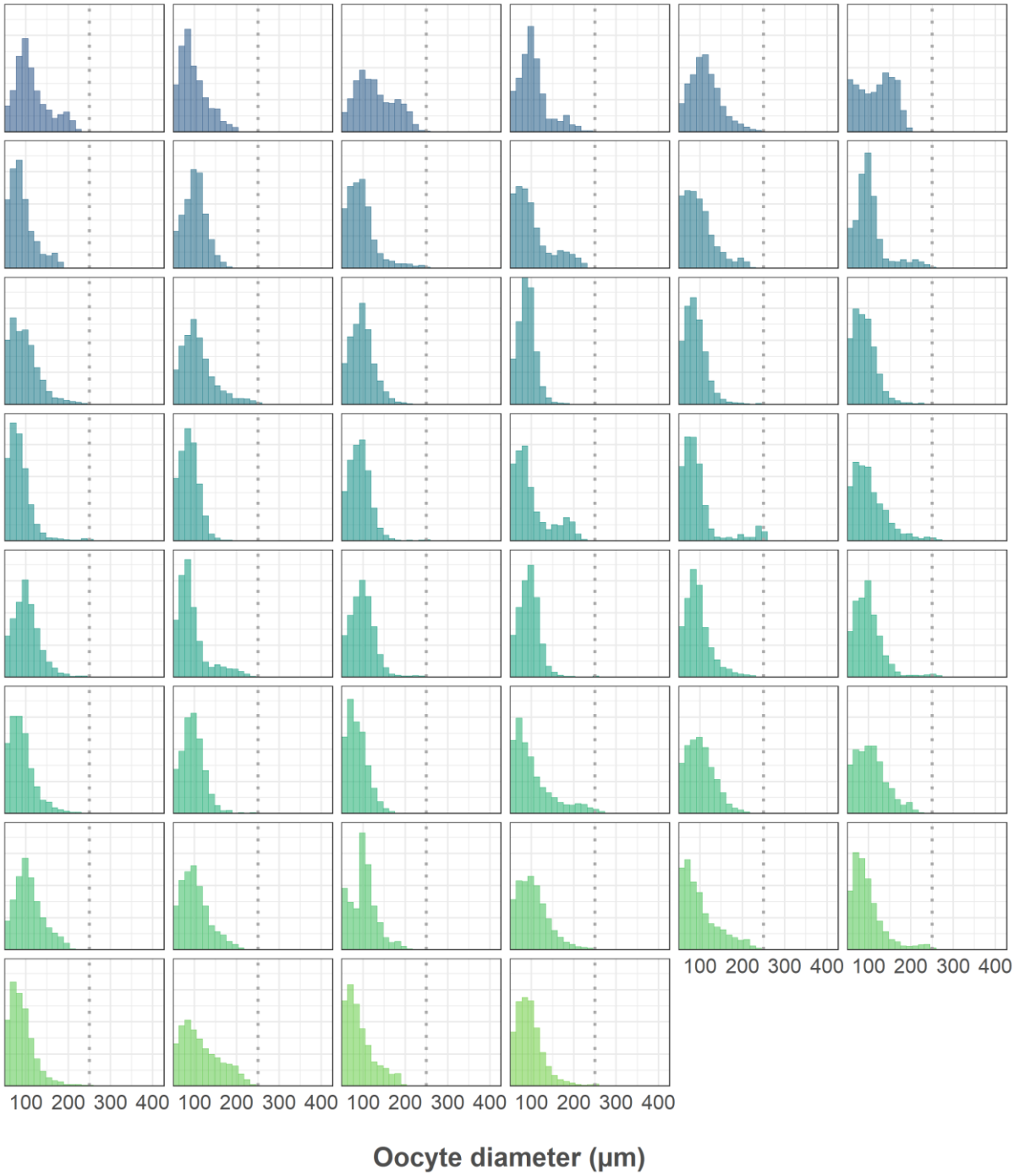

Appendix C.13. Oocyte size frequency distributions (OSFD) of the three modes of skipped spawning identified during the Winter Survey 2020: resting (brown), reabsorbing-CAO (blue) and reabsorbing-EVO (green). Histograms are overlayed with a smoothed density function (Kernel) for visualization of the distributions. A sequential reduction in the quantity of oocytes between 150 - 200 µm can be observed from resting skippers down to reabsorbing-EVO, indicating the development into secondary growth oocytes. Reabsorbing-CAO and EVO skippers possessed atretic follicles well above the 250 µm threshold (histological analysis), but due to insufficient roundness, these follicles were in most cases not detected by the image analysis system, resulting in unimodal OSFD of all three skipping modes. Descriptive statistics for the OSFD are shown in each panel as the minimum and maximum (Min, Max) oocyte diameter measured, the mean and standard deviation (Mean, SD) and the interquartile range (Q1: 25th quartile, Median, Q3: 75th quartile) of the distribution and finally, the number of oocytes measured per category (n). The vertical dotted line represents the threshold between primary and secondary growth oocytes.

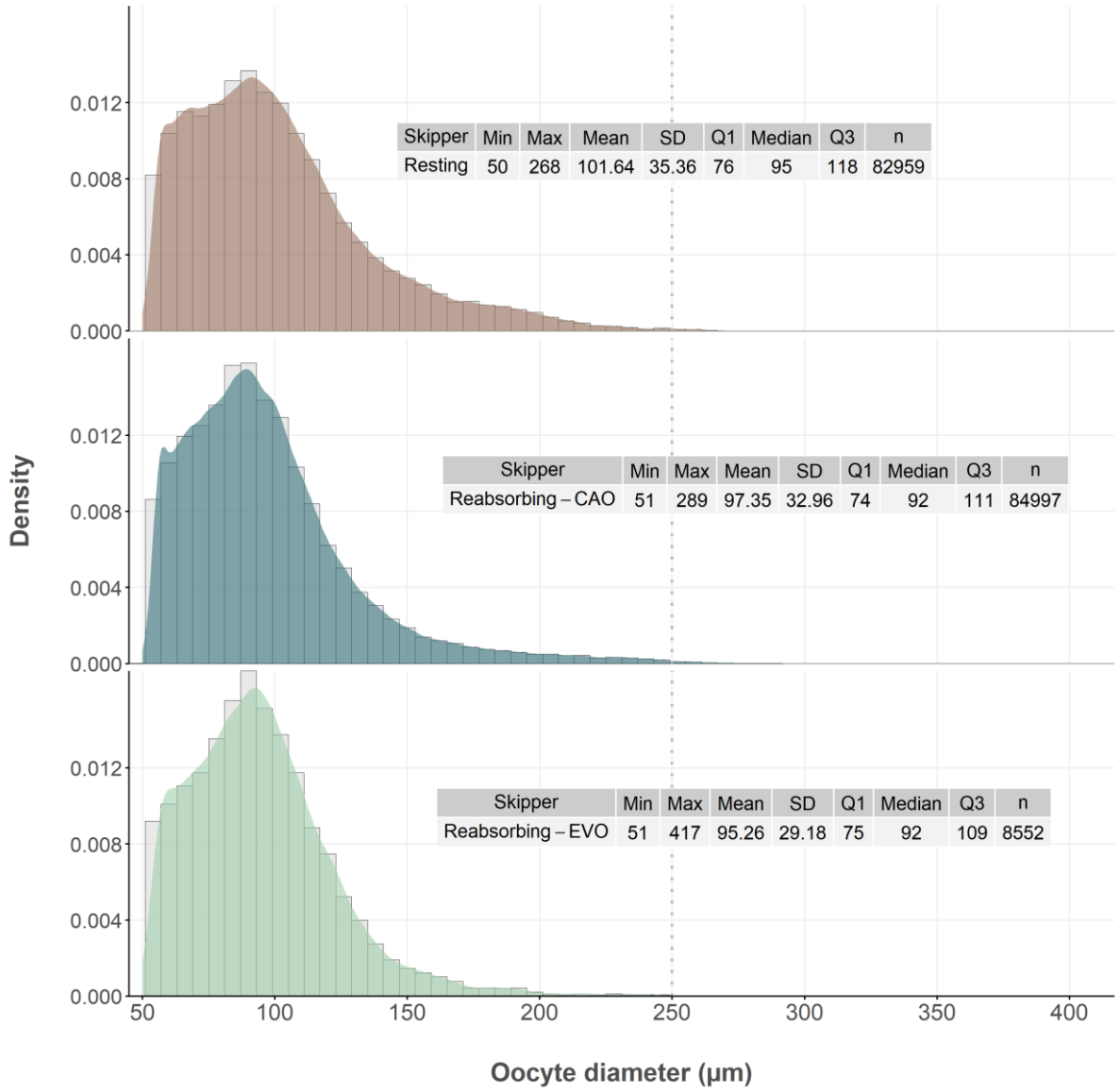

Appendix C.14. The difference in shape (skewness and kurtosis) of the oocyte size frequency distribution between immature females and the two modes of skipped spawning (i.e. resting and reabsorbing-CAO), examined with a one-way ANOVA with Tukey's HSD. The third mode of skipped spawning was excluded due to insufficient sample size (i.e. reabsorbing-EVO).

PREDICTOR VARIABLE	RESPONSE VARIABLE					
Maturity category	Skewness $F_{2,53}$ = 8.87, R^2 = 0.251			Kurtosis $F_{2,53}$ = 6.66 R^2 = 0.201		
	Estimate ± SE	*t-value*	*p-value*	Estimate ± SE	*t-value*	*p-value*
Resting - Immature	0.31 ± 0.15	1.940	0.136	0.92 ± 0.71	1.312	0.393
Reabsorbing-CAO - Immature	0.69 ± 0.17	4.106	**< 0.001**	2.50 ± 0.74	3.448	**0.003**
Reabsorbing-CAO - Resting	0.37 ± 0.14	2.686	**0.025**	1.58 ± 0.61	2.596	**0.029**

Appendix C.15. The difference in somatic gonadosomatic index (GSI_s, %) and whole-mount oocyte leading cohort (LC-W, µm) between immature females and the two modes of skipping females (i.e. resting and reabsorbing-CAO), examined with a one-way ANOVA with Tukey's HSD. The third mode of skipped spawning was excluded due to insufficient sample size (i.e. reabsorbing-EVO). One observation of GSI_s was removed due to missing value. Values of GSI_s are given on log transformed scale.

PREDICTOR VARIABLE	RESPONSE VARIABLE					
Maturity category	GSI $F_{3,52}$ = 7.617, R^2 = 0.230			LC-W $F_{2,53}$ = 50.6 R^2 = 0.656		
	Estimate ± SE	*t-value*	*p-value*	Estimate ± SE	*t-value*	*p-value*
Resting - Immature	0.30 ± 0.11	2.545	**0.036**	69.29 ± 8.88	8.542	**< 0.001**
Reabsorbing-CAO - Immature	0.49 ± 0.11	3.899	**< 0.001**	83.52 ± 9.17	9.679	**< 0.001**
Reabsorbing-CAO - Resting	0.17 ± 0.11	1.824	0.173	14.23 ± 7.61	1.992	0.123

Appendix C.16. Oocyte size frequency distributions of individual females histologically staged as uncertain (n = 22) collected during the Winter Survey 2020 in relation to thesis Objective 2.

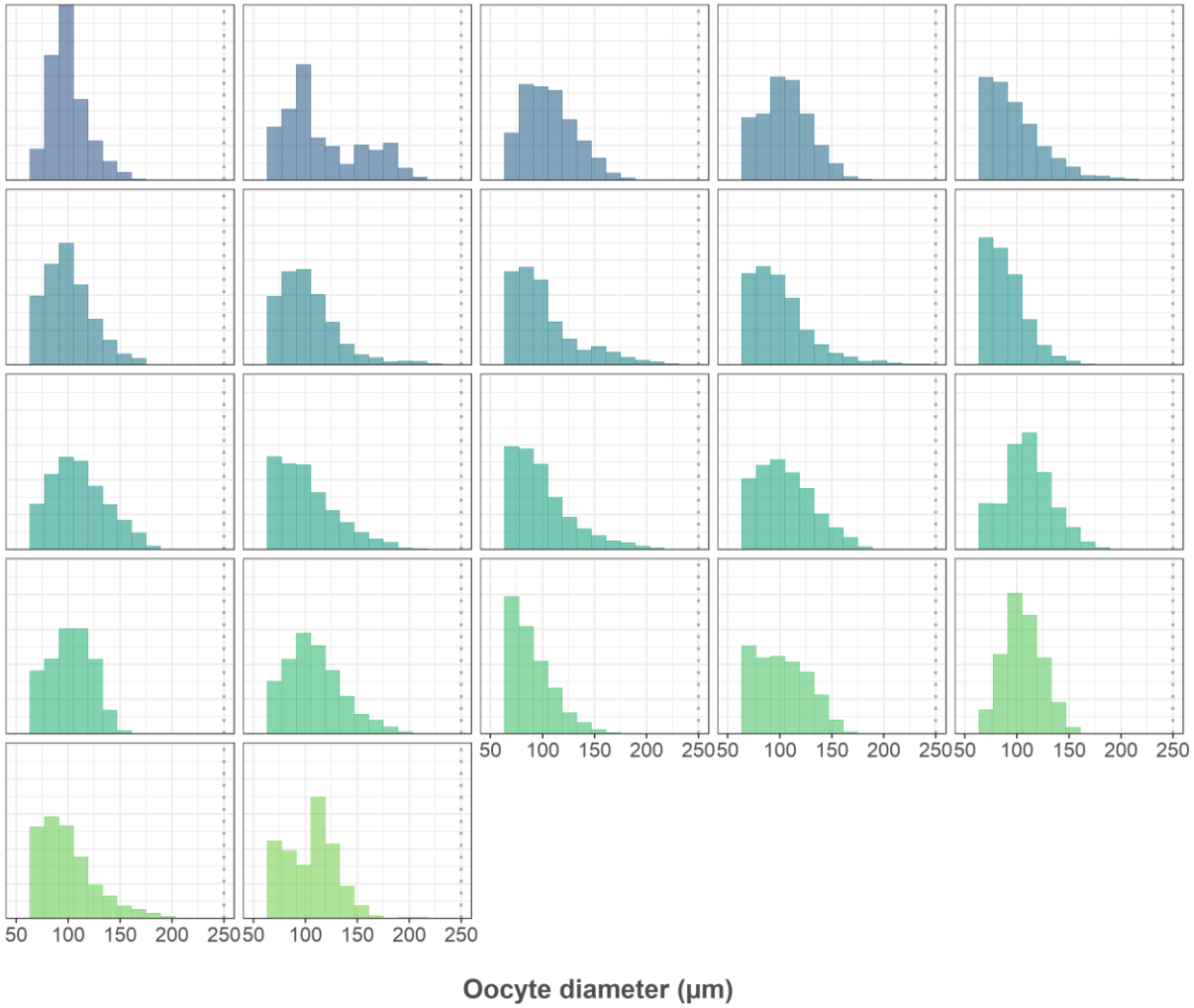

Appendix C.17. Difference in A: skewness; B: kurtosis; C: somatic gonadosomatic index (GSI_s); and D: whole-mount leading oocyte cohort (LC-W) between immature (yellow) and the three modes of skipped spawning: resting (brown), reabsorbing-CAO (R-CAO; blue) and reabsorbing-EVO (R-EVO; green) skippers, as well as 'uncertain' females (grey) (n = 80, and additional eight females from the Winter Survey 2021 have been included). Letters (letters a to c) above the boxes indicate the compact letter display of the statistically significant different groups in the one-way ANOVA after a post hoc test for multiple comparisons of groups. The F statistics, degrees of freedom and coefficient of determination of the statistical tests are shown below panel A and B, and above panel C and D.

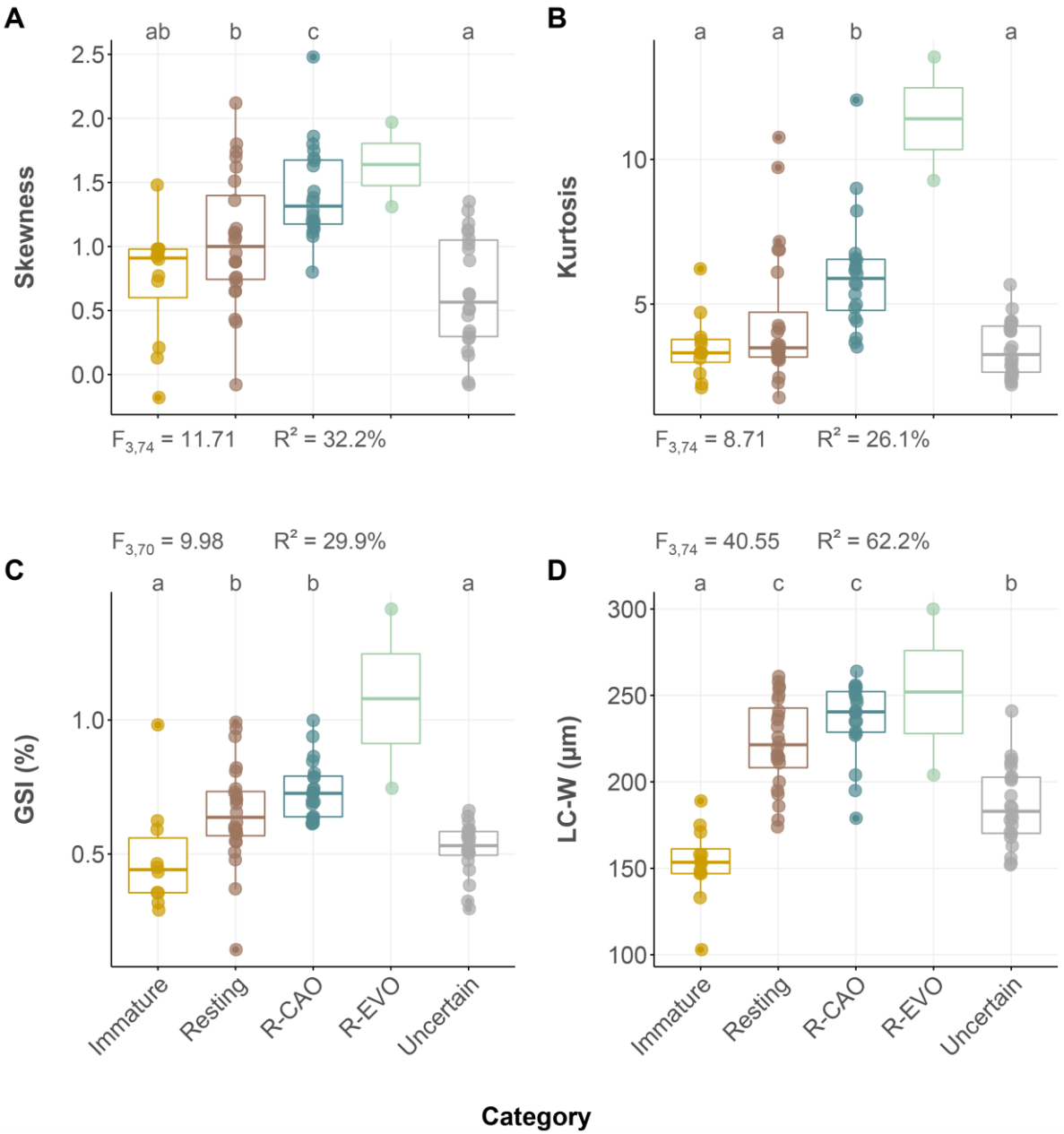

Appendix C.18. Difference in cumulative distribution of A: age; and B: length, of females histologically staged as immature, uncertain and skipping in relation to thesis Objective 2 (n = 80; eight females from the Winter Survey 2021 is included). Skipping females were significantly older than immature (t = 16.68, $p > 0.001$) and uncertain (t = 5.91, $p > 0.001$) females (one-way ANOVA, $F_{2,77} = 25.02$, $R^2 = 0.394$), but no age difference could be detected between immature and uncertain females (t = 0.50, $p = 0.868$). The same was true for total length, where skipping females were significantly longer than immature (t = 5.99, $p > 0.001$) and uncertain (t = 5.06, $p > 0.001$) females (one-way ANOVA, $F_{2,77} = 24.6$, $R^2 = 0.389$), but no difference in length could be detected between immature and uncertain females (t = 1.76, $p = 0.187$).